

Centriole disengagement: What are the relative contributions of Cohesin versus Pericentrin inactivation?

Dissertation

Zur Erlangung des akademischen Grades

- Doktor der Naturwissenschaften (Dr. rer. nat.) -

der Fakultät für Biologie, Chemie und Geowissenschaften

der Universität Bayreuth

vorgelegt von

Philip Kahlen

aus Osterholz-Scharmbeck

Bayreuth, 2023

Die vorliegende Arbeit wurde in der Zeit von April 2010 bis Dezember 2023 in Bayreuth am Lehrstuhl für Genetik unter der Betreuung von Herrn Prof. Dr. Olaf Stemmann angefertigt.

Form der Dissertation: Monographie

Dissertation eingereicht am: 14.12.23

Zulassung durch die Promotionskommission: 20.12.23

Wissenschaftliches Kolloquium: 04.07.24

Amtierender Dekan: Prof. Dr. Samimi

Prüfungsausschuss:

Prof. Dr. Olaf Stemmann (Gutachter)

Prof. Dr. Stefan Geimer (Gutachter)

Prof. Dr. Klaus Ersfeld (Vorsitz)

Prof. Dr. Benedikt Westermann

Die vorliegende Arbeit ist als Monographie verfasst.

Bisher sind keine Teile der Arbeit in Publikationen erschienen.

Table of content

1	SUMMARY	4
2	ZUSAMMENFASSUNG	6
3	INTRODUCTION	8
3.1	The eukaryotic cell cycle in general and mitosis in particular	8
3.2	The orchestration of mitotic entry, progression and exit by activity of kinases, phosphatases and targeted protein degradation	10
3.2.1	Mitotic kinases: regulation of mitotic entry and progression	11
3.2.2	The APC/C: targeted protein degradation initiates anaphase and late mitotic events	12
3.2.3	Mitotic phosphatases: regulation of mitotic exit	14
3.3	The Cohesin complex: Mediating sister chromatid cohesion	14
3.3.1	The Cohesin cycle: Loading of Cohesin in telophase and elevated dynamics in G1-phase	17
3.3.2	Establishment of sister chromatid cohesion in S-phase	18
3.3.3	M-phase: Cohesin resolution from chromosomes in two waves	20
3.3.4	Cohesin associated syndromes: Cohesinopathies	22
3.4	Microtubule organizing center, spindle pole bodies and centrosomes	22
3.5	The centrosome architecture and functions	24
3.5.1	Centrioles	24
3.5.2	The pericentriolar matrix (PCM)	27
3.6	The centrosome cycle and its coordination with the cell cycle	31
3.6.1	Procentriole formation and centriole elongation	32
3.6.2	Centrosome maturation	33
3.6.3	Centrosome separation and centriole disengagement	34
3.7	Aims of this work	37
4	RESULTS	38
4.1	Centriole disengagement: What are the relative contributions of Cohesin versus Pericentrin inactivation?	38
4.1.1	Generation and characterization of tools to study centriole disengagement	38
4.1.2	Experimental setup of the <i>in vitro</i> assay to quantify centriole disengagement	43
4.1.3	Inactivation of centrosomal Cohesin by artificial Scc1 cleavage triggers centriole disengagement	44
4.1.4	Artificial cleavage of PCNT triggers centriole disengagement	47
4.1.5	Unspecific cleavage of PCNT by HRV protease occurs at two distinct cleavage sites	53

Table of content

4.1.6	Non-cleavable versions of Scc1 and PCNT act as competitive inhibitors and reduce Separase activity	57
4.2	Phosphorylation-dependent conversion of PCNT into a suitable Separase substrate	60
4.2.1	Generation of <i>in vitro</i> tools to study the putative PCNT conversion into a suitable Separase substrate	60
4.2.2	Sequential phosphorylation by Cdk1 and Plk1 turns PCNT into a suitable Separase substrate	61
5	DISCUSSION	66
5.1	Artificial inactivation of centrosomal Cohesin or PCNT triggers centriole disengagement	66
5.1.1	Artificial cleavage of Cohesin rings induces centriole disengagement	66
5.1.2	Artificial PCNT cleavage triggers centriole disengagement	68
5.1.3	Theories for the missing additive effects upon artificial inactivation of centrosomal Cohesin and PCNT	71
5.1.4	Non-cleavable versions of Scc1 or PCNT might interfere with Separase activity	73
5.2	The fundamental role of Plk1 in licensing of centriole duplication	75
5.3	A speculative model explaining PCNTs and Cohesin's role in mediating centriole engagement	78
6	MATERIALS AND METHODS	81
6.1	Materials	81
6.1.1	Hard and Software	81
6.1.2	Chemicals and reagents	81
6.1.3	Antibodies	82
6.1.4	RNA oligonucleotides	83
6.1.5	Plasmids	84
6.1.6	Buffer, solutions and media (alphabetic order)	85
6.2	Microbiological techniques	86
6.2.1	<i>E. coli</i> strains	86
6.2.2	Cultivation of <i>E. coli</i>	87
6.2.3	Preparation of chemically competent <i>E. coli</i>	87
6.2.4	Transformation of chemically competent <i>E. coli</i>	87
6.2.5	Expression of proteins in <i>E. coli</i>	88
6.3	Molecular biological methods	88
6.3.1	Isolation of plasmid DNA from <i>E. coli</i>	88
6.3.2	Determination of DNA concentrations in solutions	88

Table of content

6.3.3	Restriction digestion of DNA	88
6.3.4	Dephosphorylation of DNA fragments	89
6.3.5	Separation of DNA fragments by gel electrophoresis	89
6.3.6	Isolation of DNA from agarose gels	89
6.3.7	Ligation of DNA fragments	89
6.3.8	Polymerase chain reaction (PCR)	89
6.3.9	Site-directed mutagenesis	90
6.4	Protein biochemical methods	90
6.4.1	SDS-polyacrylamide gel electrophoresis (SDS-PAGE)	90
6.4.2	Immunoblotting (Western blot)	90
6.4.3	Coomassie staining	91
6.4.4	Coupled <i>in vitro</i> transcription/translation (IVT/T)	91
6.4.5	<i>In vitro</i> kinase assay/cleavage assay	91
6.4.6	Ni ²⁺ -NTA affinity purification of 6x-Histidin-tagged proteins	92
6.4.7	Generation and purification of PCNT antibodies	92
6.4.8	Preparation of <i>Xenopus laevis</i> egg extract	94
6.4.9	Purification of active recombinant human Separase	95
6.4.10	Purification of active Plk1	96
6.5	Cell biological methods	96
6.5.1	Tissue culture cell lines	96
6.5.2	Cultivation of cell lines	96
6.5.3	Storage of mammalian cells	97
6.5.4	Transfection of Hek293 cells	97
6.5.5	Transfection of HeLa cells	98
6.5.6	Generation of stable Hek293 Flp-In cell lines	98
6.5.7	Synchronization of mammalian cells	98
6.5.8	Taxol-ZM override	99
6.5.9	Generation of tissue culture cell lysates for Immunoprecipitation experiments	99
6.5.10	Isolation of centrosomes	99
6.5.11	Immunofluorescence of isolated centrosomes	100
7	REFERENCES	101
8	ABBREVIATIONS	127

1 Summary

The centrosome is the main microtubule organizing center (MTOC) in animal cells. It consists of two centrioles surrounded by a proteinaceous pericentriolar matrix (PCM). In dividing cells, the centrosome duplicates once in S-phase. At the base of each centriole forms a new daughter centriole in a perpendicular orientation. This pair of centrioles stays tightly associated, or ‘engaged’, until late mitosis. This tight association suppresses the formation of further centrioles and hence, serves as an intrinsic block of reduplication and as a copy number control. How engagement between centrioles is achieved and maintained throughout interphase remains enigmatic, but most promising is a model of matrix entrapment through the surrounding PCM. In late mitosis and by concerted action of Plk1 kinase and the cysteine-endopeptidase Separase, the tight association is relieved in a process termed centriole disengagement. This step is an important licensing step for duplication in the next cell cycle. The ring-shaped multiprotein complex Cohesin and Pericentrin (PCNT) have independently been identified as centrosomal substrates for Separase. Whether the Cohesin ring is directly involved in centriole linkage or contributes, together with PCNT, to the structural integrity of the PCM remains unknown. However, proteolytical inactivation of each factor has been described as sufficient for triggering centriole disengagement. In order to solve this apparent contradiction, both factors were engineered to be cleavable by either tobacco etch virus protease (TEV) or human rhinovirus protease 3C (HRV) and corresponding transgenes were stably integrated into the same human host cell genome. Incubation of corresponding cell lysates with the TEV or HRV protease was followed by isolation of centrosomes and quantification of centriole disengagement by immunofluorescence microscopy (IFM). Individual cleavage of either Cohesin or PCNT each triggered centriole disengagement *in vitro*, confirming seemingly conflicting results from independent groups within the same experimental setup. Surprisingly, addition of both proteases at the same time revealed no additive effect regarding centriole disengagement, arguing that Cohesin and PCNT contribute to centriole engagement by different mechanisms.

Activity of the Plk1 kinase was shown to be essential for centriole disengagement in late mitosis and hence, for licensing of centriole duplication in the following cell cycle. Due to its vast number of substrates and regulated processes, e.g. centrosome maturation and centriole-to-centrosome conversion, it is hard to identify the crucial Plk1 substrate or activity for licensing centriole duplication. One possible activity could be the conversion of PCNT into a

suitable Separase substrate. This idea is inspired by the observation that Plk1-dependent phosphorylation of Cohesin substantially enhances its cleavage by Separase. Indeed, preventing phosphorylation of three sites in direct vicinity of the cleavage site by changing Ser/Thr to Ala efficiently abolished PCNT cleavage by Separase *in vitro* and *in vivo*. This result exemplifies the important nature of these phosphorylation sites and specifies another Plk1 function in mitosis.

2 Zusammenfassung

Für die Erhaltung der Genomstabilität bei der tierischen Zellteilung ist eine fehlerfreie Chromosomenverteilung auf die neu entstehenden Tochterzellen essentiell. Das Zentrosom spielt dabei für die Organisation des Zytoskeletts und der mitotischen Spindel eine entscheidende Rolle. Nach der Teilung beginnt jede tierische Zelle den neuen Zellzyklus mit einem Zentrosom, das aus zwei Zentriolen besteht. Diese wiederum sind eingebettet in eine proteinreiche perizentrioläre Matrix (PCM), die als Ausgangspunkt für die Rekrutierung und die Bildung von Mikrotubuli der Spindel fungiert. In jedem Zellzyklus wird das Zentrosom einmal dupliziert, damit in der folgenden M-Phase erneut eine bipolare Spindel ausgebildet werden kann. In Analogie zu den Chromosomen erfolgt diese Duplikation in der S-Phase. Dabei bildet sich an den proximalen Enden der bestehenden sog. Mutterzentriolen jeweils eine rechtwinklig angeordnete sog. Tochterzentriole aus. Bis zum Eintritt in die folgende M-Phase verlängern sich die Tochterzentriolen auf ihre dann volle Größe.

Die Duplikation unterliegt einer strengen Regulierung, die sicherstellt, dass nur genau eine neue Tochter- pro bestehender Mutterzentriole gebildet wird. Dies wird durch eine enge Kopplung des neu gebildeten Zentriolenpaares ab der Duplikation in S-Phase bis zum Zeitpunkt der Entkopplung in der M-Phase erreicht. Die Bildung weiterer Tochterzentriolen wird dadurch aktiv unterdrückt. Somit sichert die enge Kopplung eine korrekte Kopienanzahl an Zentriolen und verhindert die Bildung multipolarer Spindeln. Die genauen Mechanismen, die diese enge Kopplung der Zentriolen erlauben, sind bisher nur wenig verstanden. Die gängigste Theorie ist ein indirektes Zusammenhalten der Zentriolen durch Kräfte der sie umgebenden PCM. Hinweise dafür lieferten Experimente, die sich mit der Entkopplung der Zentriolen in später Mitose befassen. So konnte gezeigt werden, dass die Aktivität der Kinase Plk1 in früher Mitose sowie die Aktivität der Endopeptidase Separase in später Mitose essentiell für die Entkopplung der Zentriolen sind. Als zentrosomale Separase Substrate konnten von unabhängigen Arbeitsgruppen der aus mehreren Untereinheiten bestehende Kohäsin-Ring sowie Perizentrin (PCNT) identifiziert werden. Weitgehend unbekannt ist, ob der Kohäsin-Ring, in Analogie zu seiner Funktion bei der Schwesterchromatidkohäsion, die Zentriolen direkt zusammenhält oder gemeinsam mit PCNT zur strukturellen Integrität der umgebenen PCM beiträgt. Bemerkenswert ist, dass sowohl die Kohäsin- als auch die PCNT-Spaltung von unabhängigen Arbeitsgruppen als jeweils notwendig und hinreichend für die Entkopplung der Zentriolen charakterisiert wurden. Eine mögliche Erklärung für diesen

scheinbaren Widerspruch wäre, dass beide Faktoren synergistisch zur strukturellen Integrität der PCM beitragen. Um diesen Sachverhalt aufzuklären, wurden im Rahmen dieser Arbeit stabile humane Zelllinien generiert, die TEV-Protease (tobacco etch virus) oder HRV-Protease (human rhinovirus 3C) spaltbare Versionen der Kohäsin Untereinheit Scc1 sowie PCNT exprimieren. Die entsprechenden Zellsätze wurden mit TEV oder HRV Protease inkubiert, anschließend wurden die Zentrosomen isoliert und die zentrioläre Entkopplung mittels Immunfluoreszenzmikroskopie (IFM) quantifiziert. Auf diese Weise konnte in ein und demselben Versuchsaufbau gezeigt werden, dass sowohl die Spaltung des Kohäsin Ringes als auch von PCNT die zentrioläre Entkopplung bewirken kann. Dies bestätigt bisherige, scheinbar widersprüchliche Ergebnisse unabhängiger Gruppen. Dennoch konnten bei gleichzeitiger Spaltung von Kohäsin und PCNT durch Zugabe beider Proteasen keine synergistischen Effekte quantifiziert werden. Diese Tatsache spricht für unterschiedliche Mechanismen, mit denen Kohäsin und PCNT zur Kopplung der Zentriolen beitragen.

Desweiteren wurde im Rahmen dieser Arbeit der Zusammenhang zwischen der essentiellen Aktivität der Kinase Plk1 und der Entkopplung der Zentriolen in später Mitose untersucht. Aufgrund der großen Anzahl von Substraten und regulierten Prozessen, wie z.B. die Reifung von Zentrosomen und die Umwandlung von Zentriolen in Zentrosomen, ist es schwierig, das entscheidende Plk1-Substrat oder die Aktivität für die Lizenzierung der Zentriolenduplikation zu identifizieren. Eine mögliche essentielle Aktivität der Plk1 Kinase kann in diesem Zusammenhang die Überführung von PCNT in ein geeignetes Substrat für Separase sein. Dies konnte bereits für das mitotische sowie das meiotische Kleisin des Kohäsin Ringes, Scc1 bzw Rec8 gezeigt werden. So führte im Falle von Scc1 die Plk1-abhängige Phosphorylierung in direkter Umgebung der Separase Schnittstelle zu einer deutlich effizienteren Spaltung durch die Endopeptidase. Mit diesem Hintergrund wurden auch in der PCNT-Sequenz eine potentielle Cdk1 sowie zwei potentielle Plk1 Phosphorylierungsstellen in direkter Nähe der Separase Schnittstelle identifiziert und durch gezielte Mutagenese zu Alanin inaktiviert. Die Spaltung von PCNT konnte dadurch sowohl *in vitro* als auch *in vivo* verhindert werden. Diese Tatsache zeigt eine direkte Verbindung zwischen der Aktivität von Plk1 in früher Mitose und der Separase Aktivität sowie der Entkopplung der Zentriolen in später Mitose auf.

3 Introduction

3.1 The eukaryotic cell cycle in general and mitosis in particular

Cell reproduction in eukaryotes is an elaborate process in which one mother cell divides into two genetically identical daughter cells. The tightly regulated eukaryotic cell cycle ensures the timely separation of the two main events, the duplication of chromosomes in S-phase (synthesis phase) and their segregation in M-phase (mitotic phase) (Fig. 1). The gaps between these main phases are called G1- and G2-phase and are characterized by extensive protein synthesis in order to prepare for the subsequent DNA replication or chromosome separation, respectively. Together, G1-, S- and G2-phase are referred to as interphase and require over 90% of the time of one cell cycle. The shortest cell cycle stage, mitosis, is also the most dramatic one: Severe alterations in chromosome condensation status as well as rearrangement of organelles and the cytoskeleton occur during so-called pro-, meta-, ana- and telophase (Nurse, 1997).

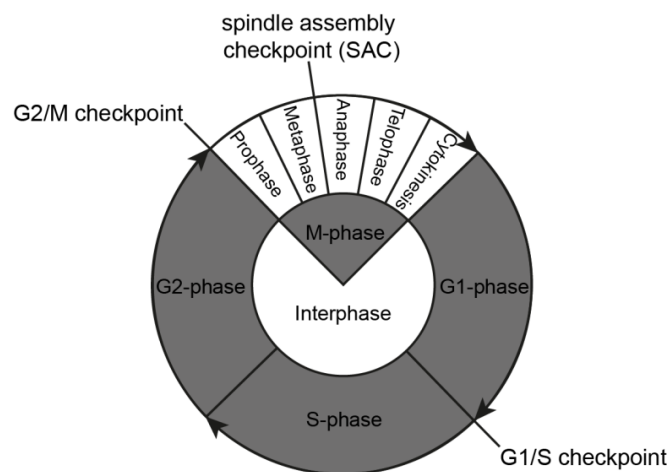


Fig. 1: Schematic overview of the eukaryotic cell cycle. Cell cycle progression is divided into four distinct phases: Chromosomes are replicated in S-phase and segregated into two daughter cells during subsequent M-phase. The G1- and G2-gap-phases provide time for preparing the next S- or M-phase, respectively. Indicated checkpoints are control mechanisms that ensure robust and all-or-nothing switches in cell cycle progression.

In prophase, the DNA condenses into chromosomes followed by nuclear envelope breakdown (Fig. 2). The mitotic spindle, a complex and highly dynamic structure composed of microtubules, mediates the segregation of chromosomes. In a typical animal cell, it originates from an important organelle, the so-called centrosome. Each cell contains two centrosomes which begin to separate in prophase and move to opposite sides of the cell in order to build a

bipolar spindle. In late prophase, sometimes named prometaphase, microtubules of the mitotic spindle start to make contact with the kinetochores, thereby enhancing congression of the chromosomes. During metaphase, the chromosomes become aligned halfway between the spindle poles (at the so-called metaphase plate) by pushing and pulling forces of the mitotic spindle. In anaphase, sister chromatids become separated and are pulled to the cell poles by the mitotic spindle. Additionally, the cell begins to elongate by pushing forces of the microtubules. Telophase is characterized by sustaining cell elongation and the beginning of DNA decondensation. The nuclear envelope reassembles and the contractile ring begins to establish a cleavage furrow which narrows at the former metaphase plate. Cytokinesis, often defined as the final stage of M-phase, terminates division of cytoplasm, organelles as well as the membrane and eventually mediates the separation of the two daughter cells (T. J. Mitchison & Salmon, 2001).

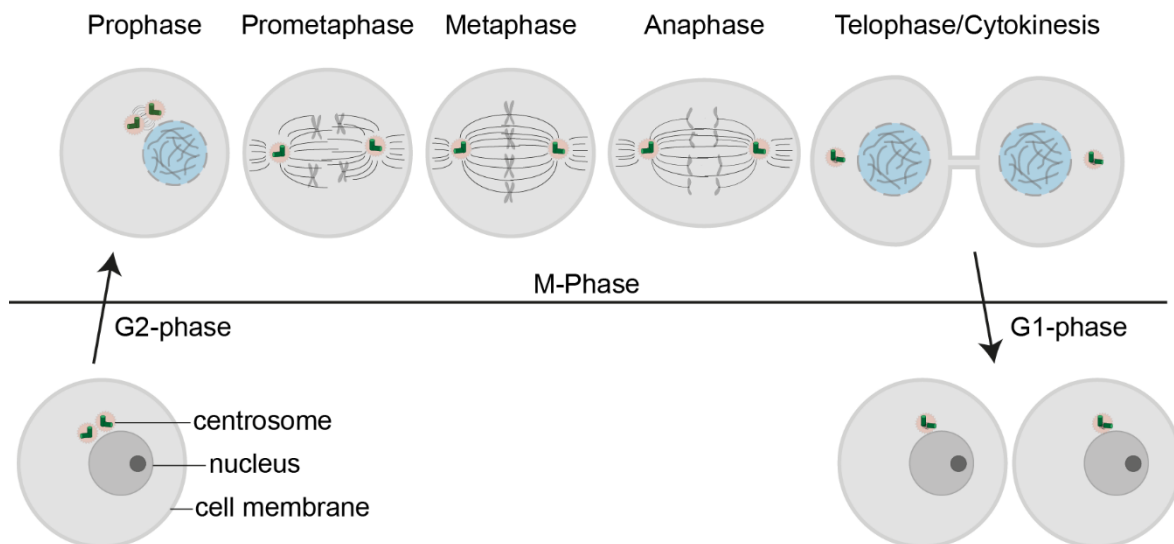


Fig. 2: The mitotic phases in more detail. Prophase is characterized by DNA condensation and centrosome splitting. In prometaphase the nuclear envelope breakdown occurs, the mitotic spindle forms and attaches to the kinetochores, followed by chromosome congression. In metaphase the chromosomes align at the metaphase plate. Anaphase is marked by sister chromatid separation. Eventually, DNA decondensation, nuclear envelope assembly, cell elongation and cleavage furrow formation are initiated during telophase. Cytokinesis is the physical process that separates the daughter cells and completes the cell cycle.

Progression through the cell cycle is controlled at different checkpoints (Fig. 1). The first one is the G1/S checkpoint which is also called restriction point or start, because cells irrevocably enter the cell cycle at this point. This entry only occurs if signals from inside (such as cell size) and outside the cell (such as mitogens) trigger transition. In case of DNA damage during S-phase, cells activate another checkpoint, the intra-S-checkpoint. Furthermore, the G2/M checkpoint has the ability to prevent entry into mitosis in case of adverse conditions such as

DNA damage. Eventually, the metaphase-to-anaphase transition is under control of the spindle assembly checkpoint (SAC), a safeguard mechanism that monitors unattached kinetochores and prevents late mitotic events until all kinetochores are correctly attached to the mitotic spindle (Iyer & Rhind, 2017; Vermeulen et al., 2003).

All of these irreversible and switch-like transitions are mainly controlled by cyclin-dependent kinases (Cdk). Cdks are activated upon interaction and complex formation with cell cycle phase-specific cyclins. In contrast to the constant kinase protein level, cyclin concentrations oscillate throughout the cell cycle in most cases (G1/S-, S-, and M-cyclins, corresponding to the cell cycle phase-specific accumulation) and lead to transient kinase activation. In addition, activity of Cdk-cyclin complexes is regulated by activating or inhibitory phosphorylation and by binding of inhibitory proteins (Pines, 1991). Furthermore, the protein levels of cyclins and regulatory proteins are altered during cell cycle by targeted degradation (Murray, 2004).

3.2 The orchestration of mitotic entry, progression and exit by activity of kinases, phosphatases and targeted protein degradation

Mitotic entry is triggered by the switch like activation of mitotic kinases. Their activity in early mitosis leads to phosphorylation of proteins that drive the already mentioned events preparing the chromosomes for segregation: disassembly of the nuclear envelope, assembly of the mitotic spindle, chromosome condensation and congression to the metaphase plate (Nasa & Kettenbach, 2018). The spindle assembly checkpoint (SAC) monitors unattached kinetochores but as soon as all kinetochores are properly captured by the mitotic spindle, the checkpoint is inactivated (Lara-Gonzalez et al., 2012). This event marks the turning point of mitosis as it leads to the activation of a giant ubiquitin ligase termed the anaphase promoting complex or cyclosome (APC/C) (Musacchio, 2015). The APC/C mediates targeted protein degradation of numerous important regulatory proteins like cyclins. As a consequence, the separation of sister chromatids is initiated and mitotic kinases become inactivated (Peters, 2006). Eventually, late mitotic events as well as mitotic exit and cytokinesis are facilitated by uprising activity of phosphatases that counteract the phosphorylations set by mitotic kinases (Nasa & Kettenbach, 2018).

3.2.1 Mitotic kinases: regulation of mitotic entry and progression

From a regulatory perspective, entry into mitosis is orchestrated by a complex network of factors that control the timely activation of Cdk1-Cyclin B1. Cyclin B1 slowly accumulates during S- and G2-phase which leads to increasing amounts of Cdk1-Cyclin B1 complexes. They are kept inactive by inhibitory phosphorylation of Cdk1 at Thr14 and Tyr15 mediated by the kinases Wee1 and Myt1 (McGowan & Russell, 1993; Norbury et al., 1991). These phosphorylations have to be removed by the Cdc25 phosphatase to achieve partial activation (Galaktionov & Beach, 1991). For full activation, Cdk1 has to be phosphorylated at Thr161 by the Cdk-activating kinase (CAK) (Kaldis, 1999). Cdk1 itself also contributes to the activation of Cdc25 and inactivation of Wee1 resulting in a positive feedback loop and a switch-like mitotic entry (Watanabe et al., 2005). Upon mitotic entry, active Cdk1-Cyclin B1 phosphorylates a vast number of substrates leading to nuclear envelope breakdown, chromosome condensation and congression (Enserink & Kolodner, 2010).

Furthermore, the family of Polo-like kinases is essential for the orchestration of mitotic events. Primarily identified in genetic screens in *Drosophila* (Sunkel & Glover, 1988), homologues of the Ser/Thr kinase Polo have since been identified in many eukaryotes. Mammals express four different Polo-like kinases (Plk1-4) with non-overlapping functions (Archambault & Glover, 2009). Among these, Plk1 is the most extensively studied kinase as it is involved in many processes related to mitotic entry as well as progression. In human cells, Plk1 promotes mitotic entry by enhancing Cdk1-Cyclin B1 activity on multiple levels: First, it phosphorylates and activates Cdc25 (Lobjois et al., 2009). Second, Plk1 phosphorylates Wee1/Myt1 and contributes to their inactivation (Watanabe et al., 2004). Third, it phosphorylates Cyclin B1 and thereby promotes its nuclear import (Lobjois et al., 2009; Peter et al., 2002). During mitosis, Plk1 localizes to the centrosomes in prophase, the kinetochores in prometa- and metaphase, the central spindle in anaphase and the midbody in telophase (Barr et al., 2004; Zitouni et al., 2014). These various subcellular localizations are mediated by its C-terminal Polo-box domain (PBD) which contains two Polo-boxes (PB), preferentially binding to phosphorylated peptides (Elia et al., 2003). This implies that other kinases, like Cdk1, act as priming kinases and hence regulate the spatial and timely activation of Plk1 (Tavernier et al., 2015). Plk1 then phosphorylates substrates via its N-terminal Ser/Thr kinase domain and thereby fulfills multiple functions like the already mentioned entry into mitosis, accumulation of proteins in the pericentriolar matrix (PCM) of the centrosomes (a process termed maturation), kinetochore assembly, chromosome arm resolution during mitosis as well as formation of a cleavage furrow during cytokinesis (Barr et al., 2004; Petronczki et al.,

2008). Plk2 and Plk3 functions are more related to cell cycle progression during interphase and DNA damage response, respectively (Ma et al., 2003; Xie et al., 2001). Plk4 is located at the centrosome throughout most of the cell cycle where it is the main regulator of centriole duplication during S-phase (Habedanck et al., 2005).

3.2.2 The APC/C: targeted protein degradation initiates anaphase and late mitotic events

Progression through mitosis is also controlled by targeted protein degradation. The majority of protein degradation in mammalian cells is carried out by the ubiquitin-proteasome pathway. Here, the small (76 aa) protein ubiquitin is covalently conjugated via an iso-peptide bond to substrate proteins which are subsequently degraded by the 26S proteasome (Collins & Goldberg, 2017). The conjugation is catalyzed in a sequential cascade reaction by three enzymes called the ubiquitin activating enzyme E1, the ubiquitin conjugating enzyme E2 and the ubiquitin ligase E3 (Kleiger & Mayor, 2014). Substrate specificity is mediated by one of the numerous E3 enzymes which are classified into two major families, the HECT and RING domain ligases. Members of the HECT domain ligases feature enzymatic activity and hence catalyze the ubiquitin transfer from E2 to the substrate via a covalent ubiquitin-HECT intermediate. Members of the RING domain ligases lack enzymatic activity and rather serve as a binding platform for the E2 enzyme and the substrate, thereby mediating the direct ubiquitin-transfer from E2 onto the substrate (Metzger et al., 2012). Two RING domain complexes are mainly dedicated to the control of cell cycle progression, namely the anaphase-promoting complex or cyclosome (APC/C) and the Skp1-Cul1-F-Box-protein (SCF) ligases (Cardozo & Pagano, 2004; Peters, 2006).

The human APC/C is a 1.2 MDa complex comprising 19 subunits (Chang et al., 2014). Its activity is regulated by phosphorylation of several subunits but furthermore strictly depends on binding of either one of its coactivator subunits Cdc20 or Cdh1 (Kraft et al. 2003; Kramer et al. 2000). While APC/C^{Cdc20} activity is essential for the initiation of the metaphase-to-anaphase transition, APC/C^{Cdh1} becomes active from late mitosis until entry into S-phase. Both coactivators recognize conserved degron sequences called destruction box (D-box) or KEN-box in substrate proteins, with APC/C^{Cdc20} more relying on the KEN-box and APC/C^{Cdh1} more relying on the D-box (Barford, 2011).

Due to its importance, APC/C activity is tightly regulated. In early mitosis APC/C activity is repressed by the SAC, a control mechanism that monitors unattached kinetochores and

generates a wait-anaphase signal until all kinetochores are stably bound by the mitotic spindle (Lara-Gonzalez et al., 2012). In more detail, unattached kinetochores catalyze the formation of a diffusible signal, the so-called mitotic checkpoint complex (MCC). The MCC is composed of Bub3, Mad2 and BubR1 which together bind Cdc20. Association of the MCC with the APC/C then blocks substrate recruitment and its activity (Joglekar, 2016). Once all kinetochores are correctly attached to the mitotic spindle, the SAC is satisfied and the MCC disassembled (Eytan et al., 2014; Yang et al., 2007). The released Cdc20 is now able to activate the APC/C and initiate anaphase with its defining event, the separation of sister chromatids. Up to this point, sister chromatids were tethered together by a multiprotein complex called Cohesin, which topologically embraces the two sisters (Michaelis et al., 1997). The resolution of cohesion occurs through Separase, a giant cysteine endopeptidase, which cleaves the kleisin subunit of Cohesin, Scc1/Rad21 (Uhlmann et al., 1999, 2000). Premature activation of Separase would lead to precocious separation of sister chromatids. Hence, Separase activity is tightly regulated by multiple, mutually exclusive inhibitors. The MCC component Mad2 for instance, was shown to further associate with shugoshin 2 (Sgo2), in order to build a competitive inhibitor complex for Separase (Hellmuth et al., 2020). Additionally, Separase can be inhibited by Securin or Cdk1-Cyclin B1 (Ciosk et al., 1998; Stemmann et al., 2001). Both inhibitors are substrates of APC/C^{Cdc20}, revealing a strictly timed order in anaphase events with inactivation of the SAC, activation of the APC/C and eventually liberation of Separase through degradation of its inhibitors. Cyclin B1 degradation additionally leads to dropping Cdk1 activity in late mitosis. As a consequence, Cdh1 is freed from its inhibitory phosphorylations and assembles with the APC/C into an active complex which supports mitotic exit. Additionally, APC/C^{Cdh1} contributes to the maintenance of G1-phase, thereby suppressing premature entry into S-phase (Jaspersen et al., 1999; Kramer et al., 2000).

The second E3 ligase important for cell cycle progression is the SCF (Skp1, Cull1 and the F-Box) ligase (Vodermaier, 2004). Cull1 and Skp1 serve as a platform for the binding of one of the many F-box proteins that mediate substrate specificity (Cardozo & Pagano, 2004; Kobe & Kajava, 2001; Pashkova et al., 2010; Yoshida et al., 2002). As a common characteristic, almost all substrates have to be phosphorylated in order to be recognized as such. This however allows targeted destruction of substrates by the SCF throughout the cell cycle (Skowyra et al., 1997).

3.2.3 Mitotic phosphatases: regulation of mitotic exit

Late mitotic events like spindle disassembly, nuclear envelope reassembly, cytokinesis and finally mitotic exit are mainly driven by declining activity of mitotic kinases and rising activity of counteracting phosphatases (Pereira & Schiebel, 2016). In mitosis, more than 1000 proteins with increased phosphorylation were identified in a mass-spectrometry approach (Dephoure et al., 2008). Over 99% of these events occur at serine and threonine residues whereas less than 1% account for tyrosine residues (Hunter & Sefton, 1980). Interestingly, the human genome encodes for more than 100 tyrosine phosphatases (TPs), but only for approximately 30 serine/threonine-specific phosphatases (STPs). This imbalance is due to the fact that STPs are able to build diverse complexes with different combinations of catalytic and regulatory subunits (Brautigan, 2013; Tonks, 2006). STPs are subdivided into three groups with the phospho-protein phosphatases (PPP) as the most important and most numerous group (Shi, 2009). They are mainly involved in cell cycle regulation, among them Cdc25, protein phosphatase 1 (PP1) and protein phosphatase 2 (PP2A) which are particularly important for mitotic entry and exit. PP2A forms more than 100 different trimeric complexes and PP1 even more than 200 dimeric complexes targeting different substrates and thereby reversing the various phosphorylations set by mitotic kinases (Heroes et al., 2013; Janssens et al., 2008; Shi, 2009).

3.3 The Cohesin complex: Mediating sister chromatid cohesion

In mammalian cells, chromosomes are duplicated in S-phase and segregated in the following M-phase. In contrast to the two centrosomes, up to dozens of chromosomes have to be properly replicated and equally distributed to the newly formed daughter cells. This major challenge is met by keeping the sister chromatids tethered together from the time of their replication in S-phase until their separation at the metaphase-to-anaphase transition in mitosis. Two mechanisms contribute to this cohesion, namely the intertwining of sister chromatids (SCI) and the Cohesin ring which physically embraces the two sister chromatids (Baxter, 2015; Haarhuis et al., 2014).

The Cohesin core complex is a tripartite ring composed of two Smc proteins (structural maintenance of chromosomes) and the kleisin subunit Scc1 (sister chromatid cohesion) (Fig. 3) (Gruber et al., 2003; Michaelis et al., 1997). Smc proteins are conserved in all

domains of live and exhibit a characteristic long and rod-shaped form. They contain a central globular hinge domain over which the proteins fold back on themselves to build intramolecular and antiparallel coiled coils. This brings the N- and C-termini in direct vicinity and together they build a nucleotide binding head domain (NBD) which characterizes Smc proteins as members of the ATP binding cassette (ABC) ATPases (Hirano, 2006; Uhlmann, 2016). In human Cohesin, Smc1 and Smc3 exclusively form heterodimers via the hinge domain on the one side and the head domains on the other side (Haering et al., 2002). Each head domain builds a partial and complementary ATPase domain meaning that the Walker A and B motif of Smc1 interact with the D-loop and the signature motif of Smc3 and *vice versa* (Lammens et al., 2004). More recent structural data suggest that SMC's coiled coils possess a flexible region in their middle, the 'elbow', which allows a collapsed conformation and contact between head and hinge domain (Bürmann et al., 2019). The kleisin subunit Scc1 closes the ring by binding to the Smc1 head domain with its C-terminus and to the coiled coil region proximal to the head domain of Smc3 with its N-terminus (Gligoris et al., 2014; Huis in 't Veld et al., 2014).

Scc1 provides binding sites for additional peripheral subunits, which regulate Cohesin dynamics on chromatin. As a common characteristic, they are all heat repeat proteins and referred to as HAWKs (HEAT Proteins Associated With Kleisins) (Wells et al., 2017). For example, permanently bound to the unstructured middle region of Scc1 is a stoichiometric subunit called Scc3 in yeast or stromal antigen (SA) in vertebrates (Losada et al., 2000; Tóth et al., 1999). The latter express two isoforms named SA1 or SA2, with non-redundant functions albeit approximately 70% sequence homology (Canudas & Smith, 2009; Carramolino et al., 1997). Both contribute to effective and stable binding of Cohesin to DNA, with SA1 binding to AT-rich telomeric sequences and with SA2 binding sequence-independent to DNA but with a higher affinity to ssDNA (Bisht et al., 2013; Countryman et al., 2018). Thereby, SA2 is associated with DNA replication and double-strand break repair (Countryman et al., 2018). Further associated with Scc1 is the kollerin complex, consisting of Nipbl/Mau2 in vertebrates or Scc2/Scc4 in yeast (Ciosk et al., 2000). Kollerin is important for the loading of Cohesin in telophase (in mammals) or G1 phase (in yeast) (Ciosk et al., 2000; Tonkin et al., 2004). During G1-phase, Cohesin association with chromatin is highly dynamic, meaning permanent loading and unloading events occur (Gerlich et al., 2006). Cohesin unloading is mediated by another peripheral Cohesin complex, namely PDS5/Wapl (Gandhi et al., 2006; Kueng et al., 2006). This complex mediates the ATP-dependent but proteolysis-independent opening of the Cohesin ring and its dissociation from DNA (Murayama &

Uhlmann, 2015). Interestingly, PDS5 (expressed in humans as isoforms PDS5A and PDS5B) has two opposing roles as it is also responsible for establishing cohesive Cohesin during S-phase. It does so in complex with Sororin, a protein mutually exclusive competing with Wapl for the same binding site at the N-terminus of PDS5 (Nishiyama et al., 2010; Rankin et al., 2005).

The discovery, that cleavage of the kleisin subunit Scc1 by Separase allows the sister chromatids to separate in anaphase led to the suggestion, that cohesion is mediated by topological entrapment of sister chromatids within the ring's lumen (Haering et al., 2002; Uhlmann et al., 2000). This widely accepted ring model was further supported by experiments with purified mini-chromosomes. Both, cleavage of the DNA by restriction enzymes as well as artificial cleavage of an engineered Cohesin ring with TEV (Tobacco Etch Virus) protease resulted in a loss of DNA-Cohesin association (Ivanov & Nasmyth, 2005). Furthermore, crosslinking all three interfaces of the integral Cohesin subunits by introduced cysteine residues creates sodium dodecylsulfate (SDS)-resistant rings around mini-chromosomes (Haering et al., 2008). However, this ring model is challenged by the handcuff, snap or bracelet model, in which sister chromatids are individually bound by a single Cohesin ring. Cohesion would then be mediated by dimerization of Cohesin rings via Scc1/STAG or the SMC hinge regions (Zhang et al., 2008; Zhang & Pati, 2009).

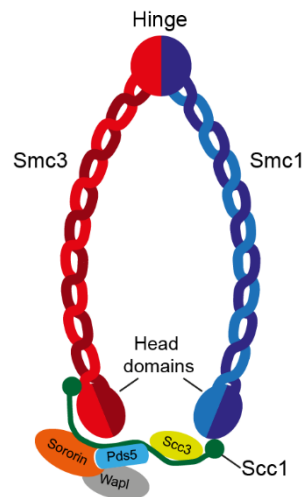


Fig. 3: The cohesin ring. Smc1, Smc3 and Scc1 together build the cohesin core complex. Smc proteins are large coiled coil proteins that fold back on themselves, thereby generating a flexible hinge domain and two ATPase head domains. Scc1 closes the ring by binding to both Smc subunits and additionally serves as a binding platform for several peripheral subunits like Scc3 and Pds5. Pds5 in turn mediates binding of the cohesin release factor Wapl or its antagonist Sororin, dependent on the current cell cycle phase.

3.3.1 The Cohesin cycle: Loading of Cohesin in telophase and elevated dynamics in G1-phase

As already mentioned, the initial loading of Cohesin occurs in late telophase (in vertebrates) or late G1-phase (in yeast) (Ciosk et al., 2000; Michaelis et al., 1997). Genome-wide mapping of Cohesin revealed a rather static accumulation at centromeres and specific sites at the chromosomal arms. These sites represent intergenic regions or CARs (Cohesin associated region) in budding yeast as well as actively transcribed genes in flies (Laloraya et al., 2000; Misulovin et al., 2008). In mouse and humans, most of Cohesin binds to sites occupied by the CCCTC binding factor (CTCF), a transcription factor involved in the organization and compaction of chromatin (Wendt et al., 2008). During G1-phase, Cohesin dynamically associates with chromatin, meaning that constant loading and unloading events occur. The mean residence time of the majority of Cohesin rings is less than 25 min (Gerlich et al., 2006). In vertebrates, Cohesin loading depends on a complex comprising Scc2-Scc4 as well as ATP hydrolysis by the SMC heads (Ciosk et al., 2000). For topological entrapment of DNA, the loading complex makes multiple contacts with all four peripheral Cohesin subunits and stimulates Cohesin's ATPase (Murayama & Uhlmann, 2013; Petela et al., 2018). The underlying mechanism and how this energy is used to achieve Cohesin loading remain controversial, however. But the fact that Cohesin associates with chromatin as a preassembled ring demands its opening at one of the three interfaces. Biochemical and Cryo-EM experiments in *S. pombe* suggest that DNA even has to pass through two interlocking Cohesin gates in order to get loaded (Murayama & Uhlmann, 2015). First, DNA has to pass through a gate between Scc1 and Smc3. This so-called N-gate opens upon binding of ATP to the Smc heads, allows DNA passage and closes as soon as the DNA is trapped in the so called 'gripping state', a narrow channel between Scc2/Nipbl, the Smc heads and the kleisin N-gate. Then, ATP hydrolysis opens the Smc gate, allowing DNA to pass and to become topologically entrapped within the Smc lumen (Marcos-Alcalde et al., 2017; Murayama & Uhlmann, 2015; Yu, 2016). For the unloading reaction, DNA has to pass the same two gates, but in the opposite direction: first the Smc head gate opens upon ATP hydrolysis, releasing the DNA into a ring formed by Scc1 and the Smc's. Rebinding of ATP then leads to engagement of the head domains again, allowing Wapl and Pds5 to disrupt the Scc1-Smc3 interaction, to open the kleisin N-gate and to release the DNA (Beckouët et al., 2016; Murayama & Uhlmann, 2015).

However, this model is challenged by other studies. The findings that fusion of the kleisin subunit to either Smc1 or Smc3 is not lethal and that, instead, artificial ligation of the Smc1-

Smc3 hinge impairs cohesion establishment favors the hinge domain as the entry gate (Buheitel & Stemmann, 2013; Gruber et al., 2006). Supporting biochemical data suggest, that DNA is entrapped in a clamp between Scc2 and the engaged Smc heads without having passed the hinge or Smc3/Scc1 gate. The SMC proteins are in a collapsed configuration, meaning that their hinge domains are bended via their elbow domains to allow contact with DNA and/or head domains. In the next step, DNA downstream of the clamp might pass through the hinge gate to achieve topological entrapment (Collier & Nasmyth, 2022).

Whether DNA passes through the hinge gate or Smc3/Scc1 gate might also depend on the function of the designated Cohesin ring. Cohesin's canonical function is the tethering of replicated sister chromatids in *trans*. In this case, topological entrapment of both sisters probably occurs in a ring build by Smc proteins and Scc1 (SK-ring) (Collier et al., 2020; Collier & Nasmyth, 2022). However, Cohesin also contributes to the organization and compaction of interphase chromatin through mediation of *cis*-contacts between loci on the same DNA molecule. This DNA compaction is achieved by a loop extrusion mechanism, in which repeated ATP hydrolysis leads to threading of the DNA through the ring's lumen (Bauer et al., 2021; Davidson et al., 2019; Kim et al., 2019). In this case, DNA is probably clamped in the 'gripping state' between Scc2, the SMC heads and the kleisin N-gate without being topological loaded (Collier et al., 2020; Davidson et al., 2019). Extruded loops allow the formation of interactions between distant loci and organize chromatin in topologically associated domains (TADs) (Wutz et al., 2017). The loop size is mainly restricted by boundary elements like CTCF, which blocks Cohesin translocation along DNA and loop extrusion (Davidson et al., 2023; Parelho et al., 2008). Thereby, CTCF serves as an anchor for Cohesin, further stabilizing it on chromatin by protecting it against Wapl's releasing activity (Li et al., 2020).

3.3.2 Establishment of sister chromatid cohesion in S-phase

The establishment of sister chromatid cohesion occurs in a co-replicative manner during S-phase (Uhlmann & Nasmyth, 1998) (Fig. 4). In coordination with the passage of the replication fork, both sister chromatids are tethered together by Cohesin. Recent yeast genetic studies suggest two independent mechanisms, namely de-novo loading and the conversion of pre-loaded Cohesin, as being capable for the establishment of cohesion (Srinivasan et al., 2020). De-novo loading behind the fork depends on the Scc2 loader and the CTF18-RFC complex, while the Cohesin conversion depends on Tof1/Csm3, Ctf4 and Chl1. Despite of

being non-essential factors for cohesion establishment, combining mutants from both epistasis groups lead to synthetic lethality or combined sickness (Srinivasan et al., 2020). For the Cohesin conversion, the replication fork would have to pass through the Cohesin ring or alternatively, transfer the ring across the replication fork in order to reassociate with DNA behind it. Irrespective of de-novo loading or Cohesin conversion, the Cohesin ring would have to entrap both sister chromatids behind the replication fork. As hinds are given, that cohesion establishment is coordinated with lagging strand synthesis, a model of sequential Cohesin capture seems to be promising (Murayama et al., 2018; Rudra & Skibbens, 2012). Cohesin might embrace dsDNA after leading strand synthesis in a first step followed by capturing ssDNA from delayed lagging strand synthesis. Cohesion would then be established upon synthesis of the duplex DNA (Rudra & Skibbens, 2012). Another essential step during cohesion establishment is the acetylation of Cohesin through the acetyltransferase Eco1 (Eco1/2 in human) (Hou & Zou, 2005; Ivanov et al., 2002). All Eco family members are localized to the sites of replication through interaction with PCNA, a ring shaped sliding clamp and processivity factor for DNA polymerases (Bender et al., 2020; Moldovan et al., 2006). Eco1 was proven to acetylate the two important lysine residues 112/113 of yeast Smc3 (Lys105/106 in human Smc3) (Rolef Ben-Shahar et al., 2008; Zhang et al., 2008). The site of modification is thought to directly interact with the entrapped DNA and the loader Scc2 (Higashi et al., 2020; Murayama & Uhlmann, 2015). With the lysine residues deacetylated, this interaction enhances ATPase activity of the Smc head domains and leads to the subsequent Wapl-dependent release of the Cohesin ring from DNA. On the contrary, acetylation of the lysine residues counteracts this process and allows establishment of stable cohesion (Beckouët et al., 2016; Çamdere et al., 2015; Murayama & Uhlmann, 2015). Furthermore, Smc acetylation facilitates the recruitment of Sororin, the antagonist of Wapl, to further stabilize Cohesin on chromatin (Nishiyama et al., 2010). The C-terminus of Sororin binds to the SA subunit of the Cohesin ring and serves as an anchor (Wu et al., 2011; Zhang & Pati, 2015). By an N-terminal YSR-sequence, a conserved binding motif shared by Sororin and Wapl, Sororin binds to Pds5 and thereby displaces Wapl (Nishiyama et al., 2010; Ouyang et al., 2016). Pds5 serves as a binding platform for both proteins, Wapl and Sororin, performing negative and positive functions in sister chromatid cohesion. It was further shown to promote Smc3 acetylation by Eco1 and prevent Hos1 mediated deacetylation throughout G2- and M-phase until Separase gets active and cleaves Scc1 (Chan et al., 2013). Importantly, only 40% of Cohesin molecules are converted to this persistent and cohesive form, whereas

60% remain dynamically associated with the chromatin during G2-phase (Ladurner et al., 2016).

3.3.3 M-phase: Cohesin resolution from chromosomes in two waves

During vertebrate M-phase, Cohesin is removed from chromosomes in two waves (Fig. 4). The first wave, the so-called prophase pathway, removes Cohesin from the chromosome arms in a non-proteolytic way upon mitotic entry (Waizenegger et al., 2000). By concerted action of Plk1, Cdk1 and Aurora B, the Cohesin associated subunits Sororin and SA2 get phosphorylated, causing the entire ring to dissociate from chromosome arms (Hauf et al., 2005; Nishiyama et al., 2013; Zhang et al., 2011). The underlying mechanisms remain enigmatic but phosphorylation of Sororin leads to its dissociation and replacement by Wapl (Nishiyama et al., 2010). As these soluble Cohesin rings are not cleaved by Separase at the metaphase-to-anaphase transition, they provide a pool of intact rings that can be loaded again on chromatin in telophase (Sun et al., 2009). Furthermore, removal of Cohesin rings from the chromosome arms might promote deconcatenation by Topoisomerase II and hence contribute to the timely resolution of sister chromatid intertwining (Farcas et al., 2011).

A small pool of Cohesin at the centromeric region of chromosomes is protected from the prophase pathway and mediates sister chromatid cohesion until anaphase onset. This protection is mediated through the 'guardian spirit' shugoshin 1 (Sgo1) by recruiting the PP2A phosphatase to the centromeric region (Kitajima et al., 2006; Liu et al., 2013; Tang et al., 2006). Here, PP2A keeps Sororin and SA2 in a dephosphorylated state, thus counteracting the activity of mitotic kinases and Wapl (McGuinness et al., 2005). When all kinetochores are stably bound by the mitotic spindle, the SAC is silenced and the MCC disassembles. Freed Cdc20 activates the APC/C, which in turn liberates Separase by targeted destruction of its inhibitors. As already mentioned, Separase is normally kept inactive by association with Securin (Ciosk et al., 1998). Securin binds to the catalytic site of Separase with a motif that partly matches the consensus cleavage site, thereby acting as a pseudosubstrate (Lin et al., 2016; Luo & Tong, 2017). Another inhibitor of Separase is Cdk1-Cyclin B1 (Stemmann et al., 2001). Formation of this complex requires initial phosphorylation of Separase at Ser1126 by Cdk1. As a consequence, Separase undergoes conformational changes in a *cis/trans*-isomerization of the proline residue at position 1127. This process is catalyzed by the peptidyl-prolyl isomerase (PPIase) Pin1. Separase in its *trans*-conformation then facilitates binding and inhibition by Cdk1-Cyclin B1 but renders itself insensitive for repeated binding

of Securin. At the same time, Separase becomes more aggregation-prone, thereby setting the timer for a well-directed and contemporary inactivation of Separase (Hellmuth et al., 2015). A third competitive inhibitor of Separase is Sgo2, which inhibits Separase in a Securin-like manner as a pseudosubstrate. It does so in complex with Mad2 in its closed configuration, providing a direct link and supervision between the SAC and Separase inhibition. Upon SAC inactivation, Separase is liberated from Sgo2-Mad2 through activity of the AAA-ATPase TRIP13 and p31^{comet} (Hellmuth et al., 2020).

During the narrow time window of anaphase onset, Separase efficiently cleaves the remaining pool of centromeric Cohesin rings, thereby allowing the separation of sister chromatids (Uhlmann et al., 1999). The efficiency of Scc1 cleavage is increased by phosphorylation of several residues in the vicinity of the Separase cleavage site, thereby turning the kleisin into a better substrate (Alexandru et al., 2001). In general, Separase preferentially cleaves phosphorylated over non-phosphorylated and chromatin bound over soluble pools of Scc1 (Hornig & Uhlmann, 2004).

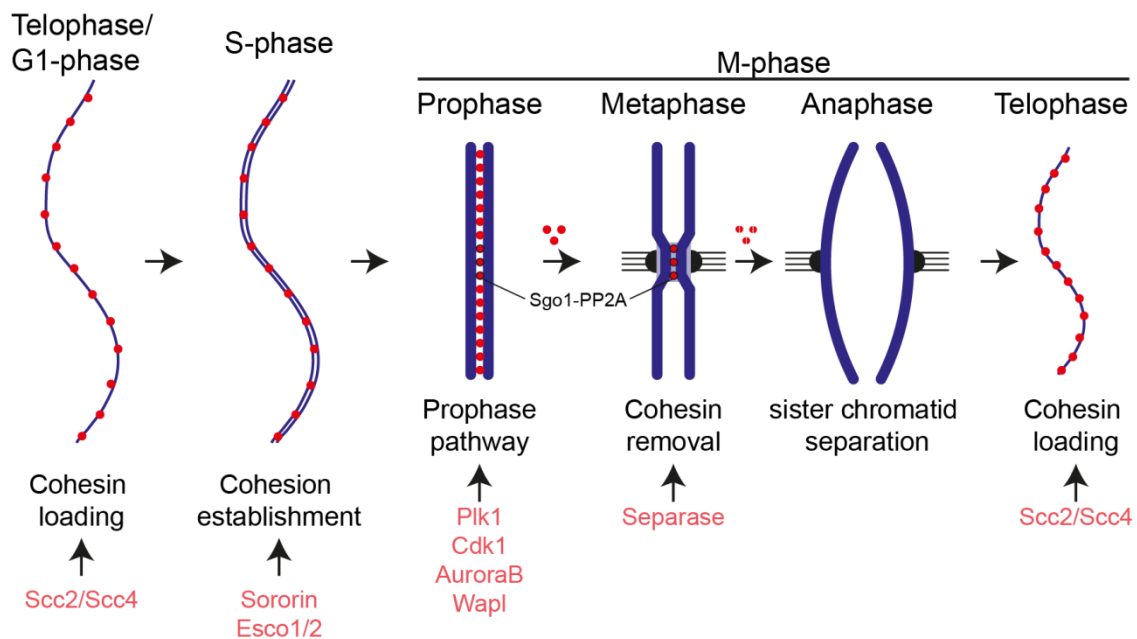


Fig. 4: The cohesin cycle. The Scc2/Scc4 dependent loading of cohesin occurs in late telophase. Throughout G1-phase, cohesin remains dynamic as it is constantly loaded and released from chromatin. During S-phase, cohesion is established through acetylation by Esco1/2 of the Smc3 subunit and subsequent binding of Sororin. In M-phase, cohesin removal occurs in two waves: 1) In prophase, the bulk of cohesin gets phosphorylated by mitotic kinases like Plk1, Cdk1 and Aurora B and dissociates from chromatin through the releasing activity of Wapl. 2) Separase cleaves the remaining centromeric cohesin rings which allows the sister chromatid separation in anaphase. In telophase, cohesin gets loaded onto chromatin and the cycle starts over again.

3.3.4 Cohesin associated syndromes: Cohesinopathies

As expected from Cohesin's importance in the depicted processes, mutations in Cohesin subunits are linked to severe diseases collectively described as Cohesinopathies. These include the Cornelia de Lange Syndrome (CdLS), Roberts Syndrome (RBS) and the Warsaw Breakage Syndrome (WBS). Overlapping phenotypes are, amongst others, mental retardation, small body stature and developmental delay (Banerji et al., 2017; Liu & Krantz, 2008). CdLS arises mainly from mutations in the Cohesin loader *Scc2*, but mild forms are also linked to mutations in *Smc1*, *Smc3* and histone deacetylase 8 (HDAC8) (Deardorff et al., 2007, 2012; Krantz et al., 2004; Pehlivan et al., 2012). However, CdLS patients do not suffer from premature sister chromatid separation (SCS), but rather from defects in *cis*-DNA tethering (Krantz et al., 2004). Patients with RBS mainly exhibit mutations in the acetyltransferase *Esco2*, partly abolishing the establishment of cohesive Cohesin, which in turn triggers premature SCS (Vega et al., 2005). WBS originates from mutations in the DNA helicase *DDX11/ChlR1*, leading to reduced level of the Cohesin loader *Scc2* and Cohesin itself by a yet poorly understood mechanism (Rudra & Skibbens, 2013; van der Lelij et al., 2010).

3.4 Microtubule organizing center, spindle pole bodies and centrosomes

Microtubules (MTs) are tubular polymers with an outer diameter of 25 nm and lengths of up to several micrometers. They are composed of $\alpha\beta$ -tubulin heterodimers that are arranged into a head-to-tail fashion and polymerize into linear protofilaments (Kollman et al., 2011). In mammals, 13 of these protofilaments oligomerize laterally to form a hollow cylinder (Tilney et al., 1973). As part of the cytoskeleton, microtubules contribute to the cellular structure and provide tracks for intracellular transport. Many of its functions depend on fast reorganization and hence the microtubule cytoskeleton is remarkably dynamic. The end of the microtubule exposing β -tubulin is capable of rapid growth or shrinkage caused by addition or loss of $\alpha\beta$ -tubulin dimers and termed the plus end. On the other hand, the end exposing α -tubulin is rather stable with a low growth or shrinkage rate and termed minus end (Roostalu & Surrey, 2017). The alteration of individual MTs between periods of growth and shrinkage is termed dynamic instability (Mitchison & Kirschner, 1984). The transition from growth to shrinkage is called catastrophe and is thought to be caused by loss of the so called 'GTP-cap', the end of a polymerizing microtubule, where GTP hydrolysis has not yet occurred. On the contrary, gain of a GTP cap is thought to reverse the process into growth and is called rescue (Bayley et

al., 1989; Brouhard & Sept, 2012). In mitosis, the frequency of catastrophe events increases, while the frequency of rescue events decreases. As a result, mitotic MTs are shorter compared to interphase MTs but become highly dynamic (Brun et al., 2009; Margolin et al., 2012). Microtubules polymerize spontaneously *in vitro* when a critical concentration of tubulin dimers is exceeded and Mg^{2+} and GTP are present (Voter & Erickson, 1984). However, in cells a nucleation factor is needed for efficient initiation of polymerization. In higher eukaryotes, the multi-subunit γ -tubulin ring complex (γ -TuRC) caps the minus end and serves as a template for microtubule nucleation (Zheng et al., 1995). These γ -TuRCs cluster at specific sites *in vivo* which are termed the microtubule organizing centers (MTOCs). MTOCs in turn are responsible for the stability of the microtubules as well as for recruitment of components for their *de novo* nucleation (Wu & Akhmanova, 2017). Since the first description of MTOCs in the late 1880s by Boveri and van Beneden (reviewed in (Scheer, 2014)), it took 70 more years and the method of electron microscopy to gain further insights into their structure and function (Amano, 1957; Ruthmann, 1959). Two of the most widely studied MTOCs today are the spindle pole bodies (SPB) in yeast and the centrosomes in animal cells.

Due to the closed mitosis in yeast, the SPBs are multilayered structures that are permanently embedded in the nuclear envelope (in case of *S. cerevisiae*) or get incorporated into the nuclear envelope upon entry into mitosis (in case of *S. pombe*) (Ding et al., 1997; Moens & Rapport, 1971). The SPB in budding yeast is well characterized and composed of 18 different proteins which organize both the nuclear and cytoplasmic microtubules (Cavanaugh & Jaspersen, 2017; Keck et al., 2011). The MTOC in animal cells is the centrosome. It is 1-2 μ m in diameter and composed of two centrioles (see below) in orthogonal orientation surrounded by a proteinaceous pericentriolar matrix (PCM). Beside its function in organizing microtubule nucleation, the centrosome is important for regulation of cell polarity, cellular transport, formation of cilia and flagella, cell cycle progression and DNA damage response (Cuschieri et al., 2007; Dawe et al., 2006; Mullee & Morrison, 2016; Tang & Marshall, 2012). Interestingly, higher plant cells contain no centrosomes but efficiently initiate microtubule nucleation on the nuclear envelope in prophase. After nuclear breakdown, the so called prospindle is formed by bipolarization (Brown & Lemmon, 2011; B. Liu & Lee, 2022). Oocytes in metazoans also lack centrosomes and nucleate their microtubules in centrosome-independent pathways like the Ran-GTP-, the chromosomal passenger complex (CPC)- or the Augmin-dependent pathway (Bennabi et al., 2016). The same pathways become relevant when centrosomes are removed from tissue culture cells by laser ablation or microsurgery as

well as in a centrosome-free *Xenopus laevis* extract where a bipolar spindle can assemble after addition of artificial chromosomes (Heald et al., 1996, 1997). These findings indicate that centrosomes are not essential for spindle assembly if only considering the following mitosis after centrosome depletion. However, permanent loss of centrosomes triggers chromosomal instability and aneuploidy in animal cells, pointing out the importance of centrosomes for a high fidelity in chromosome segregation over several cell cycles (Badano et al., 2005; Cosenza & Krämer, 2016; Sir et al., 2013).

3.5 The centrosome architecture and functions

Since the first description as tiny dot-like structures on microscope slides, MTOCs have been widely studied, revealing more of their function and architecture (Scheer, 2014). However, for further knowledge about complex structures like the amorphous PCM, it was essential to gain more information about the protein composition of the centrosome. Hence, large-scale isolation of centrosomes from different species combined with mass-spectrometry-based proteomic analysis was used and revealed more than 160 proteins as centrosomal (Andersen et al., 2003; Jakobsen et al., 2011; Müller et al., 2010). Putative protein candidates were verified in microscopy-based screens by co-localization with centrosomal markers as well as functional analyses using RNA interference (RNAi) (Andersen et al., 2003; Jakobsen et al., 2011; Müller et al., 2010). Together with these confirmed proteins, further putative proteins can be found in the database Centrosome:db. So far, more than 1000 human or fly genes are considered to encode for centrosomal proteins (Alves-Cruzeiro et al., 2014). In another study, 58 of these centrosomal proteins were used as baits in a proximity biotinylation (BioID) assay in order to generate a protein topology network. Over 7000 protein interactions at the centrosome were revealed that way (Gupta et al., 2015). Future challenges will be to further characterize centrosomal proteins in terms of their function and to understand their interaction and dynamics in dependency of particular cell cycle stages.

3.5.1 Centrioles

As mentioned above, the centrosome consists of two centrioles oriented perpendicularly to each other (Fig. 5). Each cylindrical centriole is 400-500 nm long and has a diameter of 200-250 nm (Wheatley, 1982). The centriole wall is composed of nine microtubule triplets which

are arranged around a cartwheel structure (Azimzadeh & Marshall, 2010). Each triplet contains a complete A-tubule and incomplete B- and C-tubules (Dippell, 1968). The A-tubule is oriented towards the center of the centriole and capped by a γ -TuRC complex at the proximal end (Guichard et al., 2010). The incomplete B- and C-tubules are attached to the wall of the A- or B-tubule, respectively. They are nucleated by bidirectional growth without γ -TuRC and by the time all three tubules reach their final stage of extension, the γ -TuRC from the A-tubule is removed as well (Guichard et al., 2010). Linker between the A- and C-tubule of two adjacent triplets contribute to the stability of the centriole (Li et al., 2019). Additionally, multiple post-translational modifications (PTM) like polyglutamylation, acetylation and the removal of the terminal two amino acids of α -tubulin ($\Delta 2$ -tubulin) enhance the stability of the microtubule triplets (Gundersen et al., 1987; Hirono, 2014; Paturle-Lafanechère et al., 1994; Thomas et al., 2004).

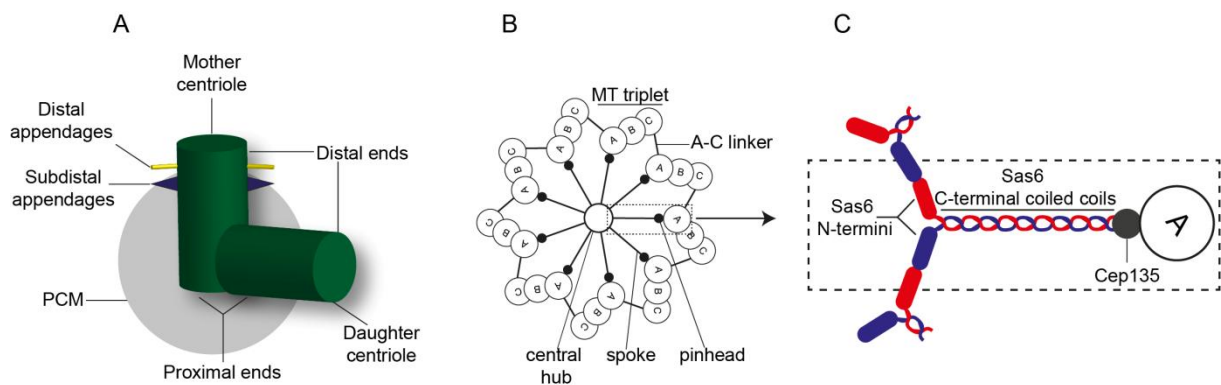


Fig. 5: The centrosome architecture. (A) Schematic view of the centrosome, which contains two orthogonally-arranged centrioles. The older mother centriole is decorated by distal and subdistal appendages. The centrioles are surrounded by a proteinaceous pericentriolar matrix (PCM) mediating the microtubule (MT) nucleation capacity. (B) Cross-section of a centriole depicting the nine-fold symmetry. Each centriole is composed of nine MT triplets arranged around a cartwheel structure. This cartwheel is composed of a central hub from which nine spokes emanate radially. The pinheads mediate the contact with the MT triplets. Two adjacent triplets are connected by an A-C linker (C) A more detailed model of the central hub, spoke and pinhead. SAS6 dimerizes via its N-terminal globular domains and its C-terminal coiled coils. Nine SAS6 dimers oligomerize to build the cartwheel structure. Cep135 serves as a pinhead and extension of the spoke, mediating contact to the A-tubule of the MT triplet.

The cartwheel is located at the proximal end of centrioles where it determines the symmetry of the newly formed procentriole and contributes to its stability. It is composed of a central hub from which nine spokes radiate towards the microtubule triplets. Each spoke is capped by a pinhead which mediates the contact with the A-tubule (Hirono, 2014). Scientists were speculating for a long time why a newly formed centriole adopts a nine-fold symmetry during the duplication cycle (Strnad & Gönczy, 2008). Elegant biophysical and structural work established SAS6 (spindle assembly abnormal protein 6 homolog), one of the key components

of the cartwheel structure, to be important for the symmetry (Kitagawa et al., 2011; van Breugel et al., 2011). Proteins of the SAS6 family are composed of an N-terminal globular domain and a C-terminal coiled coil domain. *In vitro*, the purified SAS6 ortholog Bld12 from *C. reinhardtii* is building homo-oligomers via its N-globular domain. The central hub with a diameter of approximately 20 nm is built by the oligomerization of nine Bld12 N-terminal dimers (Kitagawa et al., 2011). The C-terminal coiled coil dimers are emanating radially and thus forming the spokes of the cartwheel structure. RNAi-mediated knockdown of SAS6 in *Paramecium* and *SAS6* gene knockout in *Drosophila* or *Tetrahymena* results in variable number of triplets, underlining the importance of SAS6 in determining the nine-fold centriole symmetry (Culver et al., 2009; Rodrigues-Martins et al., 2007). Another key component is human Cep135 (Bld10 in *Drosophila*, *Chlamydomonas* and *Paramecium*) which constitutes the pinhead structure and the distal part of the spoke (Fig. 5C). The N-terminus of Cep135 was shown to directly bind to microtubules, whereas the C-terminus interacts with the SAS6 spokes and contributes to their elongation. C-terminally truncated versions of Bld10 result in shorter spokes and centrioles with an eight-fold symmetry (Carvalho-Santos et al., 2012; Hiraki et al., 2007). Usually, there are multiple layers of cartwheels within one centriole, filling up between 10-90% of the proximal lumen (Geimer & Melkonian, 2004; Gibbons & Grimstone, 1960). In mammalian centrosomes, the cartwheel is present in the procentriole, but not detectable at the end of mitosis and throughout G1-phase (Alvey, 1986; Paintrand et al., 1992).

The two centrioles of one centrosome are different in age and structure and therefore termed mother and daughter centriole. The mother centriole possesses two types of appendages at its distal end: distal (DAP) and subdistal (SAP) appendages (Hall & Hehnlly, 2021; Ma et al., 2023; Uzbekov & Alieva, 2018). When a cell exits the cell cycle and arrests in a quiescent state (termed G₀), the mother centriole migrates and attaches, via its distal appendages, to the plasma membrane (Tanos et al., 2013). In a process called ciliogenesis, the mother centriole converts to a basal body which allows the recruitment of factors important for the primary cilium formation (Choksi et al., 2014; Vertii et al., 2016). The subdistal appendages are important for anchoring of microtubules to structures other than the plasma membrane (Uzbekov & Alieva, 2018; Vertii et al., 2016).

3.5.2 The pericentriolar matrix (PCM)

In contrast to the highly ordered centrioles, the surrounding PCM was traditionally described as an amorphous, electron dense material. Its main function is the anchorage and nucleation of microtubules. The key components in these processes can be distinguished in structural and regulatory proteins (Woodruff et al., 2014). Structural proteins provide a scaffold and often contain coiled coil domains for protein-protein interactions (Salisbury, 2003). Recent improvements in microscopy methods like three-dimensional structured illumination (3D-SIM), stochastic optical reconstruction microscopy (STORM) and stimulated emission depletion (STED) enable up to ten times higher resolutions and hence deeper structural insights into the PCM organization. In 2012, four contemporary studies used 3D-SIM and STORM to spot the localization of several individual proteins and revealed a highly ordered structure of the PCM (Fu & Glover, 2012; Lawo et al., 2012; Mennella et al., 2012; Sonnen et al., 2012). Especially the interphase PCM shows a highly organized layer around the centriole wall. Structural components like Pericentrin (PCNT, PLP in *D. melanogaster*) and Cep152 (Asl in *D. melanogaster*) form elongated fibers that extend radially from the centriole wall. In contrast, components like Cep215 (Cnn in *D. melanogaster*), Cep192 (SPD-2 in *D. melanogaster*) and γ -tubulin are homogenously dispersed around the centriole, adopting a matrix that is anchored by the structural fibers (Lawo et al., 2012; Mennella et al., 2012). While animal cells approach and finally enter mitosis, the centrosome undergoes a process called maturation. The PCM accumulates more components important for microtubule nucleation, like the γ -TuRC, and increases its size up to five-fold compared to the interphase level. Notably, the localization pattern of the aforementioned proteins is less ordered and without discrete distributions in this outer centrosomal layer (Mennella et al., 2014).

Pericentrin

Pericentrin (PCNT) was first described by Stephen Doxsey and the Marc Kirschner group in 1994 (Doxsey et al., 1994). They discovered that a serum from a patient suffering from an autoimmune disease (scleroderma) efficiently stained centrosomes from plants to human. In order to identify the apparently conserved antigen(s), they performed a screening using a mouse expression library. The corresponding 220 kDa protein identified in mouse was named Pericentrin and was predicted to be a large and elongated coiled coil protein (Doxsey et al., 1994). Several years later, a 350 kDa protein was identified as the human ortholog and named Pericentrin B (PCNTB) or Kendrin. It is characterized by non-helical N- and C-termini and several central coiled coil regions (Chen et al., 1996; Li et al., 2001). The C-terminus contains

a so-called PACT domain which mediates recruitment to the centrosome (Gillingham & Munro, 2000). During recruitment, PCNT is transported together with γ -tubulin as a dynein cargo along microtubules to the centrosome (Young et al., 2000). An alternatively spliced version lacking the C-terminus and hence the PACT domain was identified as well and termed PCNTA (Doxsey et al., 1994; Flory & Davis, 2003; Lee & Rhee, 2011; Li et al., 2001). Additionally, an even shorter PCNTB isoform lacking the N-terminus was discovered in mice and flies (Martinez-Campos et al., 2004; Miyoshi et al., 2006). The functional differences of these isoforms remain to be determined, but as ectopic expression of PCNTB rescues the mitotic phenotypes of simultaneous PCNTA/B knockdown (Lee & Rhee, 2011), the B isoform seems to be of major importance for the centrosome biology and is henceforth termed PCNT.

Numerous PCNT interacting partners have been identified so far, reaching from kinases (e.g. Chk1, PKA or BCR-ABL), proteins involved in cilia formation and function (like IFT and PC2) or even nuclear proteins (like CHD3 and CHD4) (Delaval & Doxsey, 2010). Noteworthy among these interacting partners is Chk1 kinase which gets anchored at centrosomes by PCNT upon DNA damage. There, Chk1 kinase induces a signal cascade prohibiting mitotic entry, thus linking PCNT to the DNA damage response and indirectly to cell cycle control (Krämer et al., 2004; Tibelius et al., 2009). However, the best studied PCNT function is to serve as the main centrosomal scaffold that anchors proteins important for microtubule nucleation activity, like Cep215, γ -tubulin, CG-Nap, PCM1 and γ -TuRC (Buchman et al., 2010; Li et al., 2001; Takahashi et al., 2002; Zimmerman et al., 2004). Antibody staining of the N- and C-terminal domains revealed that the PCNT C-terminus is located next to the centriole wall whereas the N-terminus projects outwards and into the PCM (Lawo et al., 2012). Cep215 binds to a central region of PCNT via its very C-terminus, with both proteins adopting a hook-like structure that organizes the centriole matrix. The N-terminus of Cep215 mediates binding to the γ -TuRC suggesting that it serves as a bridge between PCNT and the γ -TuRC (Buchman et al., 2010). Interestingly, the *Drosophila* ortholog Plp seems to be dispensable for mitosis (Martinez-Campos et al., 2004) which is consistent with the observation that flies lacking centrosomes can still develop normally (Basto et al., 2006). Alterations in the human PCNT level, on the contrary, lead to severe phenotypes. Knockdown of PCNT results in smaller mitotic spindles or even monopolar spindles which come along with decreased microtubule nucleation capacity and mitotic delay (Wang et al., 2013). Especially the reduced levels of astral MTs lead to severe defects in spindle positioning (Tang & Marshall, 2012; Zimmerman et al., 2004). In contrast,

overexpression of PCNT induces formation of large PCM clouds. Hyper-recruitment of several centrosomal proteins then facilitates overduplication resulting in numerous centrioles which are not attached to the wall of the mother centriole but randomly oriented within the cloud (Loncarek et al., 2008).

Germline mutations in the *PCNT* gene are also linked to the autosomal recessive disorder microcephalic osteodysplastic primordial dwarfism type II (MOPDII). Patients suffer from small brain size (microcephaly) and short body stature (Delaval & Doxsey, 2010; Klingseisen & Jackson, 2011). Mutational analysis revealed splice site mutations as well as insertions and deletions. Among them, truncated PCNT versions which lack their C-terminal PACT domain are unable to localize to centrosomes, inducing the same severe phenotypes as described above for PCNT knockdown (Rauch et al., 2008).

γ -tubulin ring complexes (γ -TuRC) and the assembly of the mitotic spindle

In most cell types, assembly of the mitotic spindle is accomplished by the centrosome. Three different kinds of microtubules emanate from the centrosome: 1) astral microtubules make contact with the cortical protein machinery mediating the correct spindle position and orientation by exerting pulling forces; 2) polar microtubules from opposing centrosomes are not connected to kinetochores and overlap in the central region, thereby generating pushing forces; 3) kinetochore microtubules mediate a proper kinetochore-spindle connection. According to the 'search and capture' model, microtubules get in contact with kinetochores and become stabilized (Wittmann et al., 2001).

Microtubule nucleation is mainly conducted by the 2 MDa γ -tubulin-ring complex (γ -TuRC) which is composed of seven different subunits (γ -tubulin, GCP2-6 and the recruiting factor GCP-WD/NEDD1) (Sulimenko et al., 2017). Two γ -tubulins, one GCP2 and one GCP3 assemble to the tetrameric γ -tubulin small complex (γ -TuSC) (Oegema et al., 1999). This complex adopts a V-shaped structure with GCP2 and GCP3 building the arms and γ -tubulin building the tip (Kollman et al., 2008). Immunoprecipitation (IP) experiments have shown that statistically, six to seven γ -TuSC oligomerize with two to three GCP4, one GCP5 and one GCP6 to build a ring-like structure with a helical turn, the γ -tubulin-ring complex (γ -TuRC) (Kollman et al., 2011). This assembly creates the characteristic 13-fold microtubule symmetry (Kollman et al., 2010). The γ -TuRC complex is anchored at the centrosome by several structural/scaffolding components, like PCNT, CG-Nap, ninein, Cep192 and Cep215. Beside this attachment, some of these proteins even have an enhancing effect on the nucleation activity of γ -TuRCs (Choi et al., 2010; Delgehyr et al., 2005; Takahashi et al., 2002).

Given the great distance between centrosomes and kinetochores as well as the increased dynamic instability of microtubules, the probability of capturing all kinetochores during the narrow time window of spindle assembly in mitosis is almost zero (Wollman et al., 2005). As a consequence, MTs additionally have to be nucleated by non-centrosomal pathways, especially in the vicinity of chromosomes. One pathway is mediated by the small GTPase Ran. The GTP-bound form of Ran is generated by the nucleotide exchange factor RCC1 which is ubiquitously bound to chromatin, leading to local elevated activity of the Ran pathway (Carazo-Salas et al., 1999). Microtubule growth is thereby stimulated, as activated Ran increases the frequency of rescue events and enhances the activity of motor proteins and hence cargo transport towards the plus end of MTs (Margolin et al., 2012).

Additionally, at the kinetochores, the chromosomal passenger complex (CPC) consisting of Aurora B and its regulator INCENP, Borealin and Survivin, promotes spindle assembly (Carmena et al., 2012; Sampath et al., 2004). The CPC phosphorylates and thereby suppresses activity of the MT-depolymerizing kinesin MCAK and the stimulator of MT-plus end catastrophes stathmin (Andrews et al., 2004; Cassimeris, 2002; Zhang et al., 2007). Taken together, Ran and CPC mediated pathways cooperatively enrich MT nucleation capacity in the vicinity of chromatin. Another pathway is based on MT nucleation within the spindle itself. In plants, MTs branch off from preexisting ones in a well-defined 40° angle, whereas in yeast, MTs nucleate in an antiparallel manner (Chan et al., 2009; Janson et al., 2005; Murata et al., 2005). Apart from these mentioned pathways for mitotic spindle formation, MTs can also be nucleated by the nuclear membrane and the Golgi apparatus in interphase cells. This seems to be particularly important for specific cell types like skeletal muscle cells (Bugnard et al., 2005; Zhu & Kaverina, 2013).

3.6 The centrosome cycle and its coordination with the cell cycle

The centrosome and chromosome cycle have remarkable similarities with respect to their timing and regulation within the cell cycle. Centriole and chromosome duplication both start at the S-phase transition and occur in a semi-conservative manner, meaning that the older centrioles/chromosomes serve as a foundation for the synthesis of new ones. Coupling of the centrosome with the cell cycle ensures that duplication occurs only once in every cell cycle. Additionally, the copy number is tightly controlled, so that exactly one new daughter centriole is formed adjacent to the mother centriole (Delattre & Gönczy, 2004). Elegant mammalian cell fusion experiments shed light on the underlying regulatory mechanisms. Fusion of G1-phase centrosomes with S-phase cells induced duplication of both, suggesting that G1 centrosomes are already 'licensed'. On the contrary, fusing G2-phase centrosomes with S- or even G1-phase cells would only trigger duplication of the corresponding S- or G1-phase organelles, indicating an intrinsic block of reduplication (Wong & Stearns, 2003). Further studies then revealed that this intrinsic block depends on the physical proximity of the newly formed daughter and the older mother centriole. Reduplication is inhibited as long as they are tightly coupled and hence in an 'engaged status' (Tsou & Stearns, 2006). The licensing for duplication occurs in mitosis by the concerted action of Plk1 and Separase (Tsou et al., 2009; Tsou & Stearns, 2006). Upon entry into mitosis, Plk1 phosphorylation initiates hyper-recruitment of proteins important for the nucleation of microtubules. This so-called PCM maturation not only allows the formation of the bipolar mitotic spindle, but also provides the competence for duplication in the next S-phase (Woodruff et al., 2014). Furthermore, Separase needs to cleave its centrosomal substrates Cohesin and PCNT in late mitosis which leads to the spatial separation of the two daughter centrioles and hence disengagement (see Fig. 6) (Lee & Rhee, 2012; Matsuo et al., 2012; Schöckel et al., 2011; Tsou et al., 2009). This physical detachment is the most important step in licensing, explaining the intrinsic block of reduplication of G2-phase centrosomes in the cell fusion experiments (Wong & Stearns, 2003).

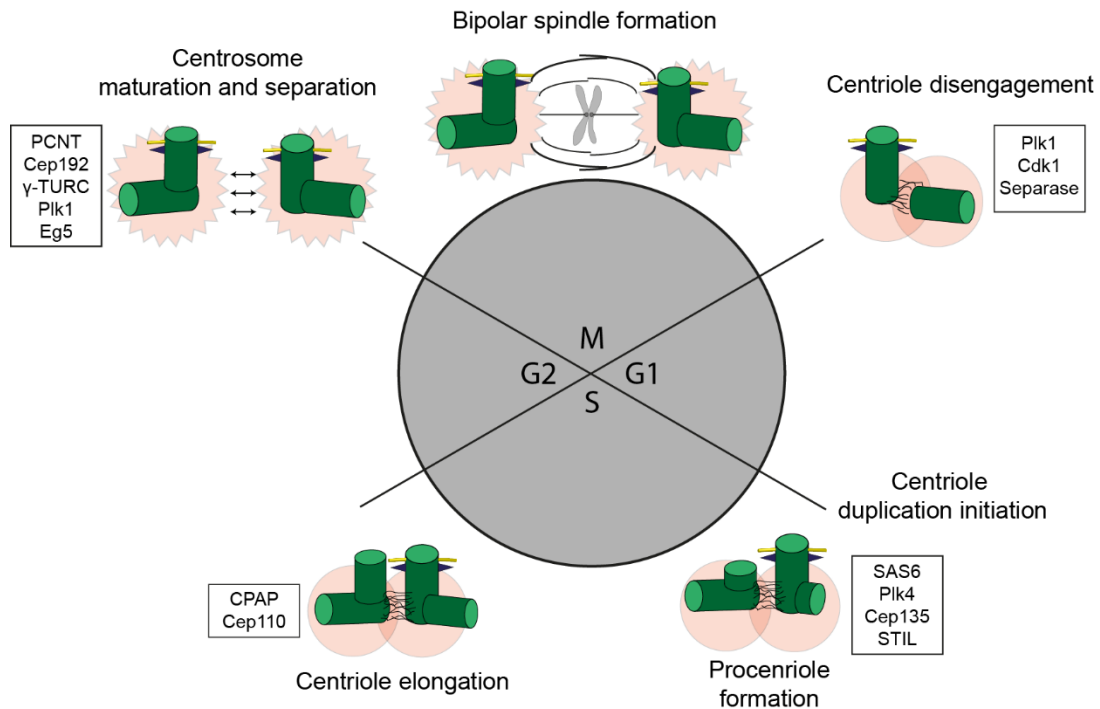


Fig. 6: The centrosome duplication cycle. Cells enter G1-phase with disengaged and hence licensed centrioles. At the G1/S-transition, centriole duplication is initiated. One procentriole per mother-centriole is formed and elongates throughout S- and G2-phase. Upon entry into mitosis, maturation of the pericentriolar matrix (PCM) occurs and the two centrosomes become separated in order to build the bipolar spindle. Activation of Separase at the metaphase-to-anaphase transition leads to cleavage of its centrosomal substrates cohesin and PCNT which in turn triggers disengagement. Essential proteins for the corresponding step in the centrosome cycle are depicted in the boxes and explained in the text.

3.6.1 Procentriole formation and centriole elongation

The regulatory mechanism that ensures the formation of exactly one daughter centriole on a radially symmetric surface remained unclear for a long time. Independent studies favor Plk4 to be the master regulator of centriole duplication (Bettencourt-Dias et al., 2005; Habedanck et al., 2005). Plk4 overexpression induces centrosome amplification, while inhibition prevents new centriole assembly (Bettencourt-Dias et al., 2005; Coelho et al., 2015). Plk4 exhibits a bimodal distribution around the centriole, showing a ring-like pattern in G1-phase which changes to a dot-like localization upon G1/S-phase transition (Sonnen et al., 2012). Initial Plk4 recruitment in G1-phase was shown to depend on the concerted action of Cep152 and Cep192. Cep192 shows a ring-like distribution around the centriole and initially recruits Plk4 to the centriole. Upon Cep152 recruitment, Plk4 translocates outwards to the newly formed Cep152 ring, arguing for a unidirectional scaffold switch (Kim et al., 2013; Sonnen et al., 2013). This translocation is achieved by a stronger affinity of Cep152 to the same negatively charged binding region within Plk4 that Cep192 is already bound to (Park et al., 2014). Plk4 is likely to be inactive in G1-phase due to autoinhibition of the kinase domain by its own L1

linker (Klebba et al., 2015). In addition to Plk4, STIL (SCL/TAL1 interrupting locus protein) and SAS6 are key components in initiating centriole duplication (Fig. 6) (Arquint & Nigg, 2016). Upon entry into S-phase both proteins start to accumulate due to inactivation of APC/C^{Cdh1} (Strnad et al., 2007). STIL was shown to directly associate with Plk4 and together they build a scaffold for SAS6 binding (Ohta et al., 2014). In a speculative model, local Plk4 activity might spread around the entire Plk4 ring by autophosphorylation. Homodimers of active Plk4 would then *trans*-phosphorylate their degrons followed by SCF-dependent degradation. Under such circumstances, STIL would not only have to activate Plk4 but also protect it from degradation to allow the observed dot-like concentration of Plk4. Alternatively, Plk4 might just move around the centriole to get enriched at the point of procentriole formation (Arquint et al., 2015; Moyer et al., 2015; Ohta et al., 2014). Plk4 phosphorylates STIL in its STAN domain, thereby facilitating binding of SAS6 and the initial formation of the cartwheel structure with its nine-fold symmetry (Kratz et al., 2015). The process of centriole elongation is much less understood, but CPAP and Cep110 were proven to be essential factors (Schmidt et al., 2009). CPAP is recruited to the Plk4/STIL/SAS6 platform and facilitates microtubule nucleation through its intrinsic tubulin dimer binding capacity (Tang et al., 2009). Once the nine MT triplets are built and start to elongate, Cep110 binds to the growing distal tip. There, it controls MT length through association with the kinesin Kif24 which in turn depolymerizes MTs (Kobayashi et al., 2011). The daughter centrioles elongate throughout S- and G2-phase, however, they are not reaching their full length until entry into M-phase (Cunha-Ferreira et al., 2009).

3.6.2 Centrosome maturation

Centrosome maturation takes place in late G2 and early mitosis and is characterized by an increase in size and MT nucleation competence of the PCM (Fig. 6) (Firat-Karalar & Stearns, 2014). This process is initiated by increasing activities of Plk1 and Aurora A at the end of G2-phase and further involves the same set of proteins that already built the highly ordered proximal PCM layer during interphase. These key components assemble and multimerize in the outer PCM but adopt a strikingly less ordered conformation compared to interphase (Firat-Karalar & Stearns, 2014; Mennella et al., 2014; Sonnen et al., 2012). One major target for Plk1 is PCNT, whose phosphorylation initiates centrosome maturation and allows recruitment of further PCM components like Cep192 and the γ -TuRC (Lee & Rhee, 2011). Cep215 recruitment is independent from PCNT, whereas their centrosomal interaction is essential for

efficient γ -TuRC anchoring (Kim & Rhee, 2014). Further Plk1 substrates like Cep192 and the γ -TuRC recruiting factor GCP-DW/NEDD1 are sequentially phosphorylated, with Aurora A and Cdk1 acting as priming kinases (Joukov et al., 2014; Zhang et al., 2009).

Another important Plk1 function at the beginning of mitosis is the centriole-to-centrosome conversion (Fu & Glover, 2016; Wang et al., 2011). Daughter centrioles hardly contribute to PCM recruitment from the time of their duplication in S-phase until entry into mitosis (Wang et al., 2011). Upon entry in mitosis, the daughter centriole is somehow modified by Plk1, thereby achieving the ability of PCM assembly and the competence to duplicate during the following interphase (Wang et al., 2011). Overexpression of several PCM components leads to formation of extra daughter centrioles emanating from the mother, while no formation of granddaughters from the daughter centrioles could be observed. This again illustrates their lacking ability of individual PCM assembly and hence duplication competence (Peel et al., 2007).

3.6.3 Centrosome separation and centriole disengagement

When vertebrate cells enter mitosis, the two centrosomes are connected through a proteinaceous linker (also called G1-G2 linker) that is composed of C-Nap1/rootletin fibers and several associated proteins like Cep68 and centlein (Bahe et al., 2005; Fang et al., 2014; Graser et al., 2007; Paintrand et al., 1992). The linker function during interphase remains unclear, but it is dissolved by Nek2A activity upon entry into mitosis and allows the separation of the centrosomes in order to build the bipolar spindle (Faragher & Fry, 2003). The centrosomes are spatially separated by pushing forces generated by MT-dependent motor proteins (Panic et al., 2015) (Fig. 6). The plus end-directed motor protein Eg5 is essential and its localization and activation is under control of Plk1 and Cdk1 (Smith et al., 2011). The linker reassembly occurs at the end of mitosis (Mayor et al., 2000).

Apart from the G1-G2 linker connecting the centrosomes, the two centrioles of each centrosome are connected by a linker as well (also called the S-M linker). This linker is established during the procentriole formation in S-phase and lasts until the end of mitosis when it is dissolved again (Firat-Karalar & Stearns, 2014). The spatial separation of the two centrioles is termed centriole disengagement and builds the main licensing step for the centriole duplication in the following S-phase (Mardin & Schiebel, 2012). The composition of this linker is not well characterized and rather complex as it is seemingly not composed of a proteinaceous linker *per se*. Instead, a matrix entrapment of the centrioles mediated by

numerous factors of the PCM seems to be the most promising model (Sluder, 2013). Supportive data came from a laser ablation study in which a mother centriole with two duplicated daughter centrioles was ablated. The movement of the daughters remained coordinated under these circumstances, strongly arguing for a matrix entrapment (Loncarek et al., 2008).

One key protein in the process of centriole disengagement is the protease Separase. In a first study, engaged centrosomes isolated from S-phase-arrested HeLa cells were incubated in a metaphase II-arrested *Xenopus laevis* egg extract. Upon release, centriole disengagement became detectable at late mitosis/early G1-phase. If the extract was supplemented with recombinant and non-degradable Separase inhibitor Securin, centriole disengagement (as well as sister chromatid separation) was blocked (Tsou & Stearns, 2006). This experiment underlined the fundamental role of Separase activity in mentioned processes and suggested that both, centrioles and chromosomes, are held together by Separase substrates. Since then, several independent studies identified Cohesin subunits at the centrosome, suggesting conserved mechanisms between mediation of sister chromatid cohesion and centriole engagement (Giménez-Abián et al., 2010; Gregson et al., 2001; Kong et al., 2009; Wong, 2010; Wong & Blobel, 2008). Indeed, either replacement of endogenous Scc1 or Smc1 with artificially cleavable versions led to disengagement upon incubation with the appropriate protease, arguing for a functional centrosomal Cohesin ring (Schöckel et al., 2011). Consistently, knockdown of Cohesin subunits led to premature disengagement whereas expression of a non-cleavable Scc1 version inhibits disengagement *in vitro* (Beauchene et al., 2010; Díaz-Martínez et al., 2010; Schöckel et al., 2011). However, these studies are challenged by similar experiments in *Drosophila*, where artificial cleavage of Scc1 by TEV protease is not sufficient to trigger disengagement (Oliveira & Nasmyth, 2013). Additionally, expression of non-cleavable Scc1 in human cell culture cells did not block disengagement, tempting the authors to speculate for another centrosomal Separase substrate (Tsou et al., 2009). And indeed, Cohesin is not the only Separase target at the centrosome as two independent studies identified PCNT as a novel substrate (Lee & Rhee, 2012; Matsuo et al., 2012). PCNT cleavage was shown to be sufficient to trigger disengagement and was further shown to be necessary as expression of a non-cleavable PCNT version suppressed disengagement. Considering that Cohesin was normally cleaved under given circumstances, these results led to an apparent contradiction regarding Cohesin's relevance in mediating centriole engagement (Lee & Rhee, 2012; Matsuo et al., 2012).

Apart from the mentioned Separase substrates, centriole disengagement and licensing for duplication seem to be additionally regulated on the level of posttranslational modifications, as the essential role of Plk1 implies (Kong et al., 2014; Lončarek et al., 2010; Mohr et al., 2015; Shukla et al., 2015; Tsou et al., 2009; Wang et al., 2008). Upon Separase inactivation, Plk1 activity at the beginning of mitosis was shown to be critical for licensing centriole duplication in the following S-phase (Tsou et al., 2009). While disengagement at late mitosis was suppressed, the majority of centrioles in these cells eventually disengaged with delay and duplicated in late S-phase. Combined downregulation of Plk1 and Separase, however, led to a complete block of duplication in the next cell cycle (Tsou et al., 2009). How Plk1 activity drives centriole disengagement and duplication is not clear, due to its vast number of substrates in early mitosis. Hence, it might be the sum of events, like the centriole-to-centrosome conversion or the PCM maturation which are critical for licensing duplication (Wang et al., 2011). In analogy to the removal of chromosomal Cohesin rings by the prophase pathway, Plk1 activity might also remove the majority of centrosomal ‘glue’ in early mitosis. Hints are given by a study in which premature activation of Plk1 during S- and G2-phase promotes the maturation of daughter centrioles (Lončarek et al., 2010; Shukla et al., 2015). Additionally, an increased distance between mother and daughter centriole of about 80 nm could be observed which they normally would not reach until prometaphase. This increased distance goes along with a certain relief of the reduplication block which, under normal conditions, allows only the mother centrioles to reduplicate (Shukla et al., 2015). The fact, that Sgo1 in complex with PP2A is also localized to and functional at the centrosome underlines a possible centrosomal prophase pathway. The Sgo1-PP2A complex might protect residual centrosomal Cohesin rings against Plk1 activity in prophase. Hence, the centrioles would not reach their full distance until Separase cleaves the residual Cohesin rings in late mitosis and thereby relieves the duplication block (Mohr et al., 2015; Wang et al., 2006, 2008). Furthermore, Plk1 was proven to phosphorylate PCNT in prophase, thereby turning it into a suitable substrate for Separase (Kim et al., 2015). This correlation was already shown for the mitotic kleisin Scc1 and the meiotic kleisin Rec8 (Alexandru et al., 2001; Katis et al., 2010).

3.7 Aims of this work

In animal cells the two centrioles of one centrosome remain tightly associated (engaged) from S-Phase until they are spatially and functionally separated in late mitosis (disengagement). Together with Plk1 activity in prophase, disengagement is a critical step for mediating licensing of duplication in the following S-phase and was proven to depend on the proteolytic activity of Separase (Firat-Karalar & Stearns, 2014). Cohesin and Pericentrin (PCNT) have each been reported to constitute centrosomal substrates of Separase, with their cleavage being necessary and sufficient for centriole disengagement (Lee & Rhee, 2012; Matsuo et al., 2012; Schöckel et al., 2011). This apparent contradiction could be explained if both factors contributed to the structural integrity of the pericentriolar matrix (PCM), which in turn mediates the tight coupling of the centrioles in an indirect manner. Cleavage of either Cohesin or PCNT might contribute to liquefaction and subsequent shrinkage of the PCM, thereby triggering disengagement. To test this hypothesis, double transgenic mammalian cell lines should be generated that inducibly express either wild type or tailored variants of Scc1 and PCNT. Artificial *in vitro* cleavage of one or both tailored proteins with the corresponding protease(s) would then be followed by isolation of the centrosomes from the lysates and quantification of the disengagement status by immunofluorescence microscopy (IFM). These experiments would allow to assess results reported by independent groups within the same experimental setup and, more importantly, would allow to determine the relative contribution of Cohesin- and PCNT-inactivation to centriole disengagement.

A further aim was to clarify whether phosphorylation of PCNT is necessary to convert it into a suitable Separase substrate. This working hypothesis was inspired by phosphorylation boosting or enabling cleavage of previously identified Separase substrates like Scc1, Rec8, MCL1 and BCL-XL (Alexandru et al., 2001; Hellmuth & Stemmann, 2020; Katis et al., 2010). Therefore, three potential Plk1 and Cdk1 consensus phosphorylation sites in direct vicinity of PCNT's Separase cleavage site were changed to alanine or aspartate, in order to inhibit or mimic phosphorylation, respectively. This was followed by assessing the effects of these mutations on PCNT cleavability *in vitro* and *in vivo*.

4 Results

4.1 Centriole disengagement: What are the relative contributions of Cohesin versus Pericentrin inactivation?

Centrosomal Cohesin and PCNT have been identified as Separase substrates by independent groups. Proteolytical inactivation of each factor has been reported to be sufficient for inducing centriole disengagement (Lee & Rhee, 2012; Matsuo et al., 2012; Schöckel et al., 2011). Inspired by these previous publications and motivated to solve this apparent contradiction, artificially cleavable versions of *SCCI* and *PCNT* were stably integrated into the same mammalian host cell genome. Targeted inactivation of each factor with the corresponding protease *in vitro* then allowed determination of the relative contribution to centriole disengagement in the same experimental setup. In order to do so, required tools like plasmids encoding for the open reading frames (ORF) of wild type and artificially cleavable versions of *SCCI* and *PCNT* had to be generated in the first place.

4.1.1 Generation and characterization of tools to study centriole disengagement

In contrast to the pre-existing wild type (WT) *SCCI* ORF (Schöckel et al., 2011), the WT-*PCNT* ORF had to be generated initially. The NCBI RefSeq accession number NM_006031 served as a reference for designing sense and antisense primers. Due to its large size of 10 kilo base pairs (kb), the *PCNT* ORF was subdivided into four overlapping fragments of approximately 2.5 kb each (Fig. 7). After successful amplification and purification, fragment 1 and 2 served as templates in an overlap extension PCR to generate the first half of the *PCNT* ORF with the corresponding outer primer. Likewise, fragments 3 and 4 were used as templates to generate the second half of the *PCNT* ORF. Both halves were sequentially cloned into an expression plasmid for mammalian cultured cells and subsequent Sanger sequencing verified successful generation of the error-free full-length WT-*PCNT* ORF. In order to increase the number of usable protein tags, the WT-*PCNT* ORF was subsequently subcloned into expression plasmids encoding for Myc- or GFP-encoding tags.

Results

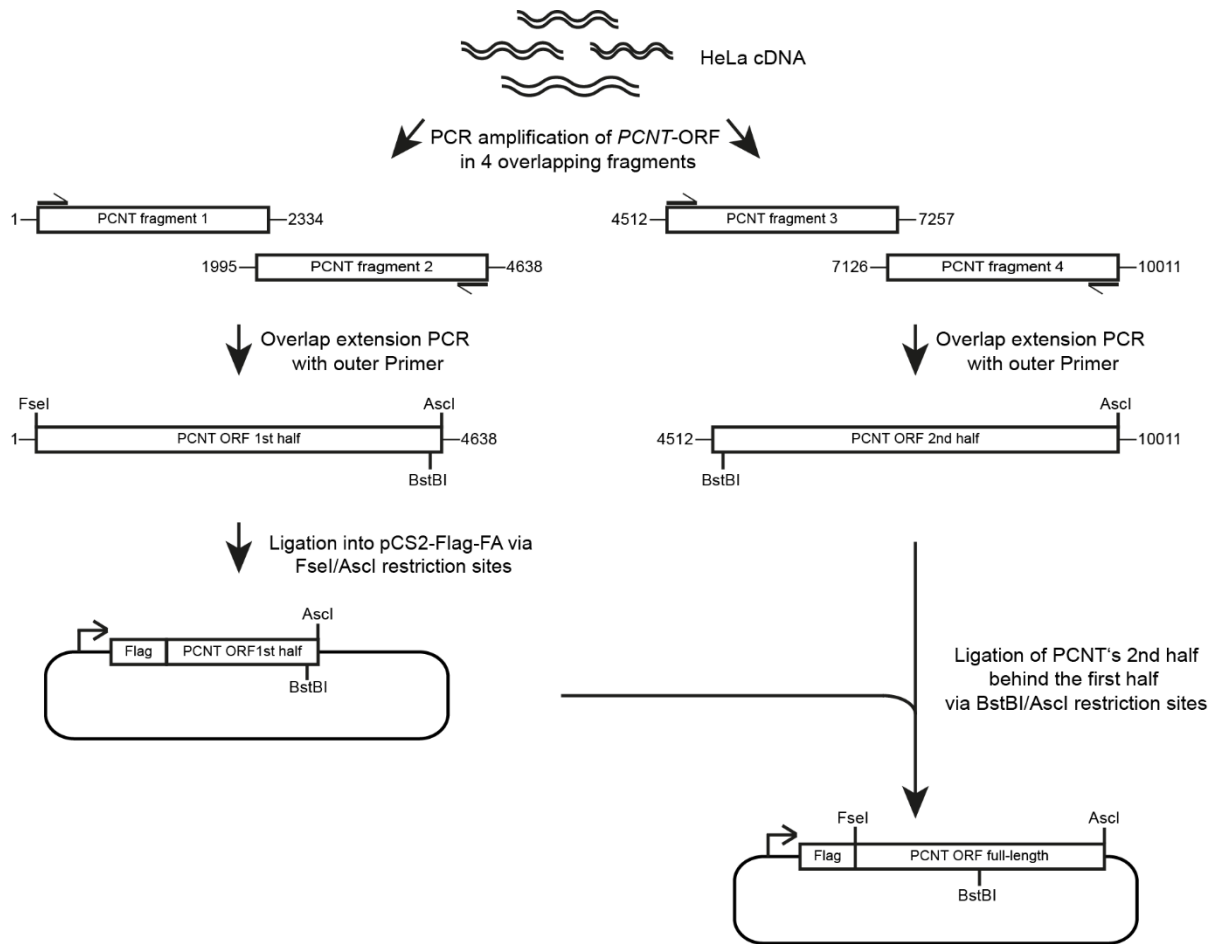


Fig. 7: Cloning strategy to generate the full-length WT-PCNT ORF. HeLa cDNA was used as template to amplify four overlapping fragments coding for the *PCNT* ORF. Fragment 1 (base pairs (bp) 1-2334) and fragment 2 (bp 1995-4638) then served as template for the follow up PCR to generate the first half, fragment 3 (bp 4512-7257) and fragment 4 (bp 7126-10011) served as template to generate the second half of the *PCNT* ORF. The first half was cloned into a standard pCS2 vector via introduced *FseI* and *AscI* restriction sites. The second half was fused with the first one via the unique restriction sites *BstBI*, located in the overlapping sequence of both halves, and *AscI*.

Furthermore, expression of full-length PCNT was confirmed by transient transfection of the corresponding plasmid in Hek293T cells and subsequent Western blot analysis (Fig. 8A). Co-staining of PCNT (via its Flag-tag) and γ -tubulin (centrosomal marker) in immunofluorescence microscopy (IFM) demonstrated a wild type-like centrosomal localization pattern of the transgenically encoded protein throughout mitosis (Fig. 8B).

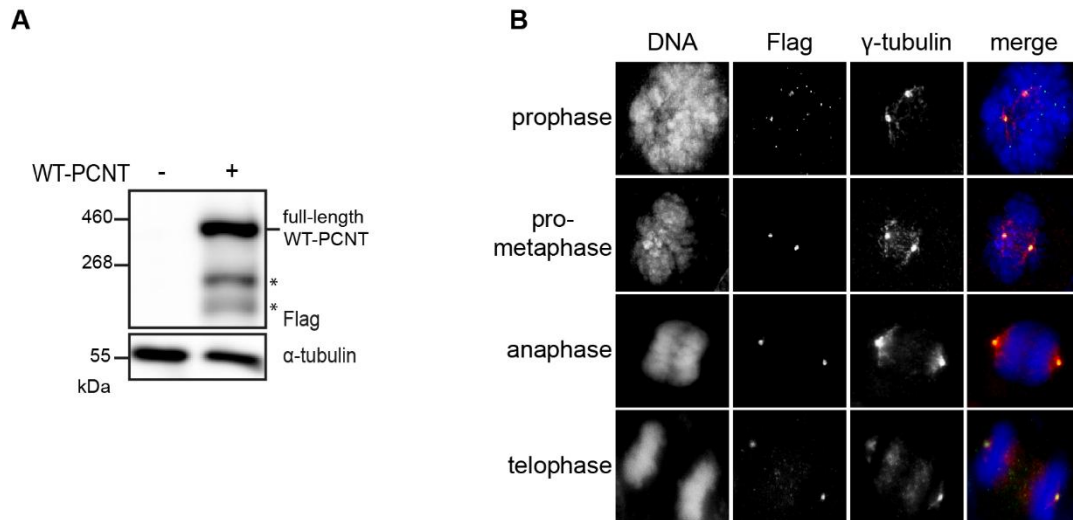


Fig. 8: Confirmation of full-length WT-PCNT expression in Western blot analysis and IFM. Hek293T cells were transiently transfected with a plasmid encoding for Flag-tagged WT-PCNT. After 48 h of growing asynchronously on cover slips cells were harvested and subjected to IFM. The remaining cells in the well were subsequently lysed for Western blot analysis. Untransfected cells served as a negative control. **(A)** Expression of transgenic PCNT was verified by immunoblotting against the Flag-tag. Detection of α -tubulin served as a loading control. Asterisks indicate truncated expression products. **(B)** Immunofluorescence staining with antibodies against the Flag-tag and γ -tubulin revealed centrosomal localization of expressed PCNT throughout mitosis. DNA was stained with DAPI.

As an additional tool for Western blot and IFM, polyclonal antibodies against PCNT were raised in rabbits and guinea pigs. A synthetic peptide representing the very N-terminal 15 amino acids (aa) of PCNT was coupled to a carrier protein and used to immunize two guinea pigs. A larger fragment, encoding for the amino acids 1968-2391, was expressed in *E. coli*, purified and used to immunize two rabbits (see 6.4.7). After purification of the antibodies from the corresponding sera (see 6.4.7), their performance was tested by Western blot analysis (Fig. 9). Here, bacterially expressed and purified fragment 1 (aa 1-778) and fragment 3 (aa 1505-2419) of PCNT were used as antigens in two different concentrations (1 and 100 ng). All four purified antibodies as well as the sera detected the corresponding antigens in the following Western blot analysis (Fig. 9A and Fig. 9B). But especially purification of the guinea pig antibodies reduced unspecific background signals (Fig. 9A).

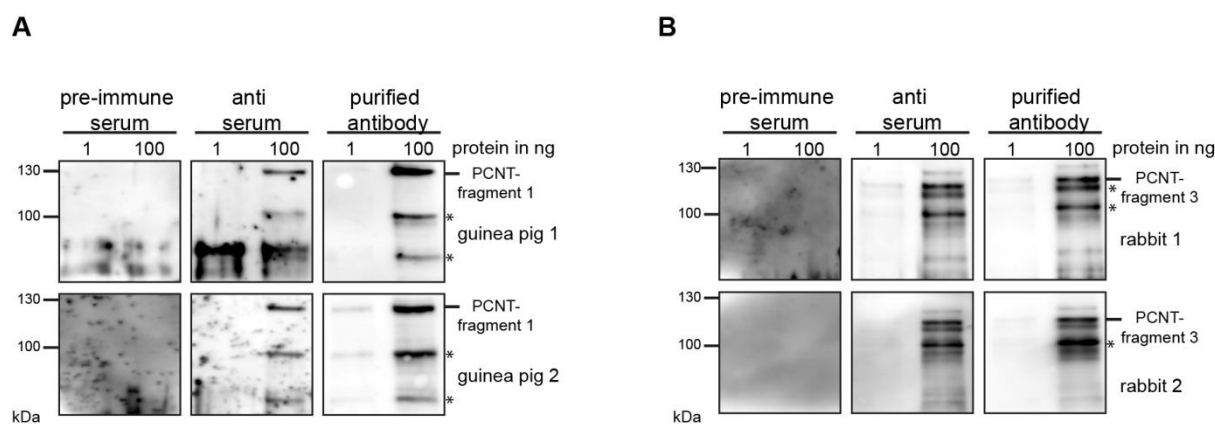


Fig. 9: Characterization of polyclonal PCNT antibodies. (A) 1 and 100 ng of recombinant PCNT-fragment 1 (aa 1-778) were used as antigen in a Western blot analysis to test the performance of pre-immuneserum (1:100 dilution), anti-serum (1:100 dilution) and the purified antibodies from guinea pig 1 (0.26 $\mu\text{g/ml}$) and guinea pig 2 (0.32 $\mu\text{g/ml}$). Asterisks indicate truncated expression products or cross-reactive bands. (B) 1 and 100 ng of recombinant PCNT-fragment 3 (aa 1505-2419) were used as antigen in a Western blot analysis to test the performance of pre-immuneserum (1:100 dilution), anti-serum (1:100 dilution) and the purified antibodies from rabbit 1 (0.19 $\mu\text{g/ml}$) and rabbit 2 (0.27 $\mu\text{g/ml}$). Asterisks indicate truncated expression products.

With the full-length ORF of WT-*PCNT* generated, the sequence could be altered by site-directed mutation in order to engineer the artificially cleavable version. Therefore, the single Separase recognition site in *PCNT* was preserved but in direct vicinity a sequence encoding for a cleavage site of the tobacco etch virus (TEV) protease was introduced (sequence encoding for the amino acids: ENLYFQ/IG) (Kapust et al., 2002) (Fig. 10A). In case of *SCC1*, the sequence encoding for one of the two Separase cleavage sites was mutated to now be recognized by the human rhinovirus 3C (HRV) protease (sequence encoding for the amino acids: ETLFQ/GP) (Cordingley et al., 1990). As expression of a non-cleavable (NC) version of *Scc1* shows cytotoxic effects (Hauf et al., 2001), the second cleavage site was left unchanged to allow cleavage by Separase and hence an unperturbed cell cycle (Fig. 10B).

After successful generation of all four *SCC1*- and *PCNT*-variants, stable isogenic cell lines could be generated in the next step. For that purpose, commercially available Flp-In 293 T-REx cells were used, which allow inducible expression of a gene of interest from a specific and mapped genomic location. These cells constantly express the Tet repressor protein, thus exhibiting low basal expression of the transgene of interest but high expression upon induction with tetra- or doxycycline. Site specific integration into the mapped Flp recombination target (FRT) site is mediated by co-transfection of a plasmid encoding for flippase (Flp) recombinase. In the context of this work, doubly transgenic stable cell lines should be generated. Hence, the described system was modified meaning that the plasmid used for the first round of integration carried an additional loxP site. This allowed site specific

integration of a second gene of interest by co-transfection of a corresponding loxP containing plasmid together with a Cre recombinase encoding plasmid (see 6.5.6).

With these tools at hand, the generation of doubly stable transgenic cell lines was started. For the first round of transfection, expression vectors containing genes for WT-*SCC1* or HRV-*SCC1* were used to generate cell line 1 and cell line 2, respectively. For the second round of transfection, expression vectors containing genes for WT-*PCNT* or TEV-*PCNT* were used to generate cell line 3 and cell line 4, respectively (Fig. 10C). Cell line 3 served as a control for the *in vitro* disengagement assay as levels of Scc1 and PCNT overexpression, together with their possible consequences for centrosome composition or engagement status are comparable to cell line 4. Additionally, possible side effects of TEV/HRV protease activity, e.g. unspecific cleavage of Scc1 or PCNT, could be monitored. Treatment of cell line 4 lysates with TEV or HRV protease allowed determination of the relative contribution of Scc1 or PCNT to centriole engagement. Incubation with both proteases together should even allow one to determine possible additive effects.

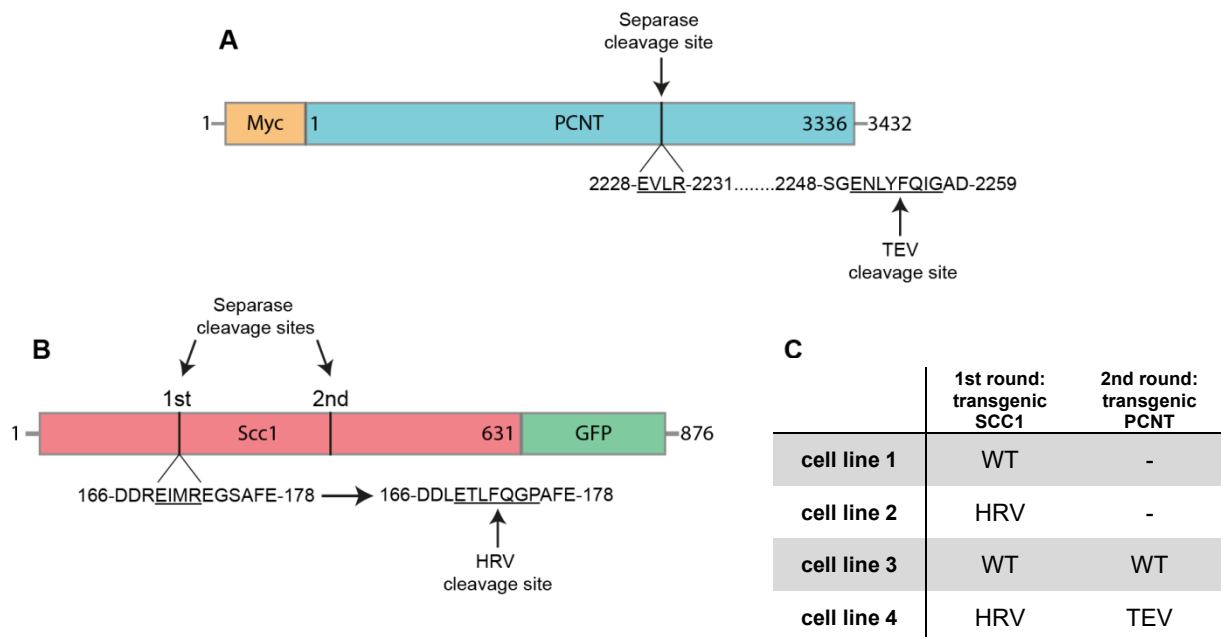


Fig. 10: Conversion of PCNT and Scc1 into artificially cleavable versions. (A) In case of *PCNT*, a TEV cleavage site was introduced next to the Separase cleavage site. **(B)** The first Separase cleavage site in *SCC1* was changed to now be recognized by HRV protease instead. The second one was left unchanged to allow for preserved cleavability by Separase and thus, unperturbed cell cycle progression. **(C)** Scheme of the generated double transgenic Flp-In 293 T-REx cell lines. For cell line 1 and cell line 2, the genes encoding for WT-*SCC1* or HRV-*SCC1*, respectively, were integrated into the genomic FRT integration site with the help of Flp recombinase. In the second round of integration the genes encoding for WT-*PCNT* or TEV-*PCNT* were integrated into the loxP integration site with the help of Cre recombinase, resulting in cell line 3 or cell line 4, respectively.

4.1.2 Experimental setup of the *in vitro* assay to quantify centriole disengagement

In order to quantify centriole disengagement triggered by treatment with TEV- or HRV-protease or both, the following *in vitro* assay was performed with the generated stable cell lines:

Expression of the transgenes was induced for at least 72 h (Fig. 11). The cells were then co-transfected with siRNA targeting endogenous *SCCI* and *PCNT* mRNA which leads to reduced levels of the corresponding endogenous proteins as well as enhanced centrosomal incorporation of the transgenically expressed proteins. Subsequently, the cells were pre-synchronized with thymidine at the G1/S-barrier for 20 h, released by washout and finally arrested with taxol in metaphase of mitosis. After harvesting the cells, the corresponding lysate was split equally into four samples and incubated without proteases as a control, with TEV- or HRV-protease and finally with both proteases together. As indicated in Fig. 11, Western blot samples were taken to monitor successful siRNA-mediated knockdown of endogenous proteins on the one hand and proteolysis of the tailored variants on the other hand. Centrosomes were isolated by centrifugation of the lysates through a sucrose cushion directly onto cover slips. Next, quantification of disengagement was carried out by immunofluorescence microscopy (IFM). Antibodies against the centrosomal proteins centrin 2 and C-Nap1 (centrosomal Nek2 associated protein 1 or Cep250) served as distal and proximal centriole marker, respectively. In case of tightly coupled engaged centrioles, the C-Nap1 signals overlap and, as a consequence of the microscope resolution limit, appear as one. Disengaged centrioles however lose their orthogonal arrangement and due to the larger spatial distance two dots become visible. In contrast, the distal marker centrin 2 is detected as two separate signals regardless of the engagement status of the centrioles. Thus, a ratio of C-Nap1 to centrin 2 signals of 1:2 indicates engaged centrioles, whereas a ratio of 2:2 indicates disengagement.

Results

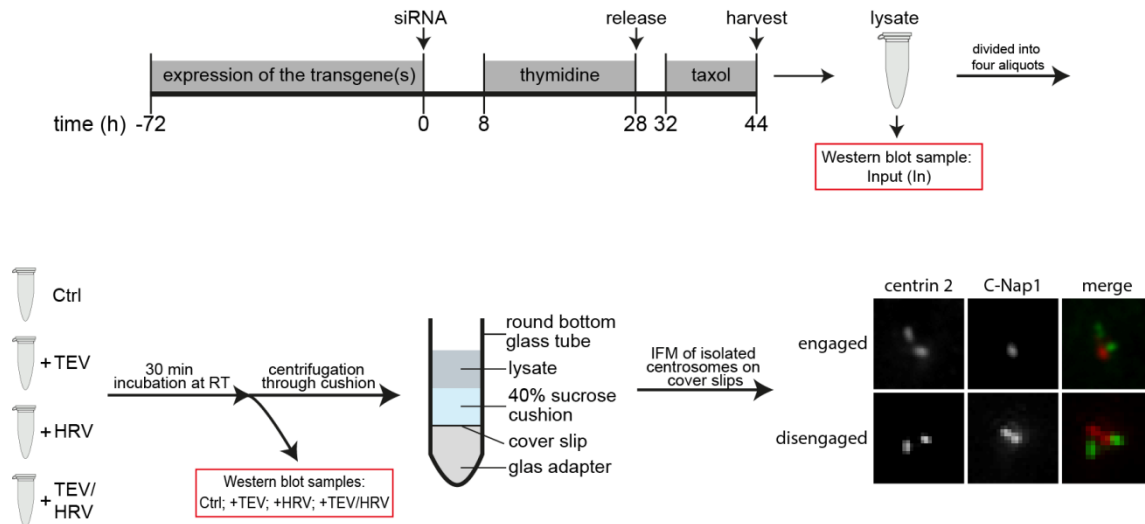


Fig. 11: Experimental workflow of the *in vitro* assay performed to quantify centriole disengagement. Transgene expression was induced for 72h before transfection of siRNAs against endogenous *SCC1* and *PCNT* was conducted. The cells were pre-synchronized at the G1/S-barrier by addition of thymidine, released after 20 h and finally arrested in metaphase by treatment with taxol. After harvesting, the corresponding lysate was divided and incubated with the depicted protease(s) or control-treated. As indicated, Western blot samples were taken to monitor the knockdown efficiency of the endogenous as well as proteolysis of the transgenically expressed proteins. The relative disengagement was quantified by IFM of isolated centrosomes. They were stained with antibodies against C-Nap1 (proximal marker) and centrin 2 (distal marker). A 1:2 ratio of C-Nap1:centrin 2 dots indicates an engaged centrosome, whereas a ratio of 2:2 indicates disengagement.

4.1.3 Inactivation of centrosomal Cohesin by artificial Scc1 cleavage triggers centriole disengagement

Several independent studies demonstrate localization of Cohesin subunits to the centrosome (Beauchene et al., 2010; Díaz-Martínez et al., 2010; Gregson et al., 2001; Kong et al., 2009; Wong & Blobel, 2008). In an elegant study, endogenous Scc1 or Smc3 was replaced by artificially cleavable versions. Co-immunoprecipitation (IP) experiments proved correct incorporation into the tripartite ring and even more important, artificial cleavage of the engineered versions triggered sister chromatid separation and centriole disengagement *in vitro* (Schöckel et al., 2011). Supportively, knockdown of individual Cohesin subunits triggered centriole disengagement while replacement of endogenous Scc1 with a non-cleavable version inhibited this crucial licensing step (Beauchene et al., 2010; Díaz-Martínez et al., 2010; Schöckel et al., 2011). Taken together, these data provide evidence for the coordination of the centrosome and chromosome cycle, as the same tripartite ring, Cohesin, mediates the tight coupling of centrioles as well as the pairing of sister chromatids.

In order to confirm previous results and determine Cohesin's contribution to centriole engagement, transfections for stable cell line 1 (plasmid encoding for WT-*SCC1*) and cell line 2 (plasmid encoding for HRV-*SCC1*) were carried out. As a proof of concept for the

chosen experimental setup and due to the time-consuming procedure of generating stable mammalian cell lines, aforementioned *in vitro* assay to quantify centriole disengagement (see Fig. 11) was already performed with selected clones after the first round of integration. At the same time, the second round of integration with WT- or TEV-cleavable *PCNT* was carried out.

Successful integration of WT-*SCC1* into the FRT site and subsequent expression of the transgenic protein upon induction was confirmed by Western blot analysis of several individual clones. Leakiness of basal transgene expression or artificially high expression level upon induction with doxycyclin was unfavorable. Therefore, experiments were carried out with a clone showing strong transgene expression only after induction (Fig. 12A). To enhance incorporation of transgenically expressed Scc1 during future assays, two siRNAs targeting the 3'UTR of endogenous *SCC1* mRNA were tested on the generated cell line, which substantially reduced the protein level (Fig. 12B). Noteworthy, induction of transgene expression itself already reduced endogenous Scc1 level, indicating that cells seek for balanced levels of this Cohesin subunit (Fig. 12B, black arrow). Unfortunately, the self-made antibody against Scc1 was raised against the very C-terminus and is incapable of detecting the inducibly expressed, GFP-tagged protein (Fig. 12B, grey arrow). For the following *in vitro* disengagement assays, determination of *SCC1* knockdown efficiency was conducted by Western blot analyses, without showing corresponding results.

Next, the selected clone was used for the *in vitro* disengagement assay. The corresponding Western blot analysis showed that treatment of the lysate with HRV and/or TEV protease caused, as expected, no detectable cleavage of expressed WT-Scc1 (Fig. 12C). Quantification of centriole disengagement revealed a marginal effect upon lysate incubation with HRV protease (5-10% disengagement). However, as this was not detectable upon incubation with TEV and HRV protease together, it might simply illustrate assay variance (Fig. 12D).

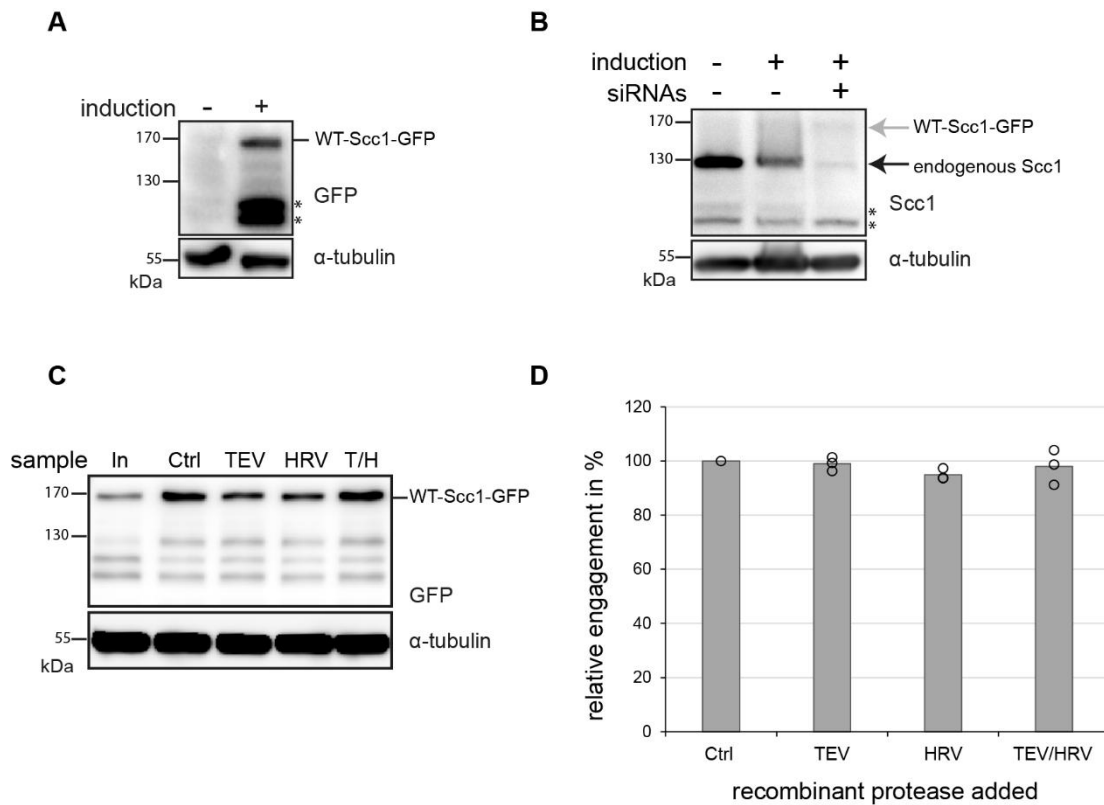


Fig. 12: Generation of a stable Hek293 cell line expressing WT-Scc1. (A) Stable transgenic Hek293 cell line expressing GFP-tagged WT-Scc1 upon induction. Detection of α -tubulin served as a loading control. Asterisks indicate truncated expression products. (B) Western blot analysis of transgenic cells described in (A) to determine siRNA mediated knockdown efficiency of endogenous *SCC1*. Two siRNAs against the 3'UTR of endogenous *SCC1* mRNA were transfected (28.5 nM each). The level of endogenous Scc1 was detected with an anti-Scc1 antibody and immunodetection of α -tubulin served as a loading control. Asterisks indicate cross-reactive bands. (C) Western blot analysis to monitor potential cleavage of the expressed WT-Scc1. As described in the experimental setup (Fig. 11), Western blot samples were taken at the indicated time points: In=Input; Ctrl=control without addition of protease; TEV=TEV protease was added; HRV=HRV protease was added; T/H=both proteases were added at the same time. The same antibodies as described in (A) were used. (D) Relative engagement of centrosomes isolated from lysates described in (C). Centrosomes were immunostained with antibodies against centrin 2 and C-Nap1. The number of engaged and disengaged centrioles was quantified by IFM in three independent experiments (circles) with at least 100 centrosomes counted each. The grey bar represents the average of these three experiments. Note that even without addition of proteases 22% of the centrioles appeared disengaged. This background was subtracted and the average amount of 78% engaged centrioles were set to 100%. All samples with proteases added were normalized to the control.

In order to confirm that artificial proteolysis of the Cohesin ring triggers centriole disengagement, transfection for stable cell line 2 was carried out with an expression construct encoding for HRV-*SCC1*. Again, several individual clones were screened by Western blot analysis to identify a clone with strong, inducible transgene expression (Fig. 13A). This clone was then used for the *in vitro* disengagement assay, in which incubation of the corresponding cell lysate with HRV protease efficiently cleaved the expressed Scc1, whereas incubation with TEV protease did not (Fig. 13B). This specific, artificial proteolysis of Cohesin rings induced about 40% centriole disengagement when quantified through IFM on isolated centrosomes (Fig. 13C). Consistent with already published data (Schöckel et al., 2011), this experiment

provides further evidence that cleavage of centrosomal Cohesin is indeed sufficient to trigger disengagement *in vitro*.

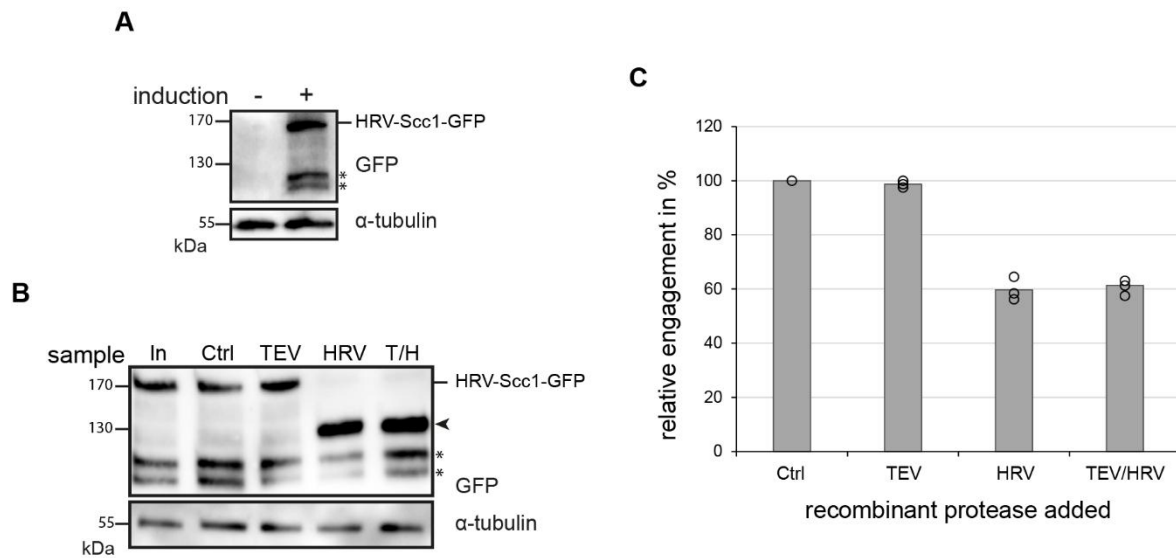


Fig. 13: Artificial cleavage of Scc1 by HRV protease triggers centriole disengagement. (A) Stable transgenic cell line expressing GFP-tagged HRV-Scc1 upon induction. Detection of α -tubulin served as a loading control. Asterisks indicate truncated expression products. (B) Western blot analysis to monitor cleavage of the transgenically expressed Scc1 during the *in vitro* disengagement assay. As described in the experimental setup (Fig 11), Western blot samples were taken at the indicated time points: In=Input; Ctrl=control without addition of protease; TEV=TEV protease was added; HRV=HRV protease was added; T/H=both proteases were added. The same antibodies as described in (A) were used. Black arrowhead indicates cleavage fragments. Asterisks indicate truncated expression products. (C) Relative engagement of centrosomes isolated from lysates described in (B). Centrosomes were immunostained with antibodies against centrin 2 and C-Nap1. The number of engaged and disengaged centrioles was quantified by IFM in three independent experiments (circles) with at least 100 centrosomes counted each. The grey bar represents the average of these three experiments. Note that even without addition of proteases 19% of the centrioles appeared disengaged. This background was subtracted and the average amount of 81% engaged centrioles were set to 100%. All samples with proteases added were normalized to the control.

4.1.4 Artificial cleavage of PCNT triggers centriole disengagement

With the confirmation of Cohesin's contribution to centriole engagement, the next question was about PCNT's contribution to it. Two independent groups reported PCNT cleavage by Separase *in vivo* to be necessary and sufficient for inducing centriole disengagement and for licensing centriole duplication in the following S-phase (Lee & Rhee, 2012; Matsuo et al., 2012). Despite a seeming contradiction to the published relevance of Cohesin in centriole engagement at first sight, Cohesin and PCNT might still cooperatively contribute to the structural integrity of the PCM (see discussion). Hence, proteolytical inactivation of each factor might be sufficient to trigger centriole disengagement. Even more interestingly, artificial inactivation of both factors at the same time might as well have additive effects, supporting the matrix entrapment theory. To address this issue, the second round of transfection with *PCNT*-encoding constructs was carried out: a gene encoding for WT-*PCNT*

was stably integrated into the selected clone expressing WT-Scc1 (cell line 1) and a gene encoding for TEV-*PCNT* was stably integrated into the selected clone expressing HRV-Scc1 (cell line 2) (Fig. 10 and 6.5.6).

Successful integration of WT-*PCNT* and expression of both transgenic proteins in cell line 3 was confirmed by Western blot analysis (Fig. 14B). Unfortunately, the siRNA mediated knockdown efficiency of endogenous PCNT could not be determined as part of the following experiments. Because of the similar molecular weight of the transgenically expressed Myc-tagged and endogenous PCNT, a separation of these two proteins on SDS-polyacrylamide gel electrophoresis (SDS-PAGE) failed. Therefore, the knockdown efficiency was confirmed in Hek293T cells and considered to be highly efficient and comparable for performed *in vitro* disengagement assays (Fig. 14A).

Against all expectations, treatment of cell line 3 lysates with HRV protease during the *in vitro* disengagement assay led to cleavage of the inducibly expressed WT-PCNT. An N-terminal cleavage fragment of approximately 120 kDa detected in the Myc-Western blot illustrated at least one unidentified cleavage site for HRV protease within PCNT (Fig. 14C). Quantification of disengagement through IFM on isolated centrosomes revealed that this highly efficient but unspecific cleavage triggered no substantial disengagement compared to controls (Fig. 14D). Considering the almost complete proteolysis of expressed PCNT, this result is quite surprising and might indicate that the position of Separase dependent cleavage is fundamental for triggering disengagement.

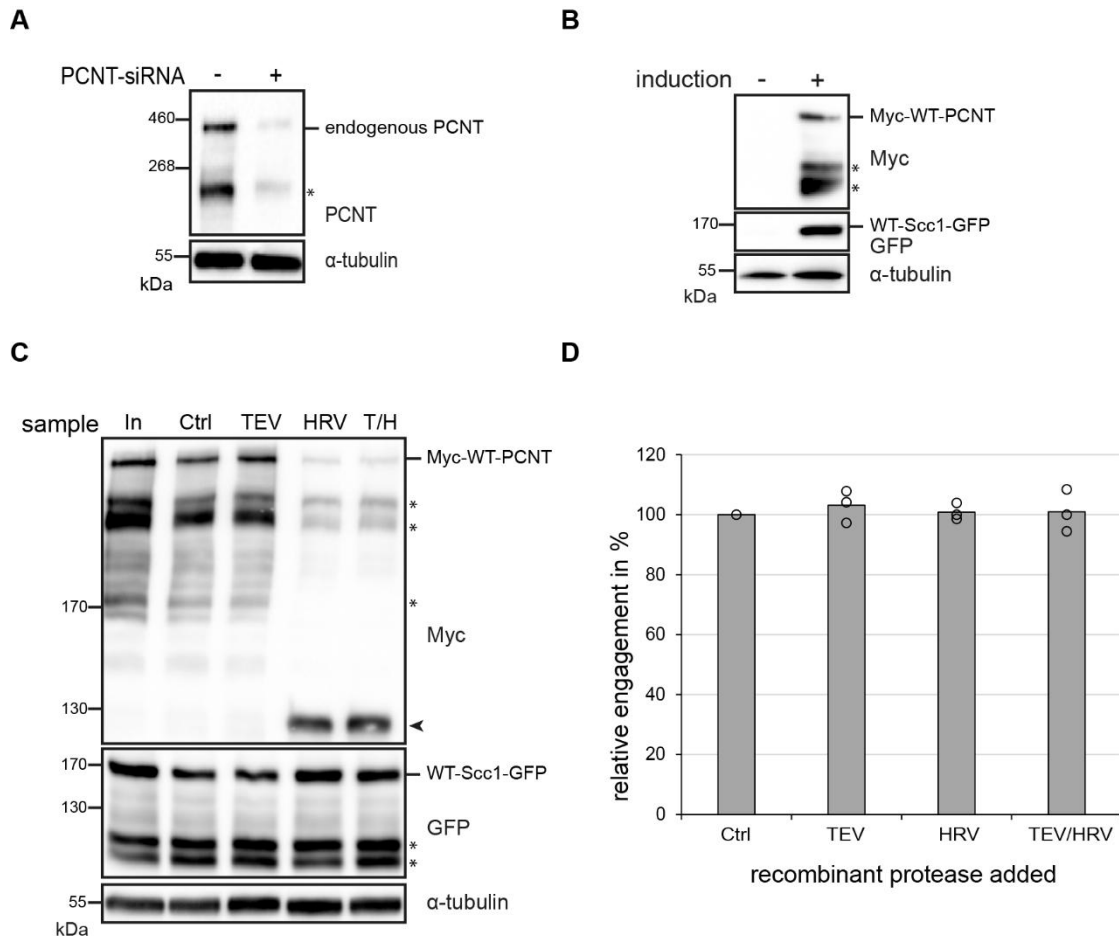


Fig. 14: PCNT is an unexpected substrate for HRV protease. (A) Determination of the siRNA mediated knockdown efficiency of endogenous PCNT by Western blot analysis. Hek293T cells were transiently transfected with *PCNT* siRNA (+, 50 nM) or *GL2* siRNA (-, 50 nM) as control. 36 h later, cells were harvested and knockdown efficiency was determined using an anti-PCNT antibody. Detection of α -tubulin served as a loading control. Asterisk indicates truncated expression product. (B) Double stable transgenic cell line expressing WT-Scc1 and -PCNT upon induction. Western blot analysis of whole cell lysates was carried out with anti-GFP and anti-Myc antibodies which detected Scc1 and PCNT, respectively. Detection of α -tubulin served as a loading control. Asterisks indicate truncated expression products. (C) Western blot analysis to monitor cleavage of expressed Scc1 and PCNT during the *in vitro* disengagement assay. As described in the experimental setup (Fig. 11) Western blot samples were taken at the indicated time points: In=Input; Ctrl=control without addition of protease; TEV=TEV protease was added; HRV=HRV protease was added; T/H=both proteases were added at the same time. The same antibodies as described in (B) were used. Black arrowhead indicates cleavage fragments. Asterisks indicate truncated expression products. (D) Relative engagement of centrosomes isolated from lysates described in (C). Centrosomes were immunostained with antibodies against centrin 2 and C-Nap1. The number of engaged and disengaged centrioles was quantified by IFM in three independent experiments (circles) with at least 100 centrosomes counted each. The grey bar represents the average of these three experiments. Note that even without addition of proteases 27% of the centrosomes appeared disengaged. This background was subtracted and the average amount of 73% engaged centrosomes were set to 100%. All samples with proteases added were normalized to the control.

Considering the unspecific cleavage of PCNT by HRV protease, the previously described experimental setup (Fig. 11) had to be modified. Incubation of cell line 4 lysates with HRV protease would cleave both factors involved in mediating centriole engagement. Hence, the artificial cleavage sites in *SCC1*- and *PCNT*-encoding constructs were swapped, resulting in

TEV-cleavable *Scc1* and HRV-cleavable *PCNT* (Fig. 15C). As a consequence, incubation of the corresponding cell lysate with HRV protease would exclusively trigger *PCNT* proteolysis, albeit at two sites. The sequence encoding for the substituted HRV cleavage site in *PCNT* was introduced in direct vicinity of the endogenous Separase cleavage site and hence, incubation with HRV protease should mimic Separase activity and trigger disengagement (Fig. 15A). In case of *SCC1* the first Separase cleavage site was mutated to now be recognized by TEV protease (Fig. 15B).

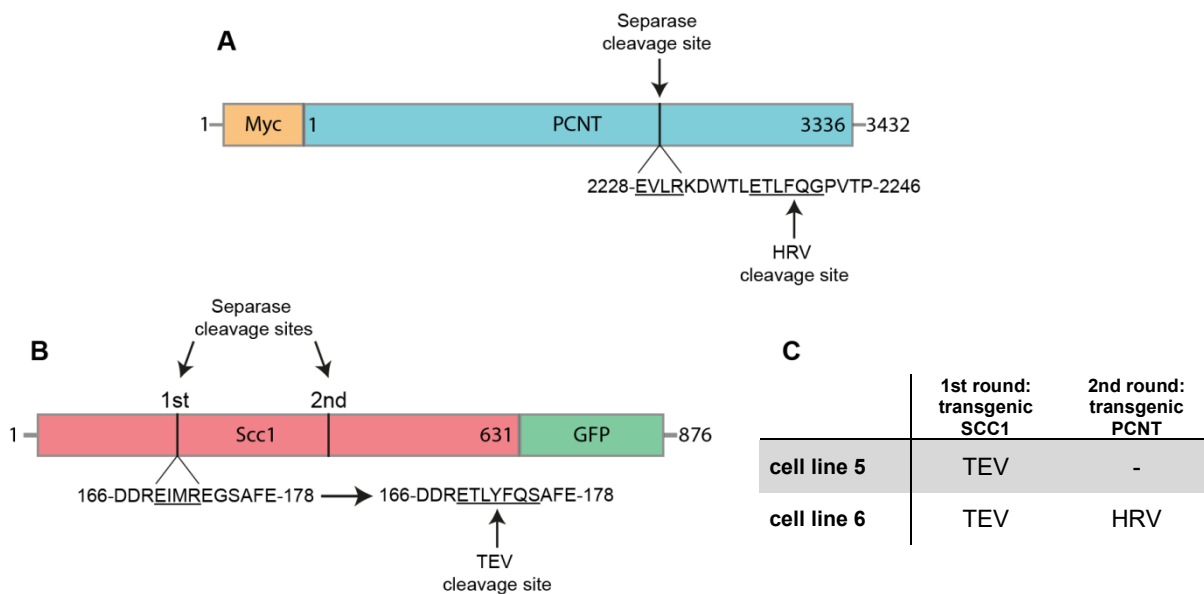


Fig. 15: Substitution of artificial cleavage sites in *Scc1* and *PCNT* encoding constructs. As a consequence to the unspecific cleavage of *PCNT* by HRV protease, the initially intended artificial cleavage sites in *Scc1* and *PCNT* had to be substituted. **(A)** In case of *PCNT*, a sequence encoding for a HRV protease cleavage site was introduced next to the single Separase recognition sequence. **(B)** The first Separase cleavage site in *Scc1* was mutated to now be recognized by TEV protease. The second one was left unchanged to allow unperturbed cell cycle progression. **(C)** For cell line 6 a gene encoding for TEV-*SCC1* was stably integrated into the genomic FRT site. In the second round of integration a gene encoding for HRV-*PCNT* was stably integrated into the loxP site.

In order to generate cell line 5, transfection with a TEV-cleavable *SCC1* encoding expression construct was carried out. Successful integration into the FRT site and expression of the transgenic protein upon induction was judged by Western blot analysis (Fig. 16A). With a selected clone, the *in vitro* assay to quantify centriole disengagement was carried out. Here, incubation of the corresponding cell lysates with TEV protease efficiently cleaved expressed *Scc1* (Fig. 16B) and triggered approximately 30% of disengagement when quantified on isolated centrosomes (Fig. 16C). This is 10% less compared to incubation of cell line 2 (expressing HRV-*Scc1*) lysates with HRV protease (Fig. 13C) and might be due to the contribution of unspecific *PCNT* cleavage or simply assay variance.

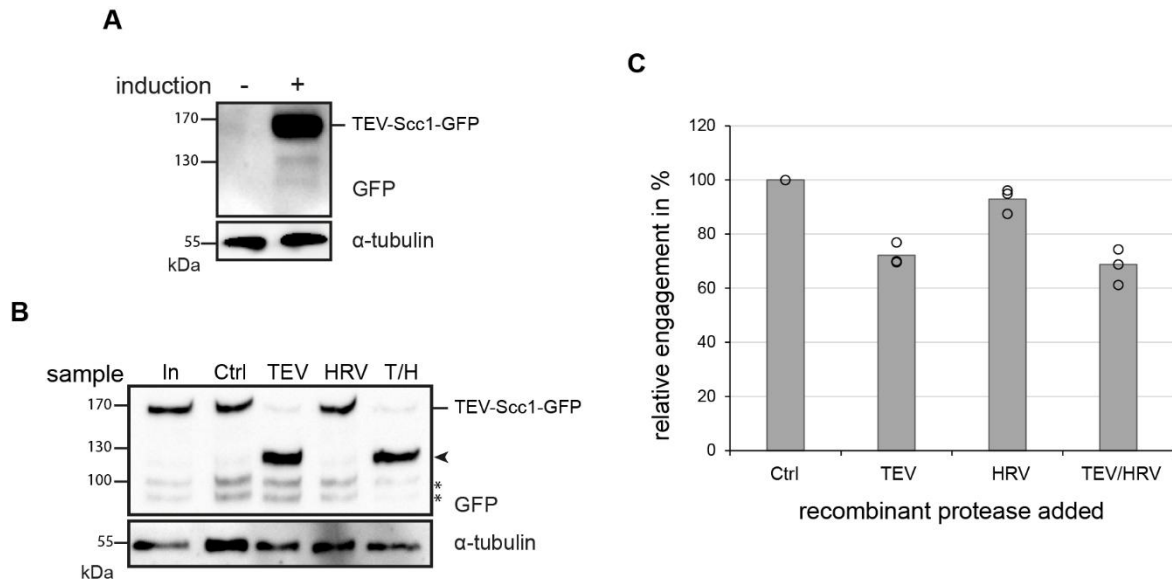


Fig. 16: Artificial cleavage of Scc1 by TEV protease triggers centriole disengagement. (A) Stable transgenic cell line expressing GFP-tagged TEV-Scc1 upon induction. Detection of α -tubulin served as a loading control. (B) Western blot analysis to monitor cleavage of transgenically expressed Scc1 during the *in vitro* disengagement assay. As described in the experimental setup (Fig. 11) Western blot samples were taken at the indicated time points: In=Input; Ctrl=control without addition of protease; TEV=TEV protease was added; HRV=HRV protease was added; T/H=both proteases were added at the same time. The same antibodies as described in (A) were used. Black arrowhead indicates cleavage fragments. Asterisks indicate truncated expression products. (C) Relative engagement of centrosomes isolated from lysates described in (B). Centrosomes were immunostained with antibodies against centrin 2 and C-Nap1. The number of engaged and disengaged centrioles was quantified by IFM in three independent experiments (circles) with at least 100 centrosomes counted each. The grey bar represents the average of these three experiments. Note that even without addition of proteases 21% of the centrioles appeared disengaged. This background was subtracted and the average amount of 79% engaged centrioles were set to 100%. All samples with proteases added were normalized to the control.

According to the modified experimental setup and in order to generate cell line 6, the HRV-*PCNT* gene was stably integrated into the selected clone expressing TEV-Scc1. Again, Western blot analysis was used to identify a positive clone expressing both transgenic proteins upon induction (Fig. 17A). Treatment of the corresponding cell lysate with TEV or HRV protease during the *in vitro* disengagement assay demonstrated efficient and specific cleavage of the engineered proteins (Fig. 17B). But even more importantly, artificial cleavage of either Scc1 or PCNT was sufficient to trigger disengagement *in vitro* when quantified on isolated centrosomes (Fig. 17C). For the first time this could be shown in the same experimental setup, confirming published results from independent groups and underlying the importance of both, Cohesin and PCNT, in mediating centriole engagement. While inactivation of Cohesin triggered approximately 35% disengagement, confirming previous results (Schöckel et al., 2011), inactivation of PCNT triggered 25% of disengagement. Compared to the published *in vivo* effects upon PCNT inactivation by the Rhee or Takahashi lab (Lee & Rhee, 2012; Matsuo et al., 2012), triggered disengagement in the chosen *in vitro* setup is rather low and

only adds up to approximately one third of the reported *in vivo* effects. However, the introduced HRV cleavage site in direct vicinity of the Separase cleavage site is sufficient to mimic Separase activity.

Surprisingly, addition of both proteases did not lead to a significantly additive effect in triggering disengagement, despite both expressed proteins being efficiently cleaved (Fig. 17C). Seemingly, Cohesin and PCNT do not cooperatively contribute to centriole engagement. These new perspectives in regulation of the centriole engagement status and duplication control are further discussed in section 5.1.3.

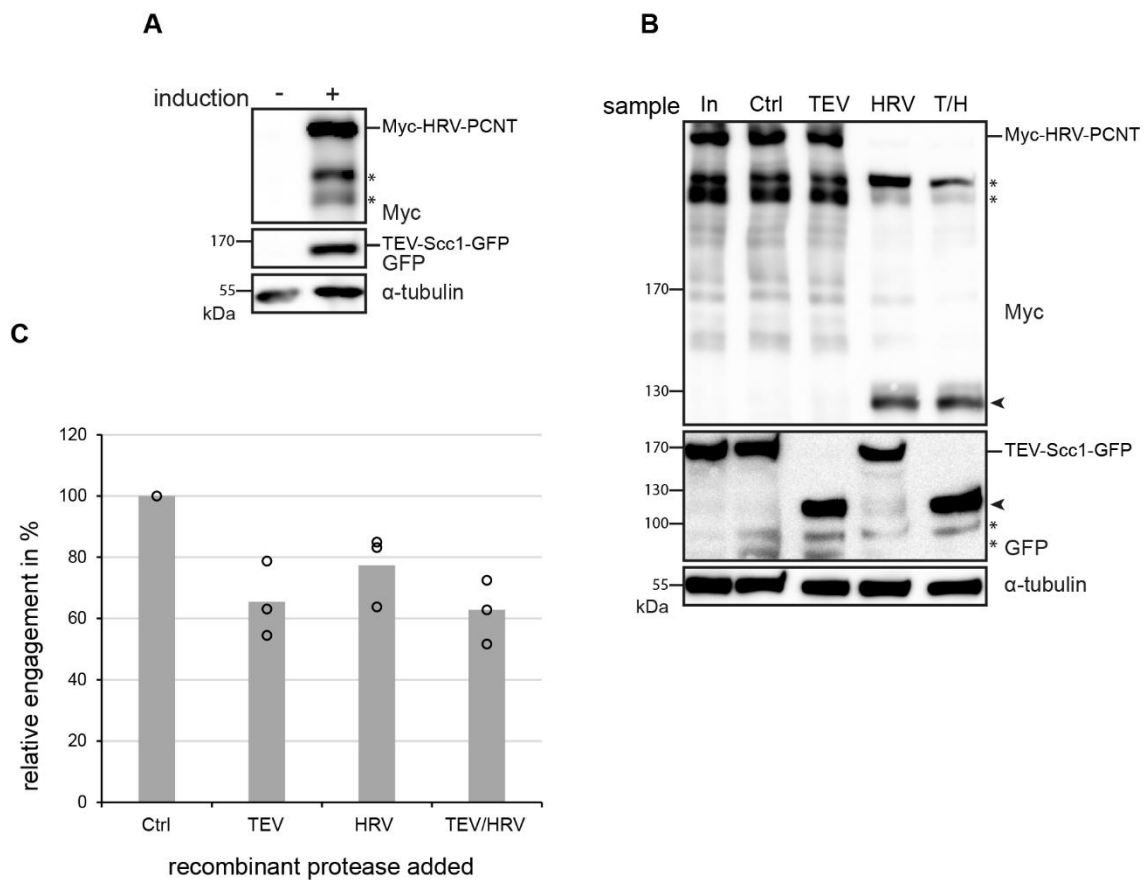


Fig. 17: Artificial cleavage of either Scc1 or PCNT triggers centriole disengagement. (A) Stable transgenic cell line expressing TEV-Scc1 and HRV-PCNT upon induction. Western blot analysis of whole cell lysates was carried out with anti-GFP and anti-Myc antibodies which detected expressed Scc1 and PCNT, respectively. Detection of α -tubulin served as a loading control. Asterisks indicate truncated expression products. (B) Western blot analysis to monitor cleavage of the expressed Scc1 and PCNT. As described in the experimental setup (Fig. 11) Western blot samples were taken at the indicated time points: In=Input; Ctrl=control without addition of protease; TEV=TEV protease was added; HRV=HRV protease was added; T/H=both proteases were added at the same time. The same antibodies as described in (A) were used. Black arrowheads indicate cleavage fragments. Asterisks indicate truncated expression products. (C) Relative engagement of centrosomes isolated from lysates described in (B). Centrosomes were immunostained with antibodies against centrin 2 and C-Nap1. The number of engaged and disengaged centrioles was quantified by IFM in three independent experiments (circles) with at least 100 centrosomes counted each. The grey bar represents the average of these three experiments. Note that even without addition of proteases 25% of the centrioles appeared disengaged. This background was subtracted and the average amount of 75% engaged centrioles were set to 100%. All samples with proteases added were normalized to the control.

4.1.5 Unspecific cleavage of PCNT by HRV protease occurs at two distinct cleavage sites

In order to map the unspecific HRV cleavage site(s) within PCNT, Hek293T cells were transfected with a plasmid encoding for GFP-tagged *PCNT*. After cell harvesting, the corresponding lysate was incubated with HRV protease and Western blot samples were taken at the indicated time points. Detection of the N-terminal GFP-tag in the following Western Blot analysis confirmed the cleavage fragment that was initially detected during the *in vitro* disengagement assays (Fig. 14C and Fig. 18A). The self-made polyclonal rabbit antibody raised against aa 1968-2391 of PCNT was used as well and detected two distinct fragments in the Western Blot. This indicated presence of a second unidentified HRV cleavage site located within this sequence (Fig. 18B and 18C).

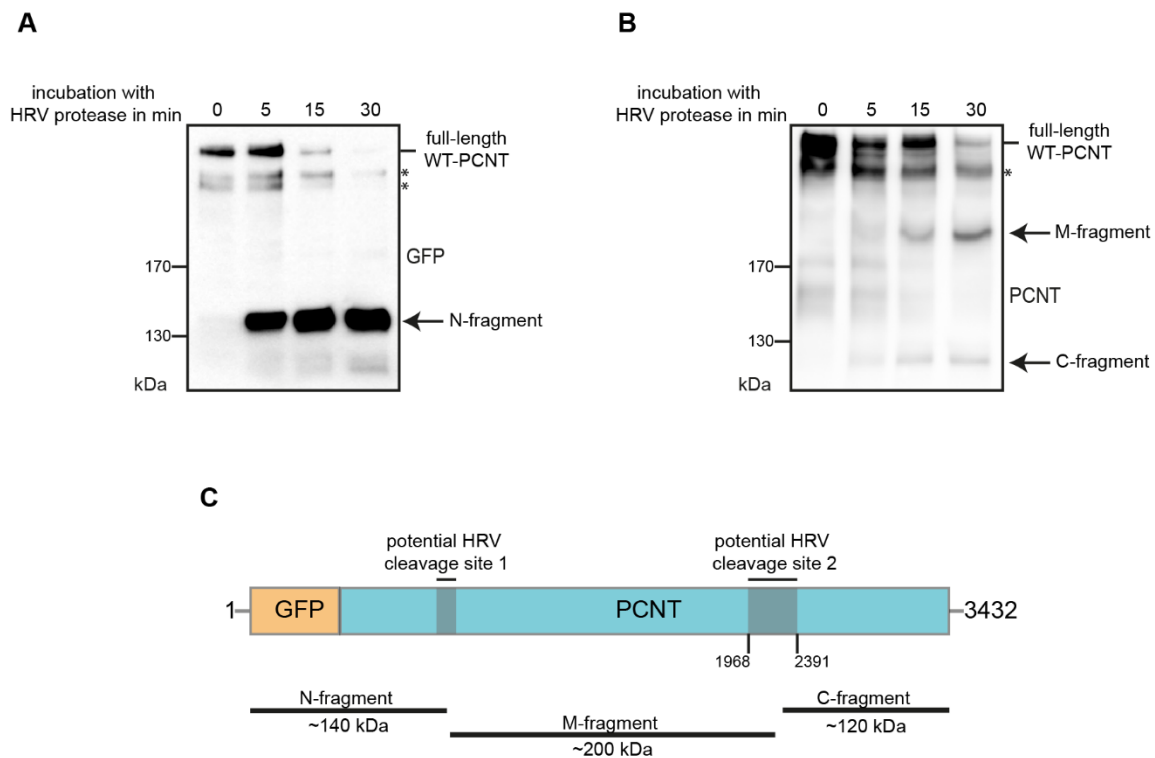


Fig. 18: HRV protease cleaves PCNT at two distinct sites. Hek293T cells were transiently transfected with a plasmid encoding for GFP-tagged WT-*PCNT*. The corresponding lysate was then incubated with HRV protease at RT and samples were taken at the indicated time points **(A)** Detection of an N-terminal cleavage fragment confirmed at least one unspecific HRV cleavage site. Western blot analysis of whole cell lysates was carried out with anti-GFP antibody which detected the N-terminally tagged PCNT. Asterisks indicate truncated expression products. **(B)** Western Blot analysis with the self-raised, polyclonal rabbit anti-PCNT antibody (antigen: aa 1968-2391) revealed a second unspecific cleavage site for HRV protease within this sequence. Asterisk indicates a truncated expression product. **(C)** Cartoon illustrating potential HRV cleavage sites and corresponding molecular weight of resulting cleavage fragments.

To further narrow it down, the plasmids encoding the four overlapping PCNT fragments (see Fig. 7) were individually transfected in Hek293T cells. Again, corresponding cell lysates were incubated with HRV protease and immunoblotted against the N-terminal Flag-tag (Fig. 19A). As expected, cleavage of fragment 1 and 3 verified the presence of two unspecific cleavage sites within PCNT. Fragment 4 was either weakly expressed or rapidly degraded and hence only visible in a long exposure (Fig. 19A, red box). Next, the online tool NetpicoRNA 1.0 server, which produces cleavage site predictions for picornaviral proteases like HRV protease, was used to generate a list of potential HRV cleavage sites within these two fragments (Fig. 19B). The glutamine in position 653 of the first fragment seemed to be the most promising hit. It and the following glycine at position 654 were mutated to alanine. In case of the third fragment, the detected cleavage product with a molecular weight of approximately 100 kDa indicated the cleavage site to be located near the C-terminus. Hence, the favored glutamine at position 2272 and the subsequent glycine were mutated to alanines, too. And indeed, mutation of these two potential cleavage sites to alanine effectively prevented cleavage of the PCNT fragments by HRV protease (Fig. 19C).

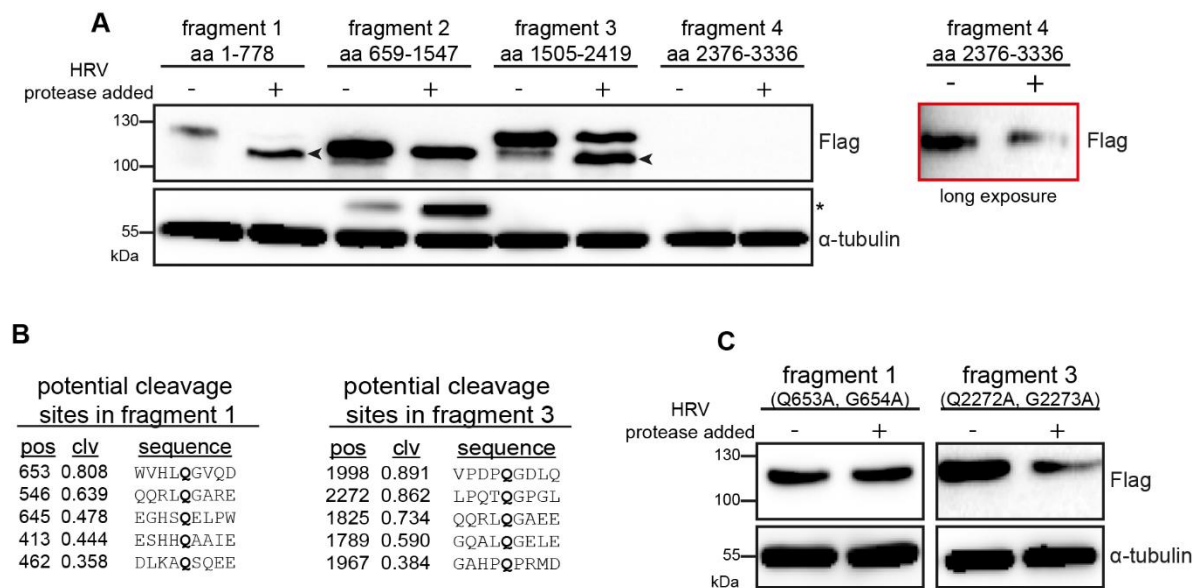


Fig. 19: Mutational inactivation of the two unspecific cleavage sites effectively prevents PCNT from cleavage by HRV protease. (A) Hek293T cells were individually transfected with plasmids encoding for fragments 1-4 of PCNT. After 48h, cells were harvested and the corresponding lysates were incubated with HRV protease for 30 min, if indicated. Expression as well as unspecific cleavage of the transgenic PCNT fragments was monitored by Western blot analysis against the Flag-tag. Detection of α -tubulin served as a loading control. Black arrowheads indicate cleavage fragments. Asterisk indicates a truncated expression product. **(B)** Prediction of the potential HRV cleavage sites in fragment 1 and 3 using the NetpicoRNA server (<http://www.cbs.dtu.dk/services/NetPicoRNA/>). Potential cleavage sites for each fragment are sorted by their position (pos), cleavage score (clv, ranges from 0,000 to 1,000 and indicates the probability of HRV cleavage at that site) and the corresponding amino acid sequence. Typically, HRV protease cleaves between Gln (Q, marked in bold) and Gly (G). **(C)** Mutation of the two HRV cleavage sites at position 653/654 and 2272/2273 to alanine prevents PCNT fragments 1 and 3 from cleavage by HRV protease.

With the exact mapping of the unspecific HRV-cleavage sites, full-length versions of the *PCNT* ORF were generated with either only the more N-terminal HRV cleavage site (2Ala-*PCNT*) or both (4Ala-*PCNT*) of the cleavage sites inactivated by mutation to alanine. Again, these constructs were transiently overexpressed in Hek293T cells and the corresponding lysates were incubated with HRV protease. As hoped, mutational inactivation of both cleavage sites in full-length *PCNT* efficiently prevents its unspecific cleavage by HRV protease (Fig. 20A).

With the full-length 4Ala-*PCNT*-ORF generated, the possible contribution of unspecific *versus* site directed cleavage by HRV protease during the *in vitro* disengagement assay could be determined in more detail. To this end, the 4Ala-*PCNT* ORF was used to generate an artificially cleavable version. Accordingly, a sequence encoding a HRV cleavage site was introduced in direct vicinity of the Separase cleavage site (see Fig. 15). This HRV-4Ala-*PCNT* encoding construct was stably integrated into the selected clone expressing TEV-Scc1, resulting in cell line 7 (Fig. 20B). Performing the *in vitro* assay to quantify centriole disengagement then allowed comparison between cell line 6 and 7 with the main focus on a possible impact of unspecific *PCNT* cleavage by HRV protease. And indeed, artificial cleavage of HRV-4Ala-*PCNT* by HRV protease caused 15% of disengagement (Fig. 20E), which is approximately 10% less compared to the obtained disengagement by treatment of cell line 6 lysates (Fig. 17 C). This might again illustrate the contribution of unspecific HRV cleavage quantified beforehand (Fig. 12D and Fig. 16C). However, proteolytic inactivation of TEV-Scc1 using cell line 5 also triggered 10% less disengagement compared to the results gained with cell line 6 (Fig. 17C). Therefore, this small deviation might illustrate normal volatility using the *in vitro* disengagement assay or could be caused by different expression levels of transgenic *PCNT*. A more detailed evaluation of these results is made in section 5.1.2.

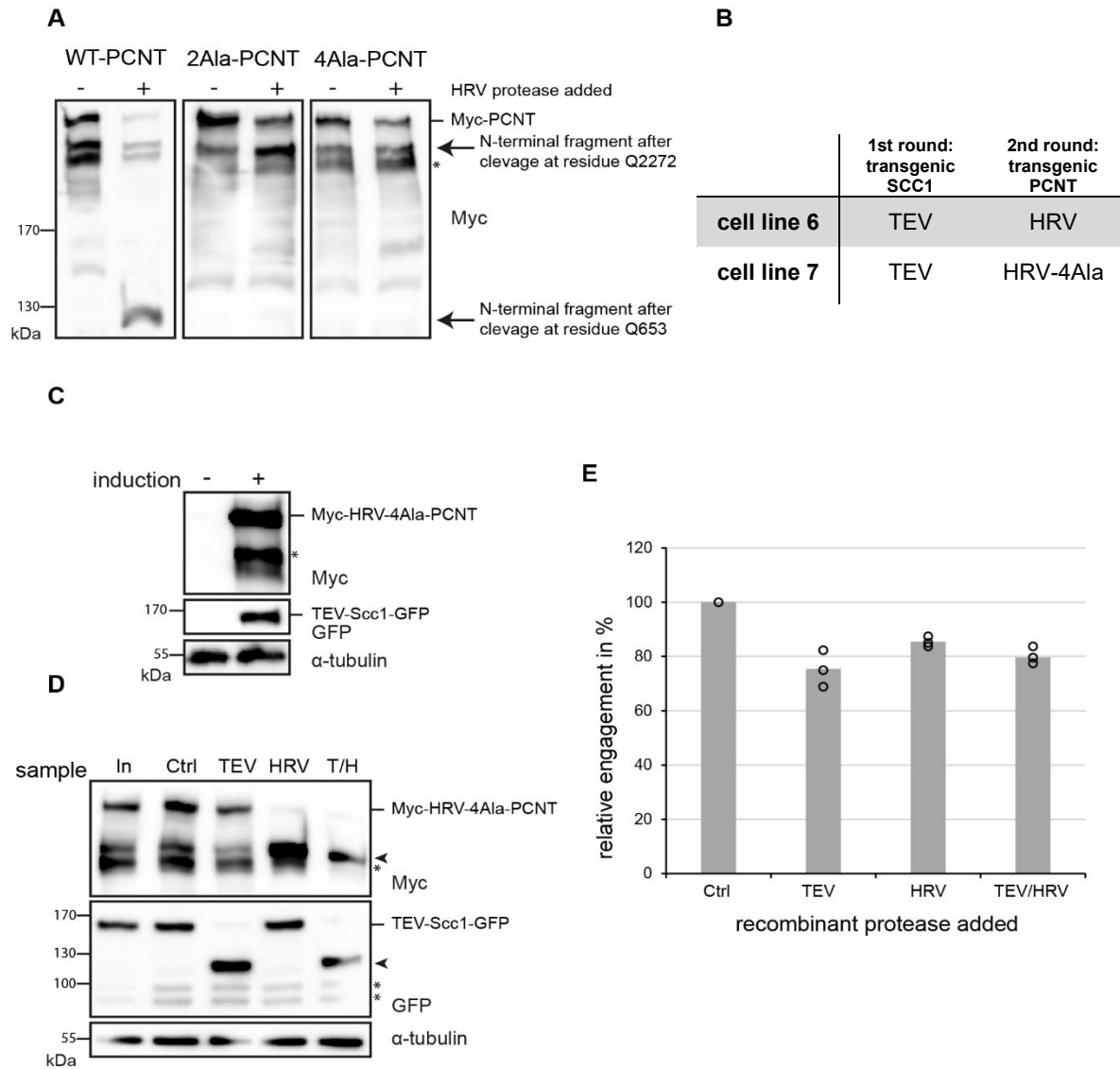


Fig. 20: Artificial cleavage of PCNT-4Ala triggers centriole disengagement. (A) Plasmids encoding for Myc-tagged WT-PCNT, 2Ala-PCNT (Q653A, G654A) and 4-Ala-PCNT (Q653A, G654A, Q2272A, G2273A) were transiently transfected into Hek293T cells. After 24h, cells were arrested in mitosis for further 15 h by addition of taxol. After harvesting, the corresponding lysates were incubated with HRV protease for 30 min at RT before Western Blot samples were taken. Western blot analysis was carried out with anti-Myc antibody which detected the depicted N-terminal cleavage fragments. Asterisk indicates a truncated expression product. (B) Scheme of the generated double transgenic Flp-In 293 T-REx cell lines. For cell line 7 a gene encoding for TEV-*SCC1* was stably integrated into the genomic FRT integration site with the help of Flp recombinase. In the second round of integration a gene encoding for HRV-4Ala-PCNT was integrated into the loxP integration site with the help of Cre recombinase. (C) Stable transgenic cell line expressing GFP-tagged TEV-Scc1 and Myc-tagged HRV-4Ala-PCNT upon induction. Detection of α -tubulin served as a loading control. Asterisk indicates a truncated expression product. (D) Western blot analysis to monitor cleavage of transgenically expressed Scc1 and PCNT. As described in the experimental setup (Fig. 11) Western blot samples were taken at the indicated time points: In=Input; Ctrl=control without addition of protease; TEV=TEV protease was added; HRV=HRV protease was added; T/H=both proteases were added at the same time. The same antibodies as described in (C) were used. Black arrowheads indicate cleavage fragments. Asterisks indicate truncated expression products. (E) Relative engagement of centrosomes isolated from lysates described in (D). Centrosomes were immunostained with antibodies against centrin 2 and C-Nap1. The number of engaged and disengaged centrosomes was quantified by IFM in three independent experiments (circles) with at least 100 centrosomes counted each. The grey bar represents the average of these three experiments. Note that even without addition of proteases 18% of the centrosomes appeared disengaged. This background was subtracted and the average amount of 82% engaged centrosomes were set to 100%. All samples with proteases added were normalized to the control.

4.1.6 Non-cleavable versions of Scc1 and PCNT act as competitive inhibitors and reduce Separase activity

While artificial cleavage of either PCNT or Scc1 was confirmed to be sufficient for triggering disengagement, expression of corresponding non-cleavable versions leads to conflicting results according to the existing literature. Two independent groups showed that expression of NC-PCNT efficiently suppressed centriole disengagement *in vivo* upon mitotic exit (Lee & Rhee, 2012; Matsuo et al., 2012). Vice versa, expression of NC-Scc1 had similar effects in another *in vitro* study (Schöckel et al., 2011). Here, centrosomes were isolated from Hek293 cells expressing NC-Scc1 together with hyperactive Separase. Quantification of centriole disengagement via IFM clearly showed inhibitory effects of NC-Scc1 (Schöckel et al., 2011). An immediate question is how expression of the non-cleavable versions can dominantly suppress disengagement if the corresponding wild type counterpart is normally cleaved? Especially as it was reproduced within this work that artificial cleavage of either Scc1 or PCNT is sufficient to trigger disengagement?

One possible explanation could be that expression of non-cleavable Scc1 has a dominant negative effect on cleavage of wild type PCNT by Separase and vice versa. This theory is based on the mechanism how Separase is normally kept inactive by Securin or Sgo2, namely by binding to the active site as a non-cleavable pseudosubstrate. Supportive data came from the Nasmyth group (Alexandru et al., 2001). A synthetic peptide resembling the cleavage site of Scc1 was a potent inhibitor of Separase when mutated to a non-cleavable version. The phosphorylated version of this peptide was even a ten times better inhibitor than the unphosphorylated peptide (Alexandru et al., 2001). Hence, limited amounts of active Separase at the centrosome might permanently bind to NC-PCNT or -Scc1 and might be titrated away from WT-Scc1 or -PCNT, respectively.

To put this theory into practice, an *in vitro* cleavage assay with active recombinant Separase was performed (Fig. 21A+B). ³⁵S-labeled full-length WT-Scc1, expressed in an *in vitro* transcription/translation (IVT/T) system, served as substrate. As competitors, bacterially expressed and purified fragments of NC-Scc1 (aa 107-271) and -PCNT (aa 2168-2331) were added in different concentrations. Before active Separase was added, substrate and competitors were incubated with Plk1 and Cdk1 in order to phosphorylate recombinant proteins, thereby enhancing binding of Separase. In accordance with this model, addition of NC-Scc1 or -PCNT clearly reduced the amount of WT-Scc1 cleavage, thus indicating an inhibitory effect of NC-substrates on Separase activity (Fig. 21). BSA was added to the

Results

reactions in order to keep the amount of added protein at a constant level of 10 μg and had no effect on the efficiency of Scc1 cleavage.

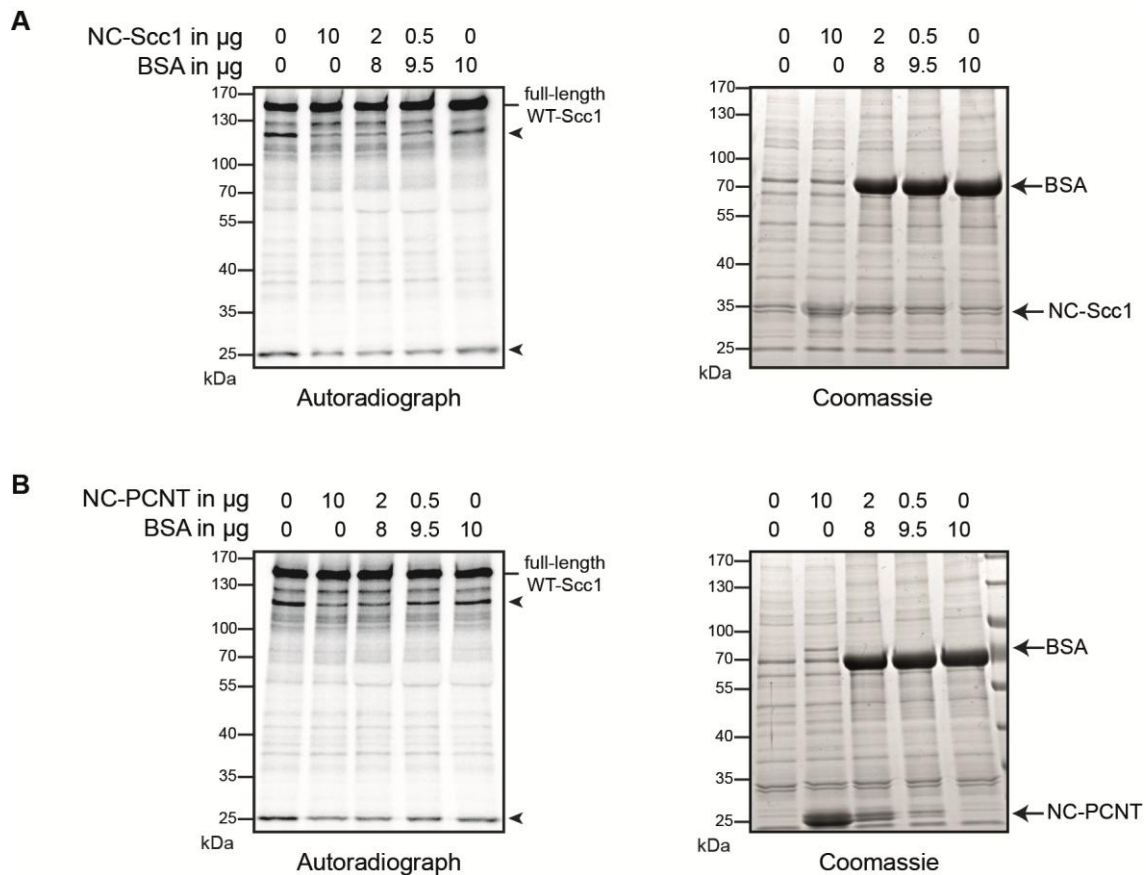


Fig. 21: Non-cleavable versions of Scc1 and PCNT act as dominant negative pseudosubstrates for Separase. Full-length ^{35}S -labeled WT-Scc1, expressed in an IVT/T reaction, served as substrate for the *in vitro* cleavage reaction with active Separase. As competitors, recombinant NC-Scc1 (aa 107-271) (**A**) or NC-PCNT (aa 2168-2331) (**B**) fragments were added in depicted concentrations. BSA was used to keep the amount of added recombinant protein at a constant level of 10 μg . Before active Separase was added, depicted reactions were incubated with Plk1 and Cdk1 kinase in presence of ATP. Samples were subjected to SDS-PAGE followed by autoradiography. Black arrowheads indicate cleavage fragments. Coomassie staining was performed prior to the Autoradiograph and served as control for the total amount of protein loaded. Note that, due to its highly acidic nature, the NC-Scc1 fragment is hardly stained by the Coomassie dye and therefore appears transparent (A).

Noteworthy, a reduced cleavage efficiency of *in vitro* expressed WT-Scc1 could also be observed when the experiment was carried out with WT-versions of Scc1 or PCNT as competitors (Fig. 22). This observation makes sense, since these versions are suitable substrates for Separase and might titrate away limited amounts of active recombinant Separase rather than inhibiting its activity. Further reasons are discussed in section 5.1.4.

Taken together, presented *in vitro* results provide an explanation for published results that the overexpression of non-cleavable Scc1 and PCNT versions efficiently suppress centriole disengagement (Lee & Rhee, 2012; Matsuo et al., 2012; Schöckel et al., 2011). These variants

might act as competitive inhibitors and might have a dominant negative effect on Separase dependent cleavage of the endogenous centrosomal substrates. With this assumption, published data that cleavage of either WT-Scc1 or -PCNT in unperturbed cells is sufficient to trigger disengagement remain valid.

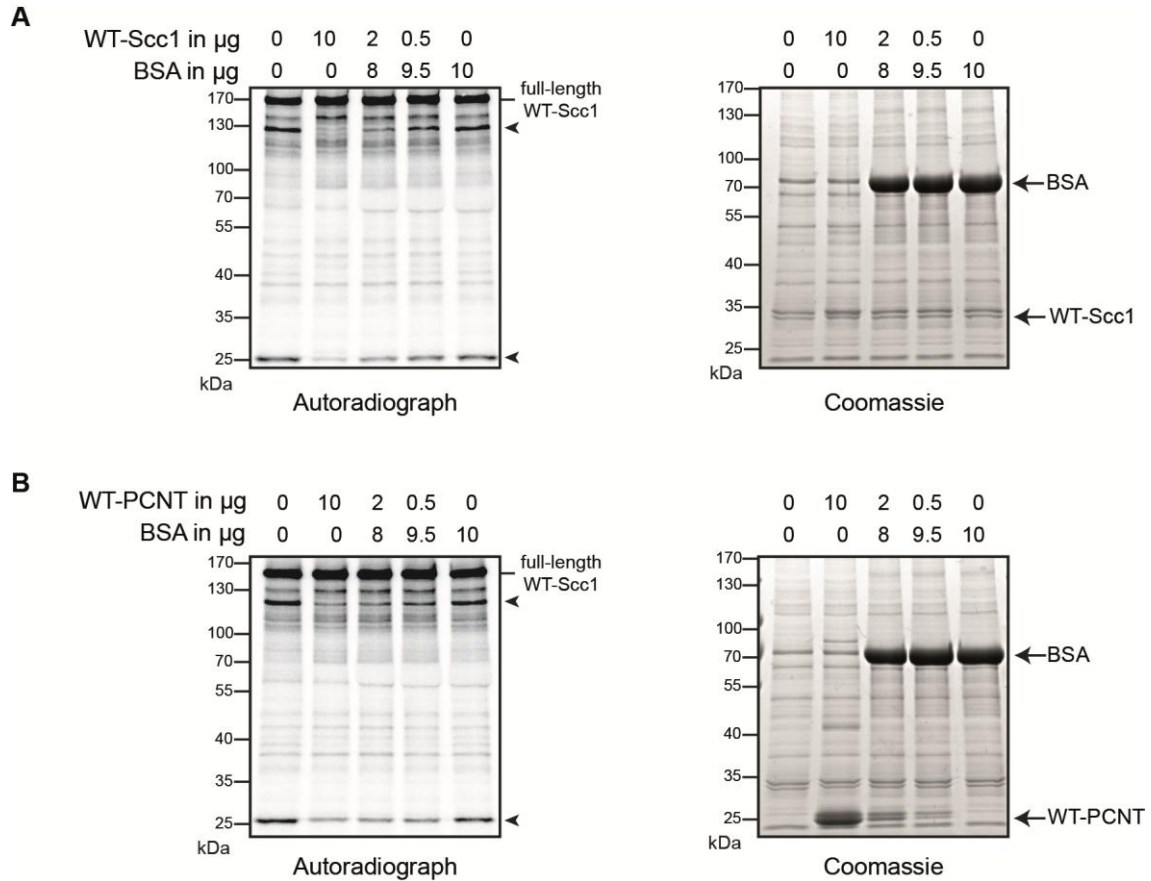


Fig. 22: Wild type versions of Scc1 and PCNT act as dominant negative pseudosubstrates for Separase. (A) Full-length ^{35}S -labeled WT-Scc1, expressed in an IVT/T reaction, served as substrate for the *in vitro* cleavage reaction with active Separase. As competitors, recombinant WT-Scc1 (aa 107-271) (A) or WT-PCNT (aa 2168-2331) (B) were added in depicted concentrations. BSA was used to keep the amount of added recombinant protein at a constant level of 10 μg . Before active Separase was added, depicted reactions were incubated with Plk1 and Cdk1 kinase in presence of ATP. Samples were subjected to SDS-PAGE followed by autoradiography. Black arrowheads indicate cleavage fragments. Coomassie staining was performed prior to the Autoradiograph and served as control for the total amount of protein loaded. Note that, due to its highly acidic nature, the WT-Scc1 fragment is hardly stained by the Coomassie dye and therefore appears transparent (A).

4.2 Phosphorylation-dependent conversion of PCNT into a suitable Separase substrate

As already mentioned in the introduction, residual centromeric Cohesin rings are cleaved by activated Separase in anaphase (Uhlmann et al., 1999). Phosphorylation of chromatin-bound Scc1 by Plk1 was shown to enhance the cleavage efficiency by Separase. Consistently, mutating ten serine residues within Scc1 to alanine reduced cleavage of chromatin bound Cohesin by nearly 50%. Six of the ten serine residues were located in direct vicinity of the two existing Separase cleavage sites (Alexandru et al., 2001; Hornig & Uhlmann, 2004). For the meiotic counterpart of Scc1, the kleisin Rec8, phosphorylation by meiotic kinases was even shown to be essential for cleavage by Separase (Brar et al., 2006; Katis et al., 2010). Further Separase substrates like MCL1 or BCL-XL also fully depend on prior phosphorylation in order to get cleaved by Separase (Hellmuth & Stemmann, 2020). Thus, given that the cleavage of Separase substrates is enhanced by or fully depend on phosphorylation, a potential impact of PCNT phosphorylation on the efficiency of cleavage by Separase remained to be determined. For that purpose, *in vitro* cleavage experiments with PCNT-fragments encoding for the Separase cleavage site were designed. As a first step, the required *in vitro* tools like active recombinant Separase and mitotic kinases had to be generated.

4.2.1 Generation of *in vitro* tools to study the putative PCNT conversion into a suitable Separase substrate

A Separase variant carrying a P1127A mutation was expressed in Hek293T cells and purified as described in 6.4.9. This mutation prevents the Pin1 mediated cis-trans isomerization of P1127 and, hence, binding of the inhibitor Cdk1-Cyclin B1 (Hellmuth et al., 2015). Bound Securin was degraded in a *Xenopus laevis* extract resulting in active (ac) recombinant Separase. Its activity was positively tested in a cleavage assay with *in vitro* expressed, ³⁵S-labeled WT-Scc1 (Fig. 23A). As a negative control served protease dead (PD) Separase (C2029S) (Stemmann et al., 2001), which was expressed and processed in the same manner like active Separase. Active Cdk1 was kindly provided by Markus Hermann from the chair of genetics. In context of this work, Plk1 was expressed in Hek293T cells as a kinase dead (KD, K82R), (Golsteyn et al., 1995) constitutively active (ca, T210D) (Qian et al., 1999) or wild type (WT) version and purified as described in 6.4.10. Their activities were successfully tested *in vitro* in a kinase assay (see 6.4.5) using the model substrate myelin basic protein

(MBP) (data not shown). Additionally, the Plk1 variants were also tested in a cleavage assay with recombinant Separase and *in vitro* expressed, ^{35}S -labeled Scc1. In consistency with published results (Alexandru et al., 2001), phosphorylation of Scc1 by WT- or ca-Plk1 clearly enhanced the cleavage efficiency of active Separase (Fig. 23B).

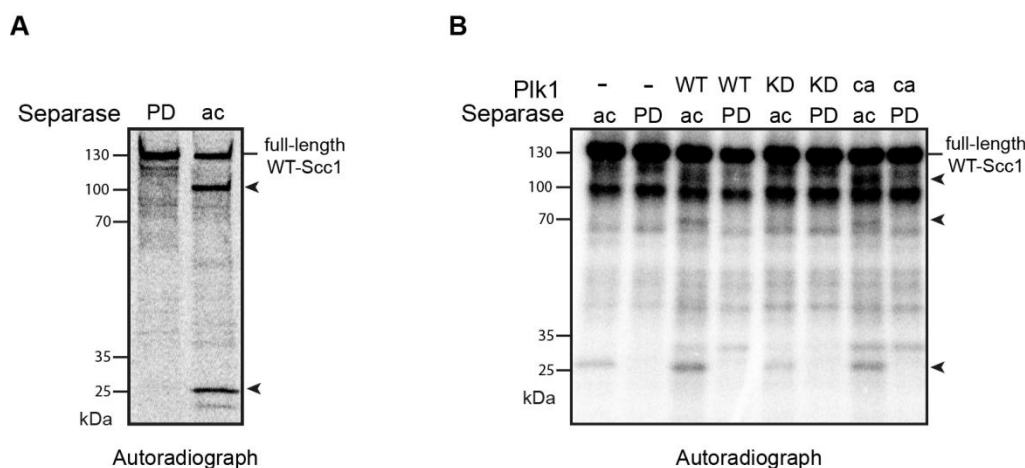


Fig. 23: Characterization of recombinant Separase and Plk1. (A) Purified recombinant protease dead (PD, C2029S) and hyperactive (ac, P1127A) Separase were tested in a cleavage assay with *in vitro* expressed, ^{35}S -methionine labeled WT-Scc1. Samples were subsequently analyzed by SDS-PAGE and autoradiography. Black arrowheads indicate cleavage fragments. (B) Constant amounts of *in vitro* expressed WT-Scc1 and recombinant Separase variants (PD or ac) were incubated with purified Plk1 variants (WT = wild type, KD = kinase-dead (K82R), ca = constitutively active (T210D)). Samples were subsequently analyzed by SDS-PAGE and autoradiography. Black arrowheads indicate cleavage fragments.

4.2.2 Sequential phosphorylation by Cdk1 and Plk1 turns PCNT into a suitable Separase substrate

With these tools at hand, the phosphorylation-dependent conversion of PCNT into a suitable Separase substrate could be studied in more detail. In an initial experiment, the residues 2211-2293 of PCNT, including its endogenous Separase cleavage site, were *in vitro*-expressed and subsequently incubated with the indicated combinations of kinases and recombinant Separase variants (Fig. 24). Strikingly, no substantial phosphorylation-induced mobility shift in the SDS-PAGE could be detected when PCNT was incubated with Plk1 alone. However, in combination with active Cdk1, Plk1 was able to substantially increase PCNT phosphorylation. This strongly favors a sequential phosphorylation with Cdk1 acting as priming kinase for Plk1. In accordance, efficient cleavage by Separase only became detectable when both active kinases were present. Hence, like for all known Separase substrates, phosphorylation seems to be important for turning PCNT into a suitable Separase substrate.

Results

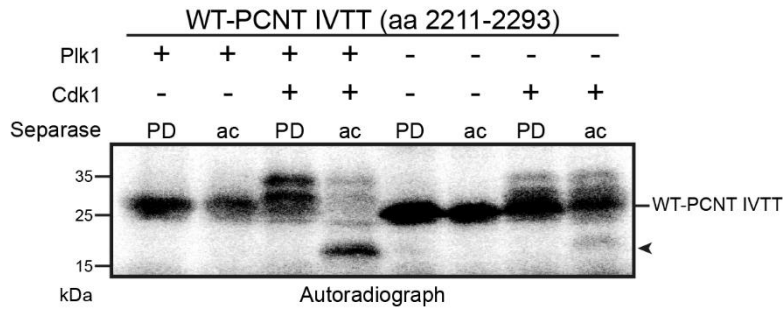


Fig. 24: Sequential phosphorylation by Cdk1 and Plk1 turns PCNT into a suitable Separase substrate. A ³⁵S-labeled WT-PCNT fragment (aa 2211-2293) encoding for the Separase cleavage site and surrounding sequences was expressed *in vitro*. Then, the PCNT fragment was incubated with active (+) or kinase-dead (-) recombinant Plk1 and/or Cdk1 for 30 min before active (ac) or protease-dead (PD) recombinant Separase was added for another 30 min. Subsequently, the reaction was stopped by addition of SDS sample buffer and samples were subjected to SDS-PAGE and autoradiography. Black arrowhead indicates cleavage fragments.

Considering these promising results, a closer look to the PCNT sequence revealed consensus phosphorylation sites for Plk1 and Cdk1 in direct vicinity to the Separase cleavage site (Fig. 25A and 25B). In a speculative model, Cdk1 might phosphorylate S2226 as a priming kinase, allowing Plk1 to bind via its PBD domain and subsequently phosphorylate the residues S2222 and/or T2235. If true, mutational inactivation of either of these residues to alanine should result in a strong decrease of Separase dependent cleavage or even prevent it. And indeed, compared to WT-PCNT, each point mutation led to a significant decrease in the cleavage efficiency by Separase. However, only mutation of all three residues to alanine (3Ala) effectively prevented cleavage by Separase *in vitro* (Fig. 25 C).

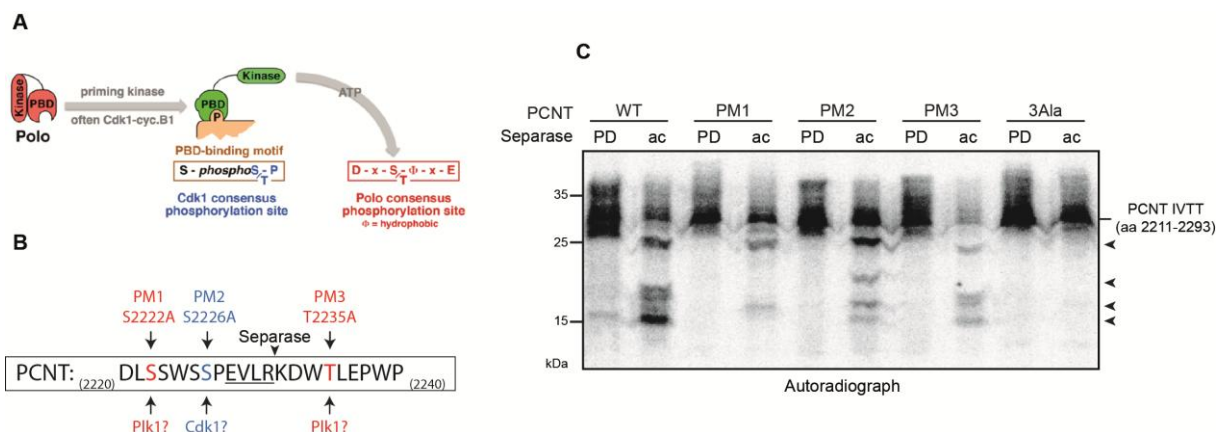


Fig. 25: Mapping of Cdk1 and Plk1 phosphorylation sites near the Separase cleavage site of PCNT. (A) Model illustrating sequential substrate phosphorylation through Cdk1 and Plk1. (B) Model depicting potential Plk1 and Cdk1 phosphorylation sites in direct vicinity of PCNTs Separase cleavage site. (C) Autoradiography of a cleavage assay performed with following PCNT fragments (aa 2211-2293): WT: wild type PCNT; PM1: mutational inactivation of S2222 to alanine; PM2: mutational inactivation of S2226 to alanine; PM3: mutational inactivation of T2235 to alanine; 3Ala: mutational inactivation of all three residues. The IVT/T reaction was performed with ³⁵S-methionine present. The PCNT fragments were incubated with active recombinant Plk1 and Cdk1 for 30min before active (ac) or protease-dead (PD) recombinant Separase was added for another 30 min. Subsequently, SDS-PAGE and autoradiography were conducted. Black arrowheads indicate cleavage fragments.

While performing depicted experiments, a study from the Rhee lab was published that also addressed the Plk1 regulation of PCNT cleavage (Kim et al., 2015). Treatment of human cell culture cells with the Plk1 inhibitor BI2536 suppressed PCNT cleavage by Separase upon mitotic exit indicating that phosphorylation is crucial for turning PCNT into a suitable substrate. Nine phosphorylation sites near the cleavage site were identified to be important for cleavage by Separase (T2154, T2160, S2183, S2189, S2222, S2259, S2267, S2318 and T2324). Mutational inactivation of all mentioned residues to alanine largely abolished cleavage, while mutating them to phospho-mimicking aspartate allowed efficient cleavage by Separase even in the presence of BI2536 (Kim et al., 2015). With the exemption of S2222, the identified residues differ from the three identified in this work.

As a consequence to this publication, a larger PCNT fragment (aa 2148-2391) including all nine identified residues from the Rhee study was used to repeat the *in vitro* kinase and cleavage assays. In accordance with the results presented in Fig. 25 and contradicting the results from the Rhee lab, mutational inactivation of the residues S2222, S2226 and T2235 to alanine was sufficient to prevent cleavage by Separase *in vitro* (Fig. 26). However, mutating the three residues to phospho-mimicking aspartate was not sufficient to allow cleavage by Separase in the absence of mitotic kinases. On the contrary, detection of cleavage by Separase upon addition of Plk1 and Cdk1 indicates an additional crucial residue to the three identified so far (see also discussion chapter 5.2).

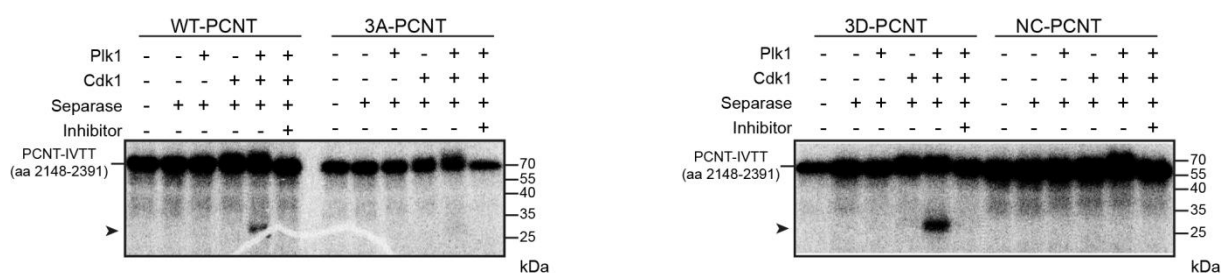


Fig. 26: Mutational inactivation of three phosphorylation sites within PCNT prevents cleavage by Separase. Autoradiography of a cleavage assay performed with following PCNT fragments (aa 2148-2391): WT: wild type PCNT; 3A: mutational inactivation of S2222A, S2226A and T2235A; 3D: phospho-mimicking mutant S2222D, S2226D and T2235D; NC: non-cleavable Separase cleavage site E2228R and R2231A. The IVT/T reaction was performed with ^{35}S -methionine present. The PCNT fragments were incubated with active (+) or kinase-dead (-) recombinant Plk1 and/or Cdk1 for 30 min before active (+) or protease-dead (-) recombinant Separase was added for another 30 min. As inhibitors, BI2536 (Plk1 inhibitor) and RO 3306 (Cdk1 inhibitor) were added when indicated (+). Subsequently, SDS-PAGE and autoradiography were conducted. Black arrowheads indicate cleavage fragments.

Given these promising *in vitro* results, the question arose whether they could be reproduced in cultured cells using full-length versions of PCNT. Therefore, PCNT constructs encoding the 3A- or 3D- variants were generated and transiently transfected into Hek293 cells. WT-PCNT and NC-PCNT encoding constructs served as positive and negative control, respectively. Transfected cells were pre-synchronized in S-phase with thymidine for 20 h before they were released and finally arrested with taxol in metaphase of the following mitosis. Addition of ZM447439, an inhibitor of the Aurora B kinase, forced these cells to override their SAC-arrest and to enter anaphase. Western blot samples were taken from the taxol arrested cells, as well as 1 h and 2 h after ZM447439 addition. Successful checkpoint override was indicated through activation and subsequent self-cleavage of Separase in a Western Blot analysis (Fig. 27A). Furthermore, degradation of the mitotic marker Cyclin B1 and dephosphorylation of histone H3 (pHH3) confirmed progression through anaphase and late mitosis. Immunodetection of the expressed PCNT versions revealed that WT- and 3D-PCNT were cleaved by activated Separase upon mitotic exit, while 3A- and NC-PCNT were not. Hence, mutational inactivation of the three residues to alanine in direct vicinity of the cleavage site is sufficient to abolish cleavage by Separase *in vivo*, confirming the *in vitro* results presented above (Fig. 26). In order to gain more information about the importance of Plk1 kinase in this process, the same assay was conducted but 2h prior to the induced SAC override, the Plk1 inhibitor BI2536 was added to the culture medium as well. Western blot analysis of Separase and the mitotic markers indicated a successful checkpoint override (Fig. 27B). However, without Plk1 activity, expressed WT- and 3D-PCNT were no longer cleaved. This observation lends further proof to the phosphorylation dependent conversion of PCNT into a suitable Separase substrate and provides a direct connection between the crucial Plk1 activity in early mitosis and centriole disengagement triggered by active Separase in late mitosis.

Taken together, the *in vitro* and *in vivo* results presented in this work shed a new light on how human cells tightly control centriole disengagement and licensing of centriole duplication during mitosis. PCNT phosphorylation by Plk1 was reported to be essential for the PCM maturation during early mitosis so far. Now, it is also directly linked to centriole disengagement, illustrating how Plk1 and Separase act cooperatively but timely separated in licensing of centriole duplication (for further discussion see chapter 5.3).

Results

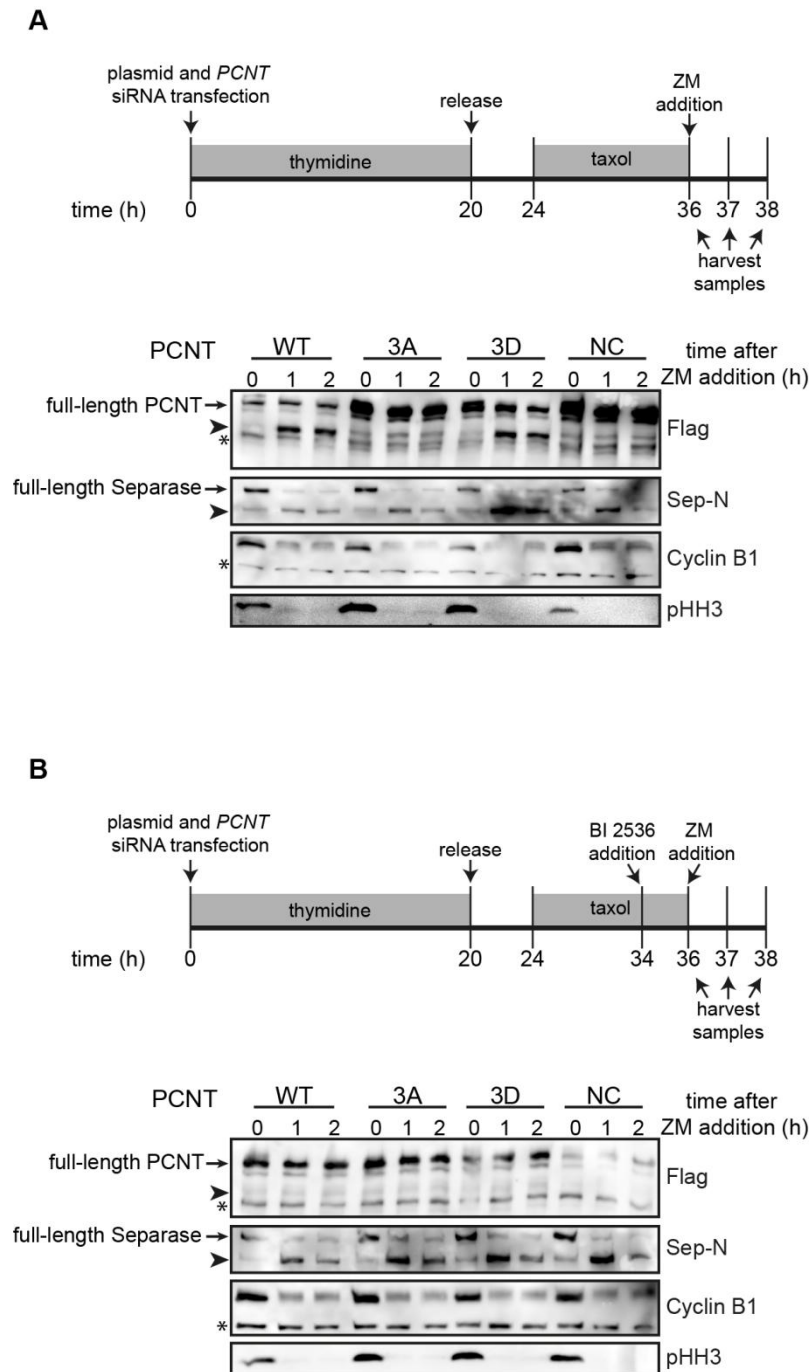


Fig. 27: PCNT phosphorylation by Plk1 is crucial for Separase dependent cleavage. (A) Plasmids encoding for following full-length *PCNT* variants were, together with siRNA against endogenous *PCNT*, transiently transfected in Hek293T cells: WT: wild type *PCNT*; 3A: mutational inactivation of S2222A, S2226A and T2235A; 3D: phospho-mimicking mutant S2222D, S2226D and T2235D; NC: non-cleavable Separase cleavage site E2228R and R2231A. At the same time, thymidine was added for 20 h in order to synchronize cells at the G1/S-barrier. Then, cells were released through washout and 4 h later, taxol was added to the media to arrest cells in mitosis. The SAC-arrest was overridden through addition of ZM447439 (ZM), an inhibitor of Aurora B kinase. Samples were taken at the indicated time points and subjected to SDS-PAGE and Western blot analysis. Antibodies against the Flag-tag (to detect *PCNT* cleavage), the N-terminus of Separase (to detect self-cleavage as a marker of activity), Cyclin B1 and pHH3 (as mitotic marker) were used. Black arrowheads indicate cleavage fragments. Asterisks indicate cross-reactive bands. (B) The same assay as described in A was performed, but 2 h prior to the addition of ZM447439, the Plk1 inhibitor BI 2536 was added to the cells as well.

5 Discussion

5.1 Artificial inactivation of centrosomal Cohesin or PCNT triggers centriole disengagement

Results presented in this thesis provide deeper insights into the complex mediation of centriole engagement. Stable cell culture cell lines were generated that inducibly express artificial cleavable version of Scc1 and PCNT. Individual and combined inactivation through the corresponding protease(s) allowed determining their respective contribution to centriole engagement. As this is the first time that both factors have been combined in the same experimental setup, obtained results contribute to solve an apparent contradiction in the centrosome field. So far, Separase dependent cleavage of PCNT or Cohesin has independently been reported to be sufficient for triggering disengagement (Lee & Rhee, 2012; Matsuo et al., 2012; Schöckel et al., 2011). Results provided in this work suggest both to be true: artificial inactivation of PCNT or Scc1 is each sufficient to trigger disengagement *in vitro*. Interestingly, combined inactivation revealed almost no additive effects when quantified on isolated centrosomes. Possible reasons should be discussed in more detail.

5.1.1 Artificial cleavage of Cohesin rings induces centriole disengagement

Tsou and Sterns were the first to directly link Separase and Plk1 activity to centriole disengagement in late mitosis (Tsou et al., 2009). Cohesin as a Separase substrate was then assumed to mediate not only cohesion between chromosomes but also centrioles. Subsequently, this speculation was supported through numerous independent localization and functional studies: Not only knockdown of Cohesin subunits led to disengagement *in vivo*, artificial, Separase-independent cleavage of the Cohesin ring within one of two different engineered subunits did also trigger centriole disengagement *in vitro* (Beauchene et al., 2010; Díaz-Martínez et al., 2010; Schöckel et al., 2011; Wong & Blobel, 2008). Results presented in section 4.1.3 of this work provide further experimental proof for Cohesin's importance in centriole engagement. Isolated centrosomes from cells expressing artificially cleavable versions of Scc1 were treated with the corresponding protease *in vitro*. With no active Separase present, treatment of TEV- or HRV-cleavable Scc1 with the corresponding protease reproducibly led to efficient proteolysis and triggered centriole

disengagement (Fig. 13 and Fig. 16). In accordance to the already mentioned published data (Schöckel et al., 2011), approximately 40% of centriole disengagement could be triggered by proteolytically inactivation of the Cohesin ring *in vitro*. Hence, Cohesin has an unquestionable function in mediating centriole engagement.

With the confirmation of Cohesin's importance in mediating centriole engagement, the immediate question is how the tight coupling of centrioles is achieved and maintained? Each mitotic centrosome consists of two centrioles embedded in a highly ordered protein matrix known as the pericentriolar material (PCM) (Mennella et al., 2014). From the time of their synthesis in S-phase until late mitosis, the newly formed daughter centriole is tightly coupled to her mother centriole, serving as an intrinsic block of reduplication and, hence, as a copy number control (Firat-Karalar & Stearns, 2014). Cohesin might contribute to centriole engagement in two different ways: First, Cohesin as a ring might entrap an unidentified substrate that directly tethers the two centrioles together (Fig. 28). Second, Cohesin could contribute to indirect tethering of the two centrioles through a matrix entrapment by the surrounding PCM (Sluder, 2013). Here, Cohesin could localize essential components to the centrosome or could positively influence their activities (Fig. 28). Cleavage of the Cohesin ring in return would weaken the structural integrity of the PCM and allow a greater spatial distance between the centrioles through the pushing and pulling forces of the mitotic spindle. This spatial distance would represent the licensing step for duplication in the next S-phase.

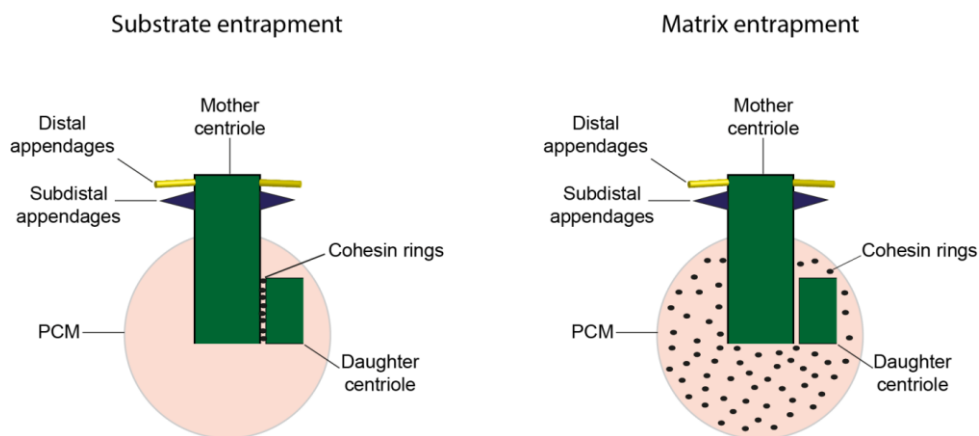


Fig. 28: Mediation of tight engagement between the mother and emerging daughter centriole in S-phase.

In dividing cells, a centriole duplicates once in S-phase. The emerging daughter centriole is formed adjacent and in perpendicular orientation to the corresponding mother centriole. From the time of their synthesis until their disengagement in late mitosis, mother and daughter centrioles remain tightly coupled. Cohesin might contribute to this centriole engagement through substrate entrapment of a yet unidentified substrate. Alternatively, cohesin could be dispersed throughout the interphase PCM and keeps centrioles engaged through a matrix entrapment. Either way, the tight coupling of centrioles prevents re- or overduplication and, hence, serves as a copy number control.

5.1.2 Artificial PCNT cleavage triggers centriole disengagement

Results presented in this work confirm that artificial cleavage of PCNT triggers centriole disengagement as well. Treatment of engineered HRV-cleavable PCNT with the corresponding protease triggered disengagement *in vitro* when quantified on isolated centrosomes (see Fig. 17. and Fig. 20). However, compared to the published *in vivo* effects of PCNT inactivation by the Takahashi and Rhee labs, the generated *in vitro* effects in this work were rather low and reduced by more than two-thirds (Lee & Rhee, 2012; Matsuo et al., 2012). In order to discuss possible reasons for this observation, it is important to understand how PCNT mediates engagement on the one hand and how cleavage by Separase triggers disengagement on the other hand.

PCNT, an elongated scaffold protein, serves as the main anchor for centrosomal proteins involved in microtubule nucleation like the γ -TuRC (Kim & Rhee, 2014; Lee & Rhee, 2011; Takahashi et al., 2002). During interphase, PCNT adopts a fiber like distribution in the highly ordered PCM, with the C-Terminus located near the centriole wall and the N-terminus extending into the PCM. Upon entry into mitosis PCM maturation takes place, thereby increasing the size and microtubule nucleation capacity of the centrosome dramatically. PCNT is strongly enriched at mitotic centrosomes, but adopts a less ordered, matrix like distribution in complex with proteins like Cep215, Cep192 and the γ -TuRC (Lawo et al., 2012). This expanding outer PCM matrix is both, source of an enhanced microtubule-nucleation capacity and a shield to resist against the pushing and pulling forces of the mitotic spindle (Sluder, 2013).

Support for the matrix entrapment theory of centrioles came from a study in Chinese hamster ovary (CHO) cells (Loncarek et al., 2008). Treatment of cells with hydroxyurea induced formation of overduplicated centrosomes consisting of one mother and two daughters (so called ‘triplosomes’). Subsequently, laser microsurgery experiments were conducted. Despite ablation of the mother centriole, movement of the two daughter centrioles remained coordinated. A possible linker tethering together mother and daughter centrioles would have been destroyed under given circumstances (Loncarek et al., 2008). In accordance, Separase depletion in *C. elegans* early embryos could be rescued by chemically induced enhancement of microtubule stability and, hence, pulling and pushing forces of the mitotic spindle. As a consequence, the PCM was disassembled and centriole separation allowed for an unperturbed duplication in the following S-phase (Cabral et al., 2013). Assuming matrix entrapment of centrioles, the question is how Separase dependent cleavage of PCNT triggers disengagement? In contrast to the Cohesin ring, which might entrap a yet unidentified

substrate, PCNT as an elongated scaffold protein fulfills its main functions through direct protein-protein interactions (Salisbury, 2003; Takahashi et al., 2002). Hence, Separase activity might directly lead to loss of crucial interactor(s) at its designated cleavage site, or it might lead to loss of protein-protein interactions through a long-range allosteric mechanism. Either way, the PCM starts to lose its integrity and forces of the mitotic spindle are more and more capable to disassemble the outer PCM. As this process takes time, it might explain the time gap between peak activity of Separase in anaphase and the visualization of disengagement in late telophase.

Interestingly, cleavage of PCNT by Separase generates a C-terminal fragment that is rapidly degraded by the N-end rule pathway (Lee & Rhee, 2012). Within this sequence lies the PACT domain, responsible for centrosomal targeting of PCNT. One might assume that its degradation leads to loss of centrosomal PCNT localization or leads to loss of crucial protein-protein interactions. However, the N-terminal fragment is retained at centrosomes after Separase dependent cleavage and only gradually decreases, concomitantly with PCM disassembly (Lee & Rhee, 2012). This indicates that the PACT domain is important for initial localization but not for persistence of PCNT at the centrosome. In accordance, a point mutation stabilizing the C-terminal fragment at the centrosome does not abolish disengagement (Lee & Rhee, 2012). Hence, it is not the rapid degradation of the C-terminus that triggers disengagement, but rather cleavage by Separase at this particular site (aa 2230). This theory is supported by results presented in section 4.1.4 in this work. During execution of *in vitro* disengagement assays, unspecific cleavage of WT-PCNT by HRV protease was detected. The first cleavage site (aa 652) could be mapped to the N-terminal coiled coil region while the second one (aa 2272) lies in vicinity of the endogenous Separase cleavage site (aa 2230) (Fig. 19). Although highly efficient, unspecific cleavage of PCNT barely triggered disengagement (<10%) when quantified *in vitro* on isolated centrosomes. This effect was furthermore only detectable in single stable cell lines expressing endogenous PCNT and a transgenic Scc1 variant (Fig. 12 D, Fig. 16C). Upon induction of PCNT expression in double transgenic cell lines, this effect was negated, probably because of higher protein levels (Fig. 14 D, Fig. 20 E). Taken together, this low impact on disengagement might simply reflect assay variance or indicate marginal effects of unspecific PCNT cleavage on the PCM composition. In future, it will be crucial to unravel mechanistic consequences of Separase dependent cleavage, e.g. in regards to loss of specific protein-protein interactions or induced conformational changes of PCNT. Furthermore, it would be interesting to investigate consequences of HRV expression *in vivo*. Transient transfection of HRV protease encoding

plasmids with subsequent high expression of corresponding protease might indicate possible impacts of unspecific PCNT cleavage on centrosome composition or centriole engagement with mitotic spindle forces present.

Additionally, PCNT as a novel HRV protease substrate might provide deeper insights into processes during the rhinovirus infection cascade. Many viruses accumulate at centrosomes, using it as the main hub for organizing cellular or particle transport (Naghavi & Walsh, 2017). Microtubule dynamics and stability can be increased or decreased, depending on the virus and its stage of infection (da Silva & Naghavi, 2023; Naghavi & Walsh, 2017). Hence, infecting cells with human rhinovirus could be used to confirm PCNT as a substrate for HRV protease and to investigate further details of the virus life cycle.

With the given information regarding PCNTs role in mediating centriole engagement, the different results obtained by mentioned *in vitro* or *in vivo* assays might become more plausible. The *in vitro* assay performed in this work used cells arrested in mitosis with nocodazole prior to harvest and isolation of centrosomes. Hence, *in vitro* cleavage with TEV and/or HRV protease was performed in a whole cell lysate without spindle microtubules and in absence of pushing and pulling forces. PCM disassembly might therefore be delayed and the percentage of centriole disengagement reduced. In the *in vivo* studies, on the contrary, expression of a non-cleavable (NC) PCNT version efficiently blocked disengagement in late mitosis (Lee & Rhee, 2012; Matsuo et al., 2012). Turning these NC-PCNTs into TEV-cleavable versions efficiently rescued disengagement and subsequent duplication upon transfection of a TEV-protease encoding plasmid (Lee & Rhee, 2012; Matsuo et al., 2012). As centrosomes were exposed to forces of the mitotic spindle, centriole disengagement might be accelerated. Noteworthy, in cells expressing NC-PCNT, the majority of centrosomes eventually disengaged and duplicated in late S-phase or G2-phase without PCNT being cleaved (Lee & Rhee, 2012). One possible explanation could be that in the absence of mitotic kinases, the outer PCM gradually shrinks throughout interphase. Below a certain threshold, the integrity of the PCM is insufficient to resist the forces of the interphase microtubule network and, especially, the pulling forces of astral microtubules. The spatial distance between the centrioles increases to an extent that allows for delayed duplication in late interphase. As a consequence, PCNT cleavage by Separase can be described as necessary for timely centriole disengagement in late mitosis, but not as an essential step for centrosome duplication in the next cell cycle.

5.1.3 Theories for the missing additive effects upon artificial inactivation of centrosomal Cohesin and PCNT

Assuming matrix entrapment of centrioles, with Cohesin rings and PCNT being dispersed throughout the PCM in order to enhance its structural integrity, one might expect additive effects upon artificial inactivation of both factors at the same time. The 40% disengagement quantified *in vitro* upon cleavage of centrosomal Cohesin would add up quite well with the 60% disengagement quantified *in vivo* upon PCNT inactivation (Lee & Rhee, 2012; Matsuo et al., 2012; Schöckel et al., 2011). However, simultaneous inactivation of Cohesin rings and PCNT through artificial cleavage revealed no substantial additive effects during *in vitro* disengagement assays (Fig. 17 and Fig. 20). One might suspect that this is caused by the chosen experimental approach, in which the centrosomes are isolated and examined in an environment that lacks spindle forces. Additionally, during the preparation, centrosomes are centrifuged through a sucrose cushion directly onto cover slips and one might suspect this procedure to exert mechanical stress and, hence, to have an impact on centrosome composition or even quantified disengagement. However, each *in vitro* assay was performed with an internal control, in which centrosomes from an untreated lysate were processed accordingly. Quantified disengagement in this sample was subtracted from the others, leaving excess disengagement solely accountable to the treatment with corresponding protease(s).

Yet, a more plausible explanation may be fundamental differences between PCNT and Cohesin in mediating centriole engagement. In particular, a spatiotemporal division of labor between both factors, strictly coordinated with the centrosome and cell cycle, seems to be possible. As mentioned before, the defining steps of the centrosome cycle are duplication in S-phase, centrosome separation at mitotic onset and centriole disengagement in late mitosis (Fujita et al., 2016). These steps are synchronized with the chromosome cycle, in which sister chromatids are duplicated in S-phase and separated in late mitosis as well (Haarhuis et al., 2014). Cohesin as a molecular ‘glue’ holds together both, centrioles and sister chromatids, from the time of their synthesis until their coordinated dissolution by the same key players, Separase and Plk1 (Schöckel et al., 2011). Due to the striking parallels between the chromosome and centrosome cycle, it is tempting to speculate that centrosomal Cohesin gets loaded and becomes cohesive during S-phase as well. Until Cohesin gets cleaved by Separase in late mitosis, it mediates substantial structural integrity of the interphase PCM and keeps the centrioles engaged. Whether this is mediated by direct entrapment of a yet unidentified substrate or by indirect tethering of centrioles through a matrix entrapment remains to be determined (Fig. 29). PCNT, on the contrary, is dispensable in interphase as artificial cleavage

of PCNT in S-phase does not trigger disengagement (Lee & Rhee, 2012). Upon entry into mitosis however, PCNT gets strongly enriched during the outer PCM expansion (Woodruff et al., 2014). It is highly unlikely but not impossible, that Cohesin gets recruited and becomes cohesive in the outer PCM as well. But as hints for a possible prophase pathway at the centrosome are existing (Mohr et al., 2015) and as the anti-cohesive factor Wapl exhibits peak activity in early mitosis (Gandhi et al., 2006), it is hard to imagine that cohesive Cohesin can be established at the outer centrosomal layer at this time. Hence, while Cohesin seems to be important for centriole engagement during S- and G2-phase, PCNT might mainly contribute to the structural integrity of the outer centrosomal layer during mitosis. The missing additive effect on centriole disengagement upon artificial cleavage of both factors could therefore originate in this spatially different localization and division of labor (Fig. 29).

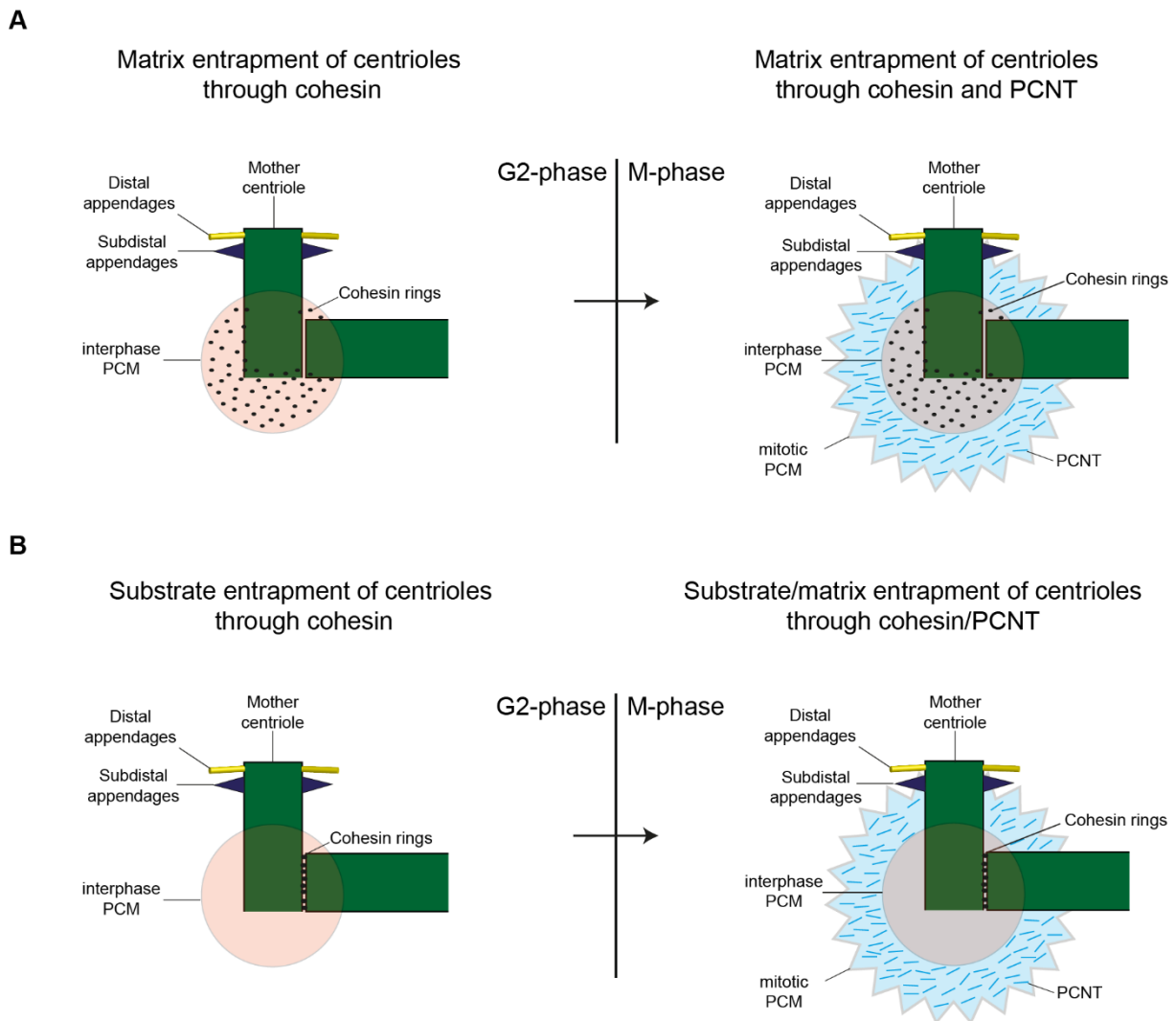


Fig. 29: Speculative model for the mediation of centriole engagement through cohesin and PCNT.

Fig. 29: (cont.) (A) Cohesin might contribute to indirect tethering of centrioles through a matrix entrapment during interphase. Upon entry into mitosis PCNT hyper accumulates at the outer PCM layer and defines its structural integrity during maturation. **(B)** Alternatively, cohesin could mediate centriole engagement through direct entrapment of an unknown substrate. PCNT becomes enriched in the outer PCM upon mitotic entry without cohesive cohesin being established as well. Hence, PCNT would solely contribute to the structural integrity of the outer PCM during mitosis. Admittedly, PCNT is also the main structural component of the interphase PCM. However, artificial cleavage of PCNT in interphase triggered no centriole disengagement (Lee & Rhee, 2012). Therefore, PCNT's role in interphase is not shown in the presented model.

Sticking to this model might also explain experimental *in vivo* results questioning Cohesin's importance in mediating centriole engagement. In a study performed with *Drosophila* embryos arrested in metaphase of mitosis, artificial cleavage of an engineered TEV-Scc1 triggered sister chromatid separation but no centriole disengagement (Oliveira & Nasmyth, 2013). This observation can simply reflect fundamental differences between flies and human cells in mediating centriole engagement. However, the PCNT homologue D-PLP has been neglected in this *in vivo* study. As D-PLP is intact in the outer layer of the PCM, it probably provides sufficient structural integrity although Scc1 is efficiently cleaved. Therefore, disengagement within the 'inner layer' of the PCM might be masked, although present and, hence, cannot be monitored in given experimental setup. This raises the immediate question why artificial cleavage of Cohesin rings triggered disengagement in presented *in vitro* assays? The answer might be that only this particular experimental setup provides conditions that allowed for the visualization and quantification of disengagement upon Cohesin inactivation. Performing artificial cleavage of Cohesin rings on isolated centrosomes with no pushing forces of the mitotic spindle present (due to added spindle poisons) probably enabled the centrioles to separate to an extent that allowed visualization of disengagement. This more direct and mechanistic approach during performed *in vitro* assays might be their great advantage. Hence, it would be interesting, to use the *in vitro* disengagement assay on a stable cell line expressing artificially cleavable Scc1 and NC-PCNT. In this scenario, cleavage of Scc1 should also trigger disengagement.

5.1.4 Non-cleavable versions of Scc1 or PCNT might interfere with Separase activity

Two independent studies reported NC-PCNT to inhibit centriole disengagement upon mitotic exit (Lee & Rhee, 2012; Matsuo et al., 2012). Given that centrosomal Cohesin rings are normally cleaved under given circumstances, these results are conflicting with the statement that artificial proteolysis of either Cohesin or PCNT is sufficient to trigger centriole disengagement.

One apparent reason for this observation could be the different levels of both centrosomal proteins. NC-PCNT as the more abundant protein might provide sufficient structural integrity of the PCM despite Cohesin being cleaved by Separase. However, this reason disregards above-mentioned statement again, that cleavage of either PCNT or Cohesin is sufficient to trigger disengagement. Another theory could be that NC-PCNT titrates away the limited amounts of active Separase at the centrosome and, hence, has a dominant-negative effect on cleavage of endogenous Scc1 and PCNT. Separase itself is kept inactive through a comparable mechanism. Securin and Sgo2 both carry non-cleavable pseudosubstrate motifs that bind to and block the active site of Separase (Boland et al., 2017; Hellmuth et al., 2020). Cdk1-Cyclin B1 uses an even more elegant mechanism by re-orienting auto-inhibitory loops from Separase itself into its active site (Yu et al., 2021). Hence, Separase could permanently bind to NC-PCNT during its short, active time window *in vivo*. In the course of this work, this theory was tested *in vitro* in a competition cleavage assay with recombinant, active Separase and a radioactively labeled WT-Scc1 generated in an IVT/T, as substrate. And indeed, it could be shown that the addition of recombinant NC-Scc1 or -PCNT fragments reduced the amount of cleaved WT-Scc1, indicating an inhibitory effect on Separase activity (Fig. 21). Noteworthy, the same could be observed when recombinant WT-Scc1 or -PCNT fragments were added as competitors (Fig. 22). Since these versions are suitable substrates for Separase as well, the cleavage reduction of radioactively labeled WT-Scc1 makes sense. Especially, if limited amount and activity of recombinant Separase are taken into account. Furthermore, added WT-Scc1 and -PCNT competitors were expressed in *E. coli* and hence came in a dephosphorylated form. Addition of mitotic kinases Plk1 and Cdk1 might not have provided sufficient kinase activity to turn the majority of recombinant proteins into suitable Separase substrates. Partial phosphorylation might even facilitate binding of Separase to the substrates without enhancing cleavage efficiency. Hence, added recombinant WT-Scc1 and -PCNT might partially have resembled NC-variants due to their phosphorylation status.

A further explanation is based on the aforementioned theory that Cohesin and PCNT separately contribute to centriole engagement within the inner and outer PCM layer, respectively (see section 5.1.3). Expression of NC-PCNT might keep the structural integrity of the outer PCM intact in mentioned *in vivo* studies (Lee & Rhee, 2012; Matsuo et al., 2012). At the same time, Cohesin cleavage at the inner PCM layer might already have primed the centrioles for subsequent duplication in S-phase. Accordingly, in cells expressing NC-PCNT, the outer PCM gradually decreases throughout interphase due to missing activity of mitotic

kinases (Lee & Rhee, 2012; Matsuo et al., 2012). Thereby, ‘inner disengagement’ caused by Cohesin cleavage could be unraveled together with the ability of centrioles to duplicate.

Sticking to the division of labor theory between Cohesin and PCNT even provides an explanation for results from a study performed by Tsou et al, in which NC-Scc1 was expressed in HeLa cells (Tsou et al., 2009). While sister chromatid separation failed completely, centriole disengagement occurred normally in these cells as judged by time lapse IFM throughout mitosis (Tsou et al., 2009). Under given experimental conditions, PCNT was cleaved by Separase in late mitosis. Centrosomal Cohesin rings, whose number might already have been decreased by a possible prophase pathway upon mitotic entry, seemed to be insufficient to resist the forces of the mitotic spindle. Furthermore, level of endogenous Scc1 was not decreased by siRNA mediated knockdown, leaving part of the residual centrosomal Cohesin rings even susceptible to cleavage by Separase.

On the contrary, expression of NC-Scc1 suppressed centriole disengagement in another study (Schöckel et al., 2011). Here, hyperactive Separase (S1126A) was inducibly expressed in Hek293 cells arrested with the spindle poison nocodazole in prometaphase. Expression of NC-Scc1 not only suppressed sister chromatid separation but also centriole disengagement (Schöckel et al., 2011). One possible reason might be that expression of hyperactive Separase caused PCNT cleavage already in prometaphase. As a consequence, PCNT transport to the centrosome together with recruitment of further crucial factors for the PCM maturation could have been compromised in these cells. Hence, Cohesin rings probably provided sufficient structural integrity despite PCNT not being enriched at the outer PCM.

5.2 The fundamental role of Plk1 in licensing of centriole duplication

Plk1 activity in early mitosis, together with Separase activity in late mitosis, was reported to be essential for centriole disengagement and their subsequent duplication in following S-phase (Tsou et al., 2009). While centrosomal Cohesin as well as PCNT have been identified and characterized as crucial Separase substrates (Lee & Rhee, 2012; Matsuo et al., 2012; Schöckel et al., 2011), numerous Plk1 targets facilitating pivotal mitotic events illustrate a rather complex regulatory network (Kalous & Aleshkina, 2023). Results presented in section 4.2.2 of this work show one particular Plk1 activity, namely the conversion of PCNT into a

suitable Separase substrate, to be one of the crucial activities upon mitotic entry. In direct vicinity of the Separase cleavage site, one putative Cdk1 and two putative Plk1 consensus phosphorylation sites could be functionally identified (S2222, S2226 and T2235). Mutational inactivation of these three phosphorylation sites efficiently abolished cleavage by Separase *in vitro* and *in vivo* (Fig. 25-27). As Cdk1 activity was crucial in performed *in vitro* experiments (Fig. 26), it might act as priming kinase, allowing binding of Plk1 via its PBD domain and subsequent phosphorylation of its designated sites. The potential Cdk1 phosphorylation site (S2226) is located six residues upstream (P6) of the Separase cleavage site (P1). This P6 position was shown to be important for enhancing cleavage of Scc1 or Meikin by Separase, probably by binding to a positively charged patch in direct vicinity of the Separase cleavage site (Alexandru et al., 2001; Maier et al., 2021). In case of the pseudosubstrate Securin, a glutamate at the P6 position resembles phosphorylation and probably enhances binding to the active site of Separase (Boland et al., 2017). Unfortunately, mutating the important P6 residue of PCNT, together with the two further residues, to aspartate did not turn PCNT into a constitutive substrate and hence, did not facilitate cleavage *in vivo* when Plk1 was inhibited (Fig. 27). Therefore, it would be interesting to repeat *in vitro/in vivo* assays with the serine residues at Position P7 and/or P9 taken into account (see Fig. 25).

While performing the assays shown in this work, a publication from the Rhee lab identified nine phosphorylation sites within PCNT to be crucial for Separase dependent cleavage (Kim et al., 2015). Except for one residue, they differ from the identified residues in this work and are more distant in the primary structure from the Separase cleavage site. Although these results could be partly contradicted in this work, it might still be interesting to mutate each single of these residues to aspartate in a combinatorial approach with the three phosphorylation sites identified in this work. Thereby, another crucial phosphorylation site could be found allowing cleavage by Separase when Plk1 was inhibited. Taken together, presented data provide a direct link between crucial Plk1 activity in early mitosis and Separase activity in late mitosis. Like it was already shown for the Separase substrates Scc1, Rec8, BCL-XL, MCL1 and Meikin (Alexandru et al., 2001; Brar et al., 2006; Hellmuth & Stemmann, 2020; Hornig & Uhlmann, 2004; Katis et al., 2010; Maier et al., 2021), PCNT phosphorylation clearly enhances cleavage efficiency by Separase in late mitosis.

This novel function adds another layer of regulation to the complex network of Plk1 activity in terms of licensing centriole duplication. As already mentioned before, Plk1 activity is also crucial for the outer PCM maturation during mitotic onset (Blanco-Ameijeiras et al., 2022). Phosphorylation of PCNT, amongst other components, initiates centrosome maturation and

leads to recruitment of crucial components for nucleation of the mitotic spindle (Haren et al., 2009; Lee & Rhee, 2011). Interestingly, Plk1 activity fulfills both, recruitment of PCNT to the centrosome and its conversion into a suitable Separase substrate, thereby mediating its timely destruction. Recent data shed a new light on the PCNT recruitment to the centrosomes (Remsburg et al., 2023; Sepulveda et al., 2018). Apparently, PCNT mRNA is enriched and translated near the centrosome. In a co-translational manner, nascent PCNT polypeptides interact with the dynein motor complex via a putative N-terminal LIC1-domain (Sepulveda et al., 2018). Within this domain, two crucial Plk1 phosphorylation sites were identified and thought to be essential for mediating PCNT-dynein interaction (Lee & Rhee, 2011; Sepulveda et al., 2018). Translation of PCNT under spatiotemporal control of Plk1 prohibits the danger of non-centrosomal PCNT accumulations, with the dire consequence of recruiting further centrosomal components and formation of non-centrosomal MTOCs (Sepulveda et al., 2018). Co-translational transport of PCNT might directly be entangled with another crucial Plk1 activity in early mitosis, the centriole to centrosome conversion. Engaged daughter centrioles barely contribute to the PCM recruitment in early mitosis (Wang et al., 2011). Only after essential Plk1 phosphorylation upon mitotic entry, daughter centrioles gain the function of PCM recruitment in late mitosis. This limitation might be a control mechanism, preventing daughter centrioles to produce granddaughters during interphase (Wang et al., 2011). The exact chain of events, as well as all the total number of substrates and crucial modifications for inducing the centriole-to-centrosome conversion, remains enigmatic. But the spatiotemporal expression and transport of PCNT, the main scaffold protein of interphase and mitotic PCM, under control of Plk1 activity probably is one of the most important steps.

Another interesting aspect of Plk1 activity in early mitosis is the release of Cohesin from chromosome arms in the so called prophase pathway (Waizenegger et al., 2000). This pathway guarantees that the bulk of Cohesin is removed in a phosphorylation dependent, but Separase independent manner (Gandhi et al., 2006; Hauf et al., 2005; Nishiyama et al., 2013). A small subpopulation at the centromeres is kept dephosphorylated by concerted action of Sgo1 and PP2A, thereby mediating cohesion until Separase becomes active at the metaphase to anaphase transition (Hauf et al., 2001; McGuinness et al., 2005; Uhlmann et al., 1999). As hints are given that the prophase pathway is also functional at centrosomes, the majority of centrosomal Cohesin rings might also be removed by Plk1 activity in early mitosis (Mohr et al., 2015). Supportive data came from a study performed in HeLa cells. In an unperturbed cell cycle, the wall-to-wall distance between mother and daughter centriole in S- and G2-phase is approximately 45 nm. In mitotic prophase however, they reach a distance of approximately 80

nm, concomitantly with a certain relief of reduplication block (Shukla et al., 2015). Activation of Plk1 in G2-arrested cells allowed the same spatial distance, with the dire consequences of centrosome maturation and even reduplication (Lončarek et al., 2010). Hence, unperturbed cells might enter mitosis with a distance between centrioles, which already allows for duplication in the following S-phase. If this distance originates from a possible prophase pathway, Plk1 activity fundamentally regulates the licensing of centriole duplication on multiple levels: the outer PCM expansion by hyper-recruitment of PCNT provides a shield against the pushing and pulling forces of the mitotic spindle. At the same time PCNT is converted into a suitable Separase substrate, thereby ensuring its timely destruction. At the inner PCM layer, spatial distance between mother and daughter centriole might be increased by a possible prophase pathway together with a certain relief of duplication block. Full distance of more than 80 nm is only reached at the end of mitosis, arguing for residual centrosomal Cohesin rings that are protected by Sgo1-PP2A complex until Separase becomes active. Alternatively, disassembly of the outer PCM might allow this spatial distance.

5.3 A speculative model explaining PCNTs and Cohesin's role in mediating centriole engagement

Results presented in this work, alongside with discussed theories regarding the mediation of centriole engagement and especially its dissolution through concerted action of Plk1 and Separase can be summarized in a speculative model (Fig. 30).

During S-phase, centrosomes are duplicated. A newly formed daughter centriole is formed at the base of each mother centriole in a process termed procentriole formation. Until late mitosis when Separase drives its dissolution, the daughter centriole is closely tied to the mother. This centriole engagement prevents re- or overduplication and is mainly mediated by Cohesin rings and the structural integrity of the interphase PCM. Whether a substrate has to be directly entrapped or Cohesin contributes to this bond through a matrix entrapment mechanism has to be determined. Either way, thanks to Cohesin the PCM integrity is strong enough to resist the pushing and pulling forces of interphase microtubules. Upon entry into mitosis, Plk1 as a key player in regulating centriole duplication fulfills several functions. First, Plk1 activity is crucial for the centriole-to-centrosome conversion. Second, Plk1 activity in prophase already leads to a substantial distance between mother and daughter centriole

which goes along with a certain relief of the intrinsic reduplication block. This is achieved by phosphorylation dependent but Separase independent removal of centrosomal Cohesin rings and resembles events of the chromosomal prophase pathway. Spatial separation of centrioles might be limited by residual Cohesin rings, protected through Sgo1-PP2A, as well as the increasing outer PCM. The latter, which is referred to as maturation, is induced by Plk1 activity and is mainly achieved through hyper-recruitment of PCNT. As the main scaffold protein, PCNT helps to recruit and anchor several important factors, like the γ -TuRC in order to build the bipolar spindle. In this scenario, Plk1 would induce a certain relief of the reduplication block at the inner PCM layer and at the same time, by recruiting PCNT and other components to the outer PCM, support the matrix entrapment of centrioles. This outer PCM provides enough structural integrity to resist the pushing and pulling forces of the mitotic spindle until Separase gets activated at the metaphase-to-anaphase transition. Cleavage of PCNT would disintegrate the outer PCM and cleavage of residual centrosomal Cohesin at the inner PCM layer would allow the total separation of the mother and daughter centriole. This disengagement is the licensing step as it relieves the reduplication block and allows duplication of centrioles in the next cell cycle. As a further layer of control, Plk1 phosphorylation turns PCNT into a suitable Separase substrate. This directly links crucial Plk1 activity in early mitosis to Separase activity in late mitosis, underlining the outstanding importance of Plk1 activity in licensing centriole duplication.

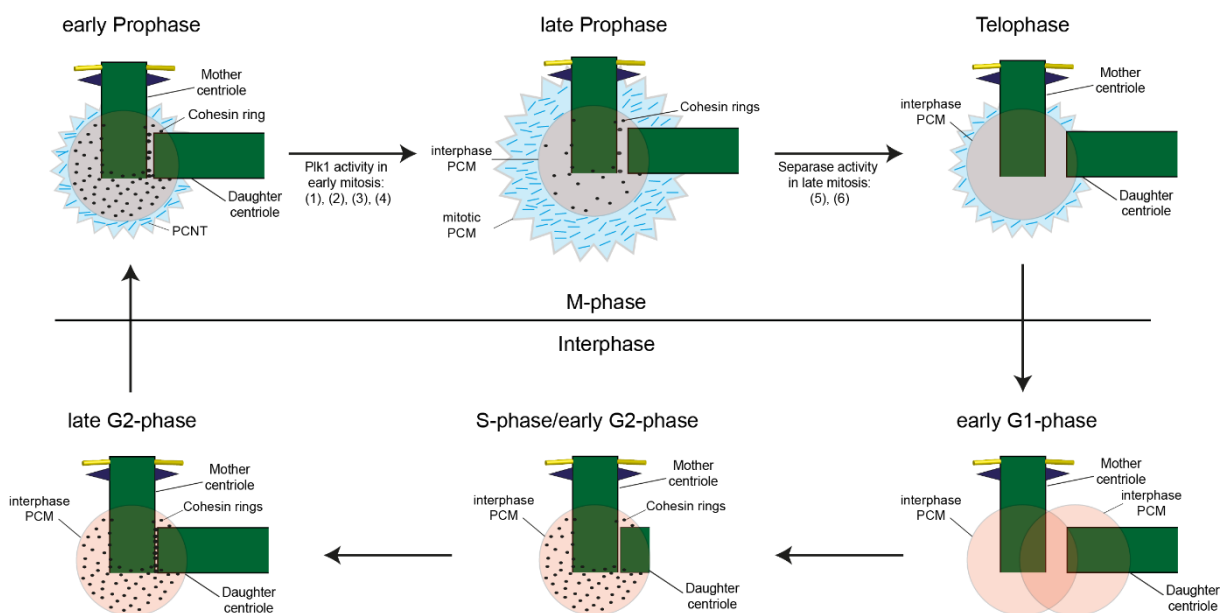


Fig. 30: Speculative model for the mediation of centriole engagement through cohesin and PCNT and its dissolution through concerted action of Plk1 and Separase in mitosis.

Fig. 30: (cont.) In this model, cohesin is assumed to mediate centriole engagement through a matrix entrapment in interphase. Upon exit from mitosis, cells start the next cell cycle with one centrosome consisting of two disengaged (mother-) centrioles. During S-phase, each mother centriole duplicates once through formation of a daughter centriole. The newly formed daughter centrioles further elongate throughout G2-phase. Upon entry in mitosis, the kinase Plk1 fulfills several important activities in licensing centriole duplication: (1) PCM maturation: hyper recruitment of PCNT and further factors important for microtubule nucleation. (2) Conversion of PCNT into a suitable Separase substrate. (3) Centriole-to-centrosome conversion. (4) Possible centrosomal prophase pathway: the majority of cohesin rings at the inner PCM layer might be removed. Hence, the spatial distance between centrioles might be increased to ≈ 80 nm. In late mitosis, Separase dependent cleavage of residual centrosomal cohesin rings at the inner PCM layer allows a spatial distance between centrioles of ≈ 150 nm. This distance is concomitant with a relief of the reduplication block. Furthermore, Separase dependent cleavage of PCNT induces disassembly of the outer PCM (5), which allows visualization of centriole disengagement (6).

6 Materials and Methods

6.1 Materials

6.1.1 Hard and Software

This work was created using “Microsoft Office 2008” (Microsoft Corporation, Redmond, USA). It was written using Microsoft Word 2008 and diagrams were generated with Microsoft Excel 2008. Chemiluminescence signals of immunoblots and Coomassie stained gels were detected using the “LAS-4000” or the “LAS-3000” system (FUJIFILM Europe GmbH, Düsseldorf, Germany) respectively. Immunofluorescence pictures were generated with the “Axio Imager A1” microscope (Zeiss, Jena, Germany). Radioactively labeled proteins were detected using the “FLA-7000” system (FUJIFILM Europe GmbH, Düsseldorf, Germany). Image processing was performed using “Adobe Photoshop CS6” (Adobe System Inc., San Jose, CA, USA).

6.1.2 Chemicals and reagents

All chemicals and reagents were purchased from the following companies unless stated otherwise: Abcam (Cambridge, UK), AppliChem (Darmstadt, Germany), BD Biosciences (Heidelberg, Germany), Fermentas/Thermo Fisher Scientific (Schwerte, Germany), GE Healthcare (Munich, Germany), Invitrogen/Life Technologies (Darmstadt, Germany), Merck (Darmstadt, Germany), Millipore/Merk (Schwalbach, Germany), New England Biosciences (NEB, Frankfurt a. M., Germany), Pierce/Thermo Fisher Scientific (Bonn, Germany), Qiagen (Hilden, Germany), Roche Diagnostics (Mannheim, Germany), Serva (Heidelberg, Germany), Sigma-Aldrich (Munich, Germany) and VWR (Darmstadt, Germany).

6.1.3 Antibodies

Primary antibodies

target protein	species and clonality	Use; dilution/ concentration	origin
C-Nap1	guinea pig, polyclonal	IFM: 1:2500	self-made, for details see (Schöckel et al., 2011), affinity purified
Centrin 2	rabbit, polyclonal	IFM: 1 µg/ml	self-made, for details see (Schöckel et al., 2011), affinity purified, LG10 Run1
Cyclin B1	mouse, monoclonal	WB: 1:1000	Millipore, 05-373
Flag	rabbit, polyclonal	IFM: 1:200; WB: 1:1000	Sigma-Aldrich, F7425
GFP	mouse, monoclonal	WB: 4 µg/ml	hybridoma cells kindly provided by Simona Sacconi, affinity purified
Myc	mouse, monoclonal	WB: 0.2 µg/ml	self-made, hybridoma cells (clone 9E10) derived from Developmental Studies Hybridoma Bank, affinity purified
p-histone 3	rabbit, polyclonal	WB: 1:2000	Millipore, 06-570
PCNT	two rabbits, polyclonal	WB: 0.27 µg/ml	self-made, raised against bacterially expressed aa 1968-2391 of PCNT, affinity purified
PCNT	two guinea pigs, polyclonal	WB: 0.32 µg/ml	self-made, peptide antibody raised against aa 1-14 of PCNT, affinity purified
Separase N	rabbit, polyclonal	WB: 0.5 µg/ml	self-made, raised against aa 2-16 of hSeparase, affinity purified
Scc1	rabbit, polyclonal	WB: 1:1000	self-made against a C-terminal peptide, for details see (Stemmann et al., 2001), affinity purified
α-tubulin	mouse, monoclonal	WB: 1:200	hybridoma supernatant, Developmental Studies Hybridoma Bank, clone 12G10
γ-tubulin	mouse, monoclonal	IFM: 1:1000	Sigma-Aldrich, T6657

Secondary antibodies

name	use	dilution	origin
HRP-conjugated goat anti-mouse IgG	WB	1:15000	Sigma, A9917
HRP-conjugated goat anti-rabbit IgG	WB	1:15000	Sigma, A0545
AlexaFlour488 goat anti-mouse IgG	IFM	1:500	Invitrogen
AlexaFlour488 goat anti-rabbit IgG	IFM	1:500	Invitrogen
Cy3 goat anti-mouse IgG	IFM	1:500	Invitrogen
Cy3 goat anti-rabbit IgG	IFM	1:500	Invitrogen
Cy3 goat anti-guinea-pig IgG	IFM	1:500	Jackson Immunoresearch Laboratories
Cy5 goat anti-mouse IgG	IFM	1:500	Jackson Immunoresearch Laboratories
Cy5 goat anti-rabbit IgG	IFM	1:500	Invitrogen

DNA oligonucleotides

name	sequence
PK_Pericent_5'F	5'-AATGGCCGGCCGATGGAAGTTGAGCAAGAGCAG-3'
prsc-clea.-nr2-a	5'-GGCGCGCCTTAAGCCTTTTCTCTCAGTTCAAGTAG-3'
prsc-clea.-nr3-f	5'-ATAGGCCGGCCTGACTTGGAGGCCGACACAGAGCG-3'
prsc-clea.-nr4-a	5'-GGCGCGCCTTACAATTCATTAATTCATCCAAC-3'
prsc-clea.-nr5-f	5'-ATAGGCCGGCCTCAGCTCCGCCAGGCGGCCAAGCC-3'
prsc-clea.-nr6-a	5'-GGCGCGCCTTACTCGCCGCTTGGGGGTGCAAGG-3'
prsc-clea.-nr7-f	5'-ATAGGCCGGCCTCAGCCGCTGCCGGAAGCCATGAA-3'
hPericentr_3'Asc	5'-ATTGGCGCGCCTCATCGGGTGGCAGGATTTCTTTG-3'
hScc1_Tev_5'	5'-CGTGAGACCCTGTACTTCCAGAGTGCTTTTGGAGATG-3'
hScc1_Tev_3'	5'-GCACTCTGGAAGTACAGGGTCTCACGATCATCCATTC-3'
hPCNT_HRV_5'	5'-CCTGGAGACCCTGTTCCAGGGCCCCGTGACACCCAC-3'
hPCNT_HRV_3'	5'-CGGGGCCCTGGAACAGGGTCTCCAGGGTCCAGTCCTT-3'
hPCNT_Tev_5'	5'-GAGACCCTGTACTTCCAGTCCAGTGCCGACACATCCCTGGGGGA-3'
hPCNT_Tev_3'	5'-GGACTGGAAGTACAGGGTCTCTCCTGAGTCGGGTGTACGGCGA-3'
PCNT_S2222A_5'	5'-TCGGGATGCTGGACCTGGCTTCTGGAGCTCCCCT-3'
PCNT_S2222A_3'	5'-AGGGGAGCTCCAGGAAGCCAGGTCCAGCATCCCGA-3'
PCNT_S2226A_5'	5'-GACCTGTCTTCTGGAGCGCCCCTGAGGTCTCAG-3'
PCNT_S2226A_3'	5'-CTGAGGACCTCAGGGCGCTCCAGGAAGACAGGTC-3'
PCNT_T2235A_5'	5'-CCCTGAGGTCTCAGGAAGGACTGGGCCCTGGAGC-3'
PCNT_T2235A_3'	5'-GCTCCAGGGCCCAGTCCTTCTGAGGACCTCAGGG-3'
5'BamH1_Scc1 ab Ala107	5'-ACCGGTGGATCCGCCATTACTTTACCTGAAGAATTC-3'
Scc1 bis Ser271_3'Hind3	5'-CTTGTAAGCTTATGATACATTATCATCCTCATCCATATC-3'
5'BamH1-PCNT ab Ser2168	5'-ACCGGTGGATCCTTGATACCAGATGAAATGCC-3'
PCNT Gly2331_3'Hind3	5'-CTTGTAAGCTTATCCAGGAGGAGGTGAACTTAATG-3'

6.1.4 RNA oligonucleotides

target	name	sequence	final concentration
Scc1	hScc1_3'UTR1	5'-ACUCAGACUUCAGUGUAUA-3'	28.5 nM
	hScc1_3'UTR2	5'-AGGACAGACUGAUGGGAA-3'	
Luciferase	GL2	5'-CGUACGCGAAUACUUCGA-3'	variable
PCNT	siPCNT	5'-GCAGCUGAGCUGAAGGAGA-3'	50 nM

6.1.5 Plasmids

name	insert	tag	backbone	origin
pPK3054	hPCNTB fragment 1 (aa 1-778)	N-Flag ₃ -TEV ₂ -	pCS2	this study
pPK3055	hPCNTB fragment 2 (aa 659-1547)	N-Flag ₃ -TEV ₂ -	pCS2	this study
pPK3056	hPCNTB fragment 3 (aa 1505-2419)	N-Flag ₃ -TEV ₂ -	pCS2	this study
pPK3057	hPCNTB fragment 4 (aa 2376-3336)	N-Flag ₃ -TEV ₂ -	pCS2	this study
pPK3338	hPCNTB full-length	N-Flag ₃ -	pCS2	this study
pDB535	hPlk1 wild type	N-HA ₃ -Tev-	pCS2	Dominik Boos
pDB536	hPlk1 kinase dead (K82R)	N-HA ₃ -Tev-	pCS2	Dominik Boos
pPK3528	hPlk1 constitutively active (T210D)	N-HA ₃ -Tev-	pCS2	this study
pPK3327	hScc1 wild type	...C-GFP	pcDNAL	this study
pPK3119	hScc1 TEV-cleavable	...C-GFP	pcDNAL	this study
pPK3326	hScc1 HRV-cleavable	...C-GFP	pcDNAL	this study
pPK3062	hPCNTB full-length	N-Myc ₆ -	pcDNA5	this study
pPK3059	hPCNTB TEV-cleavable	N-Myc ₆ -	pcDNA5	this study
pPK3140	hPCNTB HRV-cleavable	N-Myc ₆ -	pcDNA5	this study
pPK3414	hPCNTB 4-Ala (Q653A, G654A, Q2272A, G2273A), HRV-cleavable	N-Myc ₆ -	pcDNA5	this study
pPK3158	hPCNTB fragment 1 (aa 1-778), 2-Ala (Q653A, G654A)	N-Flag ₃ -TEV ₂ -	pCS2	this study
pPK3159	hPCNTB fragment 3 (aa 1505-2419), 2-Ala (Q2272A, G2273A)	N-Flag ₃ -TEV ₂ -	pCS2	this study
pMF2984	hPCNTB aa 1-1877	N-Myc ₆ -	pCS2	Martina Färber
pMF2986	hPCNTB full-length	N-Myc ₆ -	pCS2	Martina Färber
pMF2954	hPCNTB aa 2211-2293	N-myc ₆ -	pCS2	Martina Färber
pMF2961	hPCNTB aa 2211-2293; S2222A	N-Myc ₆ -	pCS2	Martina Färber
pMF2962	hPCNTB aa 2211-2293; S2226A	N-Myc ₆ -	pCS2	Martina Färber
pMF2963	hPCNTB aa 2211-2293; T2235A	N-Myc ₆ -	pCS2	Martina Färber
pMF2964	hPCNTB aa 2211-2293; S2222A, S2226A, T2235A	N-Myc ₆ -	pCS2	Martina Färber
pMF2989	hPCNTB aa 1968-2391	N-KSI-...-His ₆ -C	pET31b	Martina Färber
pPK3850	hScc1 wild type (aa 107-271)	N-His ₆ -Sumo-1	pET28M	this study
pPK3851	hScc1 non-cleavable (aa 107-271)	N-His ₆ -Sumo-1	pET28M	this study
pPK3852	hPCNTB wild type (aa 2168-2331)	N-His ₆ -Sumo-1	pET28M	this study
pPK3853	hPCNTB non-cleavable (aa 2168-2331)	N-His ₆ -Sumo-1	pET28M	this study
pPW3502	hSeparase P1127A, C2029S	N-GFP-TEV ₄	pCS2	Peter Wolf
pMF3218	hPCNTB fragment 1 (aa 1-778)	N-His ₆ -Sumo1-	pET28M	Martina Färber
pMF3220	hPCNTB fragment 3 (aa 1505-2419)	N-His ₆ -Sumo1-	pET28M	Martina Färber
pPK3339	hPCNTB full-length, 3A: S2222A, S2226A, T2235A	N-Flag ₃ -	pCS2	this study
pPK3340	hPCNTB full-length, 3D: S2222D, S2226D, T2235D	N-Flag ₃ -	pCS2	this study

pPK3341	hPCNTB full-length, RxxE: E2228R, R2231E	N-Flag ₃ -	pCS2	this study
pFL3463	hSeparase P1127A	N-GFP-TEV ₄	pCS2	Franziska Langhammer
pSX100	hSecurin	-	pCS2	Hui Zou
pAG1786	Flp-recombinase	-	pCS2	Amelie Gutmiedel
pIC-Cre	Cre-recombinase	-	pMC1	(Gu et al., 1993)

6.1.6 Buffer, solutions and media (alphabetic order)

Binding buffer: 50 mM Tris-HCl, pH 7.2, 10 mM Imidazole, 6 M GuaHCl; **Blocking solution:** 1x PBS, 3% (w/v) BSA; **Blotting buffer:** 192 mM glycine, 25 mM Tris, 15% (v/v) methanol, 0.01% (w/v) SDS; **BRB 80 (5x):** 400 mM Pipes-KOH pH 6.8, 5 mM MgCl₂, 5 mM EGTA; **CaCl₂ (25x):** 15 mM CaCl₂ in sperm dilution buffer; **Coomassie staining:** 10% (w/v) (Na)₂SO₄, 12% (v/v) phosphoric acid, 20% (v/v) methanol, 1% (w/v) Coomassie brilliant blue G250; **CSF-XB:** 100 mM KCl, 0.1 mM CaCl₂, 2 mM MgCl₂, 10 mM HEPES/KOH, pH 7.7, 50 mM sucrose, 5 mM EGTA/KOH, pH 8.0, adjust pH to 7.7 with KOH; **Cytochalasin B:** 10 mg/ml Cytochalasin B in DMSO; **Dejelling solution:** 2% (w/v) Cysteine (free base), 0.5x XB-salts, adjust pH to 7.8 with KOH; **DNA loading buffer (6x):** 50% (v/v) glycerol, 0.1 M EDTA, 0.02% (v/v) xylene cyanol, 0.02% (v/v) bromophenol, 0.02% (v/v) SDS; **Elution buffer:** 50 mM Tris-HCl, pH 7.2, 250 mM imidazole, 6 M GuaHCl; **HBS (2x, 50ml):** 800 mg NaCl, 37 mg KCl, 10.65 mg Na₂HPO₄, 100 mg Glucose, 500 mg HEPES, pH 7.05 adjusted with NaOH, sterile filtered (0.2 µm pore size); **Kinase buffer (5x):** 25 mM MOPS, pH 7.2, 12.5 mM β-glycerol-phosphate, 25 mM MgCl₂, 5 mM EGTA, 2 mM EDTA, 0.25 mM DTT; **Laemmli running buffer (1x):** 192 mM glycine, 25 mM Tris, 0.1% (w/v) SDS; **LB agar:** LB medium with 1.5% (w/v) agar; **LB medium:** 1% (w/v) tryptone, 0.5% (w/v) yeast extract, 1% (w/v) NaCl, dissolved in ddH₂O and sterilized by autoclaving; **LP2 buffer:** 20 mM Tris-HCl, pH 7.6, 100 mM NaCl, 10 mM NaF, 20 mM β-glycerolphosphate, 5 mM MgCl₂, 0.1% (v/v) Triton-X-100, 5% (v/v) glycerol, 1x protease inhibitor cocktail (Roche Diagnostic); **Lysis buffer:** 1x PBS, 400 mM NaCl, 5 mM imidazole; **MMR (25x):** 2.5 M NaCl, 50 mM KCl, 25 mM MgCl₂, 50 mM CaCl₂, 2.5 mM EDTA-NaOH, pH 8.0, 125 mM HEPES-NaOH, pH 7.8, adjust pH to 7.8 with NaOH; **Mounting medium:** 2.33% (w/v) 1,4-diazabicyclo-[2,2,2]-octaneglycerol, 20 mM Tris-HCl, pH 8.0, 78% (v/v) glycerol; **PBS (10x):** 1.37 M NaCl, 80 mM Na₂HPO₄, 27 mM KCl, 14 mM KH₂PO₄, pH 7.4; **Resolving gel (6%, 25 ml):** 9.3 ml 1 M Tris-HCl, pH 8.8, 10.4 ml ddH₂O, 5 ml 30% (w/w) acryl amide-bisacryl amide (37.5:1), 280 µl 10% (w/v) ammonium persulfate (APS), 14.3 µl 20% (w/v) SDS, 20 µl

TEMED; **Resolving gel (8%, 35 ml)**: 13.1 ml 1 M Tris-HCl, pH 8.8, 12.4 ml ddH₂O, 9.3 ml 30% (w/w) acryl amide-bisacryl amide (37.5:1), 160 µl 10% (w/v) ammonium persulfate (APS), 20 µl 20% (w/v) SDS, 11 µl TEMED; **Resolving gel (17%, 37.5 ml)**: 21.3 ml 30% (w/w) acryl amide-bisacryl amide (37.5:1), 14 ml 1 M Tris-HCl, pH 8.8, 2 ml 2.5 M sucrose, 160 µl 10% (w/v) ammonium persulfate (APS), 20 µl 20% (w/v) SDS, 11 µl TEMED; **SDS sample buffer (4x)**: 250 mM Tris-HCl, pH 6.8, 40% (w/v) glycerol, 8% (w/v) SDS, 2 M β-mercaptoethanol, 0.04% (w/v) bromophenol; **SOB medium**: 2% (w/v) tryptone, 0.5% (w/v) yeast extract, 0.5% (w/v) NaCl, 2.5 mM KCl, pH 7.0; **Sperm dilution buffer**: 1 mM MgCl₂, 100 mM KCl, 150 mM sucrose, 5 mM HEPES/KOH, pH 7.7; **Stacking gel (5%)**: (10 ml): 6.9 ml ddH₂O, 1.7 ml 30% (w/w) acryl amide-bisacryl amide (37.5:1), 1.3 ml 1 M Tris-HCl, pH 6.8, 100 µl 10% (w/v) ammonium persulfate (APS), 6.2 µl 20% (w/v) SDS, 5.6 µl TEMED; **Stacking gel (7%)**: (32.5 ml): 20.6 ml ddH₂O, 7.6 ml 30% (w/w) acryl amide-bisacryl amide (37.5:1), 4.1 ml 1 M Tris-HCl, pH 6.8, 160 µl 10% (w/v) ammonium persulfate (APS), 20 µl 20% (w/v) SDS, 11 µl TEMED; **Sucrose cushion**: 1x BRB 80, 20 mM EDTA, 0.01% (v/v) Triton X-100, 40% (w/v) sucrose; **T4 DNA ligase buffer (10x)**: 50 mM Tris-HCl, pH 7.5, 10 mM MgCl₂, 10 mM DTT, 1 mM ATP; **TEV-cleavage buffer**: 10 mM HEPES/KOH, pH 7.7, 20% (w/v) glycerol, 50 mM NaCl, 25 mM NaF, 1 mM EGTA, 2 mM DTT; **TBE buffer**: 90 mM Tris, 90 mM boric acid, 2.5 mM EDTA; **TBS-Tw**: 137 mM NaCl, 25 mM Tris-HCl, pH 7.5, 2.6 mM KCl, 0.05% (v/v) Tween-20; **Tbf1 buffer**: 30 mM KAc, 50 mM MnCl₂, 100 mM KCl, 15% (v/v) glycerol, pH 5.8; **Tbf2 buffer**: 10 mM MOPS-NaOH, 75 mM CaCl₂, 10 mM KCl, 15% (v/v) glycerol, pH 7.0; **TPE buffer**: 50 mM Tris, 2 mM EDTA, 0.13% (v/v) H₃PO₄; **Washing buffer**: 50 mM Tris-HCl, pH 7.2, 25 mM imidazole, 6 M GuaHCl; **Washing solution**: 1x PBS, 0.1% (v/v) Triton-X-100; **XB salts (20x)**: 2 M KCl, 2 mM CaCl₂, 20 mM MgCl₂

6.2 Microbiological techniques

6.2.1 *E. coli* strains

The *E. coli* XL-1 blue strain with the following genotype was used for molecular cloning and plasmid amplification: *E. coli supE44 hsdR17 recA1 gyrA46 thi relA1 lac⁻ F'[pro AB⁺ lacI^qΔ(lac Z)M15 Tn10 (tet^r)]* (Stratagene/Agilent Technologies, Santa Clara, CA, USA).

The *E. coli* strain Rosetta DE3 with the following genotype was used for protein expression: *E. coli* F- ompT hsdSB (rB- mb-) gal dcm λ (DE3 [*lacI lacUV5-T7 gene 1 ind1 sam7 nin5*] *Cam*^R (Novagen/Merck).

6.2.2 Cultivation of *E. coli*

E. coli strains were grown in LB medium by shaking at 37°C and 200 rpm in a vertical shaker using Erlenmeyer flasks. Culture densities were determined by measuring the absorbance at a wavelength of 600 nm (OD₆₀₀) using an OD600 DiluPhotometer (Implen, Munich, Germany). Antibiotics for selection of transformed bacteria were added to the media at 100 µg/ml (ampicillin) or 30 µg/ml (kanamycin) final. LB agar plates were incubated at 37°C and stored at 4°C for up to two weeks. For long time storage 20% (v/v) glycerol was added to the liquid culture, incubated for 30 min on ice and finally stored at -80°C.

6.2.3 Preparation of chemically competent *E. coli*

300 ml of LB medium was inoculated with 4 ml of an overnight culture and grown at 37°C with 200 rpm in a vertical shaker until the OD₆₀₀ reached a value of 0.5. The culture flask was then chilled on ice for 15 min and pelleted by centrifugation (4°C, 3000 g, 15 min). All following steps were performed with sterile materials and solutions prechilled to 4°C. Pelleted bacteria were resuspended in 90 ml of Tbf1 buffer and incubated on ice for 15 min. After additional centrifugation (4°C, 1500 g, 15 min) bacteria were resuspended in 15 ml Tbf2 buffer and chilled on ice for 5 min. Finally, the suspension of bacteria was aliquoted, snap-frozen and stored at -80°C prior to use.

6.2.4 Transformation of chemically competent *E. coli*

Competent bacteria were thawed on ice. 50 µl of suspension were carefully mixed with 50-100 ng of plasmid DNA or 10 µl of ligation mix and incubated for 30 min on ice. A heat shock was performed at 42°C for 45 s and subsequently put on ice for 2 min. 1 ml of LB medium without antibiotics was added and incubated at 37°C for 30 min (for vectors carrying ampicillin resistance) or 60 min (for vectors carrying kanamycin resistance) respectively. After recovery the transformation mix was transferred on LB agar plates containing the respective antibiotic and incubated overnight at 37°C.

6.2.5 Expression of proteins in *E. coli*

For expression of recombinant proteins, chemically competent Rosetta DE3 cells were transformed with the relevant plasmid and let grown overnight at 37°C and 200 rpm in a vertical shaker in LB medium supplemented with the desired antibiotic. The next morning prewarmed (37°C) LB medium was inoculated with a 1:100 dilution of the preculture and the appropriate antibiotic again. The culture was grown at 37°C and 200 rpm in a vertical shaker. Expression was induced by addition of IPTG (1 mM final concentration) at an OD₆₀₀ of 0.5-0.7. After shaking for another 3 h at 37°C cells were harvested by centrifugation (4°C, 5000 g, and 15 min). Pellets were snap-frozen and stored at -80°C or processed directly.

6.3 Molecular biological methods

6.3.1 Isolation of plasmid DNA from *E. coli*

3 ml LB medium containing the appropriate antibiotic was inoculated with a single transformed *E. coli* XL1-Blue colony. After incubation for 8-14 h with shaking at 200 rpm in a vertical shaker and 37°C the cells were harvested. Plasmid DNA was purified via alkaline lysis of the bacteria and subsequent isolation by anion exchange columns according to the manufacturer's instructions (Fermentas/Thermo Scientific, Schwerte, Germany). Larger amounts of DNA were isolated from 50-500 ml overnight culture according to the manufacturer's instructions (Qiagen, Hilden, Germany).

6.3.2 Determination of DNA concentrations in solutions

DNA concentrations were determined by using the ND-1000 Spectrophotometer (Peqlab, Erlangen, Germany), measuring the absorbance at a wavelength of 260 nm (OD₂₆₀). An OD₂₆₀ of 1 corresponds to 50 µg/ml double stranded DNA.

6.3.3 Restriction digestion of DNA

Sequence-specific cleavage of DNA was performed with restriction enzymes from either NEB (Frankfurt a. M., Germany) or Fermentas/Thermo Scientific (Schwerte, Germany) according to manufacturer's instructions. Usually, 1-5 units of restriction enzyme were used for the digestion of 1 µg DNA. Samples were incubated in the appropriate buffer at the recommended temperature for 5-60 min. The reaction was stopped by adding DNA loading buffer or heat inactivation.

6.3.4 Dephosphorylation of DNA fragments

To avoid religation of linearized vectors, the 5'-end of the vector was dephosphorylated by addition of 5 U/ μ g antarctic phosphatase (NEB, Frankfurt a. M., Germany) and the appropriate buffer. After incubation for 30 min at 37°C, the enzyme was heat inactivated for 10 min at 75°C.

6.3.5 Separation of DNA fragments by gel electrophoresis

For analysis or preparative isolation, DNA fragments were electrophoretically separated on 1-2% agarose gels. TPE buffer was used for separation of fragments which were larger than 1 kb and TBE buffer was used for fragments smaller than 1 kb. Ethidium bromide was added to a final concentration of 0.5 μ g/ml. The DNA samples were mixed with loading buffer (to 1x) and separated at 100 V in TPE or TBE buffer. Due to the intercalation of ethidium bromide into double stranded DNA, fragments could be visualized using a UV transilluminator (324 nm). The fragment-size was estimated by comparison to a self-made standard (SPP1 bacteriophage DNA digested with restriction enzyme *EcoR1*).

6.3.6 Isolation of DNA from agarose gels

After gel electrophoresis the desired DNA fragments were isolated from the gel by excising with a scalpel. The DNA was extracted using the GeneJet Gel Extraction Kit (Fermentas/Thermo Scientific, Schwerte, Germany) according to the manufacturer's instructions.

6.3.7 Ligation of DNA fragments

The amount of DNA inserts and linearized, dephosphorylated vector was estimated on an agarose gel. For the ligation reaction, a molar ratio of vector and insert of 1:2 to 1:5 was used. In a total volume of 10 μ l, the reaction mix also contained 1 μ l of T4 DNA ligase (selfmade) and 1 μ l of T4 DNA ligase buffer (enzyme and buffer were self-made in the lab). For efficient ligation, the reactions were carried out for 1 h at RT or overnight at 14°C.

6.3.8 Polymerase chain reaction (PCR)

PCR reactions were performed in a total volume of 50 μ l with 0.2 μ l of 5'- and 3'-oligonucleotide (100 mM each), 1 μ l deoxyribonucleotide triphosphate mix (10 mM, NEB, Frankfurt a. M., Germany) 0.5 μ l of Phusion polymerase (Fermentas/Thermo scientific, Schwerte, Germany) in the corresponding buffer (GC or HF buffer). As template, 50 ng of

plasmid DNA or 250 ng of genomic DNA was used. Amplification was carried out in a TC-512 cycler (Techne, Burlington, NJ, USA). Usually, the denaturing step was done at 98°C for 15 s, annealing for 15 s at a temperature optimized for the corresponding primer pairs, and elongation at 72°C for 15 s/kbp.

6.3.9 Site-directed mutagenesis

Site-directed mutagenesis was performed using the primer extension approach. Four primers were needed, two internal reverse complement oligos carrying the desired mutation and two outer primers. In two separate PCR reactions, an upstream and a downstream fragment were generated. The outer primers were designed to terminate at 5'- or 3' ends of the corresponding gene or at useful restriction sites within. The two resulting, overlapping amplicons were purified via gel electrophoresis and served as templates for the following PCR reaction using only the outer primers. Finally, this fragment was purified again via gel electrophoresis, ligated into a suitable vector and the mutations were verified by sequencing (SeqLab, Göttingen, Germany).

6.4 Protein biochemical methods

6.4.1 SDS-polyacrylamide gel electrophoresis (SDS-PAGE)

For the separation of proteins under denaturing conditions, SDS-PAGE was performed using self-poured 8-17% gradient gels (with the "SG100" system, Hoefer Inc). For PCNT samples, self-poured 6% resolving gels, topped by 5% stacking gels were used. Samples were supplemented with SDS-sample buffer (to 1x) and denatured at 95°C for 5-10 min. Electrophoresis was carried out at 120-140 V in a "Mighty Small II for 8x7 cm gels (Hoefer Inc)" chamber containing 1x Laemmli buffer. As a molecular weight standard, PageRuler Plus Prestained Protein Ladder or HiMark Prestained Protein Standard (Fermentas, St. Leon-Rot) was used.

6.4.2 Immunoblotting (Western blot)

After separation via SDS-PAGE, proteins were transferred electrophoretically to a nitrocellulose (GE healthcare, Munich, Germany) or polyvinylidene fluoride (PVDF) membrane (Serva, Heidelberg, Germany). The PVDF membrane was incubated in 100% methanol for 5 min, washed with ddH₂O and incubated in blotting buffer for further 5 min.

Protein transfer was carried out in a wet blot chamber (Bio-Rad Mini Protean II, Bio-Rad Laboratories GmbH, Munich, Germany) for 60-90 min at 100 V. The membrane was blocked for unspecific binding with 5% milk powder in TBS-Tw for 30-60 min at RT. Then, the membrane was incubated overnight at 4°C with the primary antibody diluted in 1x PBS supplemented with 3% (w/v) BSA and 0.02% (v/v) NaN₃. Next day, the membrane was washed three times briefly with TBS-Tw followed by 1 h incubation at RT with the secondary antibody in 1x PBS supplemented with 3% (w/v) BSA. Finally, the membrane was washed three times with TBS-Tw for 10 min each, followed by incubation with "ECL ultra" (Lumigen, Southfield, MI, USA) or "HRP Juice" (p.j.k, Kleinblittersdorf, Germany) according to the manufacturer's instructions. The generated luminescence signal was detected using a "LAS-4000" detection system (FUJIFILM Europe GmbH, Düsseldorf, Germany).

6.4.3 Coomassie staining

For staining, SDS-gels were incubated in Coomassie staining for several hours or overnight on a shaker. To remove unspecific staining, gels were washed in ddH₂O for at least 1 h. For storage, the gels were vacuum-dried on a 3MM blotting paper (Whatman, GE Healthcare, Munich, Germany) in a gel dryer (GD2000, Hoefer, Holliston, MA, USA).

6.4.4 Coupled *in vitro* transcription/translation (IVT/T)

For coupled *in vitro* transcription/translation of *SCCI*- or *PCNT*-encoding plasmids (pCS2 based vectors) TNT coupled reticulocyte lysates (Promega, Mannheim, Germany) were used. For a standard reaction 25 µl of Rabbit Reticulocyte Lysate was mixed with 2 µl reaction buffer, 1 µl RNA Polymerase (SP6 or T7, 0.5 µg/µl), 1 µl Amino Acid Mixture (minus methionine, 1 mM), 2 µl of [35S]-labeled methionine, 1 µl of Ribonuclease Inhibitor (40 U/µl), 2 µl DNA template (0.5 µg/µl) and 16 µl nuclease-free water. The reaction was incubated for 90 min at 30°C. The reaction was either stopped by addition of SDS sample buffer and boiling of the sample at 95°C for 10 min, or the IVT/T product was used for *in vitro*-kinase assays (see 6.4.5).

6.4.5 *In vitro* kinase assay/cleavage assay

For a standard reaction, 0.5 µl IVT/T were mixed with 2 µl Plk1 (self-made) and/or 2 µl Cdk1 (self-made in the lab), 0.5 µl ATP (200 µM), 2 µl kinase buffer (5x) and filled up with ddH₂O to 9.5 µl. If necessary, the Plk1 inhibitor BI-2536 and/or the Cdk1 inhibitor RO-3306 were added (final concentration: 100 nM each). The reaction was incubated at 30°C for 30 min,

before 0.5 μ l of active or protease-dead recombinant Separase was added. After 30 min of incubation at 30°C the reaction was stopped by addition of SDS-sample buffer and boiling at 95°C for 5 min. The samples were subjected to SDS-PAGE followed by fixation of the gel in 40% (v/v) methanol/10% (v/v) acetic acid for 30 min. Then, the gel was washed with ddH₂O for 15 min before it was placed on a blotting paper (Whatman, GE Healthcare, Munich, Germany) and dried for 1 h at 80°C on a "Model 483" vacuum drier (BioRAD). The dried gel was then placed into a developing cassette and covered with an imaging plate (FUJIFILM Europe GmbH, Düsseldorf, Germany). After exposure overnight, the imaging plate was analyzed using the "FLA-7000" system (FUJIFILM Europe GmbH, Düsseldorf, Germany).

6.4.6 Ni²⁺-NTA affinity purification of 6x-Histidin-tagged proteins

Ni²⁺-NTA affinity purification was used to isolate His₆-tagged PCNT fragments from *E. coli* lysates (see 6.2.5). Therefore, the harvested bacteria from 500 ml culture medium were resuspended in 25 ml lysis buffer and lysed in a homogenizer (EmulsiFlex Microfluidizer, Avestin, Canada) by cycling the cell suspension for 10 min. The lysate was then centrifuged at 10000 g for 30 min at 4°C to pellet the cellular debris. The supernatant was incubated with 250 μ l Ni²⁺-NTA agarose (Qiagen, Hilden, Germany) for 2 h at 4°C on a turning wheel. The beads were then washed twice with lysis buffer supplemented with 20 mM imidazole. Bound protein was eluted with two times 250 μ l lysis buffer supplemented with 250 mM imidazole (pH 8.0). The eluate was then dialyzed against 1x PBS before it was aliquoted, snap-frozen using liquid nitrogen and stored at -80°C.

6.4.7 Generation and purification of PCNT antibodies

6.4.7.1 Generation and purification of PCNT_{aa1968-2391} specific antibodies from rabbit

Affinity purification of the KSI-PCNT_{aa1968-2391}-His tagged antigen

Protein expression was performed as described in 6.2.5. The pET31 vector was used, which allowed fusion of the PCNT-encoding sequence with the N-terminal insoluble KSI-tag and a C-terminal His₆-tag. Protein purification was performed by Ni²⁺-NTA affinity purification from isolated inclusion bodies under denaturing conditions. To this end, the harvested bacteria from 500 ml culture medium were resuspended in 50 ml lysis buffer and lysed in a homogenizer (EmulsiFlex Microfluidizer, Avestin, Canada) by cycling the cell suspension for 10 min. Then, the inclusion bodies were pelleted by centrifugation in a JA-25.50 rotor (Beckman Coulter) at 15000 g for 20 min. The supernatant was discarded and the pellet was

resuspended with lysis buffer (to remove residues of soluble proteins) and pelleted again by centrifugation in a JA-25.50 rotor at 15000 g for 10 min. Subsequently, the pellet was resuspended in 50 ml binding buffer, supplemented with 0.5 ml Ni²⁺-NTA agarose (Qiagen, Hilden, Germany) and incubated over night at 4°C on a turning wheel. Beads were washed four times with washing buffer and then incubated with 4 ml elution buffer for 1 h at 4°C. The eluate was then dialyzed overnight at 4°C using ‘slide a lyzer’ membranes (Pierce, Thermo Fisher Scientific, Bonn, Germany): in part against 1x PBS for the immunization of rabbits and against coupling buffer for coupling to NHS columns (see below). Next day, the dialysate was cleared by centrifugation for 10 min at 10000g and 4°C before they were aliquoted, snap-frozen in liquid nitrogen and stored at -80°C until use.

Purification of specific antibodies from rabbit serum

For the generation of polyclonal antibodies from rabbit, the PCNT-antigen was expressed and purified as described above. Two rabbits were immunized with 1 mg of antigen each, splitted into 4 injections over a period of ten weeks (Charles River Laboratories, Chatillon-sur-Chalaronne, France). The obtained serum from the final bleed was then purified in two steps: 1) Antibodies against the KSI- and His-tag were removed from the serum by pumping the serum over a CnBr-activated sepharose (Sigma-Aldrich, Munich, Germany) ‘pre’-column coupled with bacterially expressed KSI-His protein according to the instructions of the manufacturer at a rate of 0.5 ml/min; 2) the ‘flow through’, serum cleared from antibodies against the tags, was then pumped over a HiTrap N-hydroxy-succinimide (NHS)-activated column (GE Healthcare, Munich, Germany) coupled with the bacterially expressed antigen (see above) according to the instructions of the manufacturer at a rate of 0.5 ml/min. After washing with 1x PBS, antibodies were eluted with 100 mM glycine/100 mM NaCl (pH 2.5) and rapidly neutralized with 1 M Tris-HCl (pH 9). Each collected fraction was analyzed by SDS-PAGE followed by Coomassie staining and fractions containing antibodies were pooled and dialyzed against 1x PBS/10% glycerol overnight. Next day, the dialysate was cleared by centrifugation for 10 min at 10000g and 4°C before the concentration was determined (Rabbit 1: 0.19 mg/ml Rabbit 2: 0.27 mg/ml). Subsequently, the dialysates were aliquoted, snap-frozen in liquid nitrogen and stored at -80°C until use.

6.4.7.2 Generation and purification of peptide derived (aa 1-14) PCNT-specific antibodies from guinea pig

Coupling of a PCNT peptide antigen to a KLH-carrier protein

In order to raise antibodies against PCNT, a peptide representing the very N-terminal 14 amino acids (MEVEQEQRRRKVEA, synthesized by Eurogentec, Köln, Germany) was used to immunize two guinea pigs. Per animal, 2 mg of peptide were coupled to 2 mg of maleimide activated Keyhole limpet Hemocyanine (mcKLH) according to manufacturer's instructions ("Imject Maleimide Activated mcKLH Kit", Thermo Scientific, Bonn, Germany). EDTA was removed by dialysis against PBS and the resulting antigen was used for four injections over a period of eight weeks (Charles River Laboratories, Chatillon-sur-Chalaronne, France) before the animals were bled to obtain the antibody containing sera.

Affinity purification of the PCNT peptide antibody

4 mg of the corresponding peptide (see above) were coupled to a 2 ml gel bed of sulfhydryl reactive agarose according to the manufacturer's instructions ("Sulfolink Immobilization Kit for peptides, Thermo Scientific, Bonn, Germany). 3 ml of antibody containing serum was diluted with 7 ml 1x PBS and cycled overnight through the peptide column at 4°C. After washing with 1x PBS, antibodies were eluted with 100 mM glycine (pH 2.7) and rapidly neutralized with 1 M Tris (pH 9). Each collected fraction was analyzed by SDS-PAGE followed by Coomassie staining and fractions containing antibodies were pooled and dialyzed against 1x PBS/10% glycerol overnight. Next day, the dialysate was cleared by centrifugation for 10 min at 10000g and 4°C before the concentration was determined (GP1: 0.26 mg/ml GP2: 0.32 mg/ml). Subsequently, the dialysates were aliquoted, snap-frozen in liquid nitrogen and stored at -80°C until use.

6.4.8 Preparation of *Xenopus laevis* egg extract

Prior to use, all glassware were rinsed twice with ddH₂O to remove residual calcium ions which would trigger release of the metaphase II arrested *xenopus laevis* eggs. Work with frogs and frog eggs was performed at 18°C, whereas prepared egg extracts were kept on ice and exclusively pipetted with cut tips. To induce egg laying, female frogs were injected with human chorionic gonadotropin (hCG, 1000 U/ml in ddH₂O, Intervet). Between 0.7-1 ml, depending on the size of the frog, were injected into the dorsal lymph sac using a 27-gauge needle (B. Braun, Melsungen, Germany). After 8 h, the frogs were transferred into containers

filled with 1.5 l 1x MMR buffer. 12-16 h later, laid eggs were collected in glass dishes and washed briefly with 1x MMR. Eggs with abnormal morphology were removed followed by incubation in dejellying solution for 5 min to remove the jelly coats of the eggs. Subsequently, the eggs were intensively washed for four to six times with CSF-XB to remove residual amounts of the cytotoxic cysteine. Again, eggs with abnormal morphology were removed and the remaining eggs were transferred to a 4 ml centrifuge tube (Beckman Coulter, Krefeld, Germany) containing 0.5 ml CSF-XB and 5 μ l Cytochalasin B. Centrifugation in a JS 13.1 swing-out rotor (Beckman Coulter, Krefeld, Germany) for 1 min at 200 g followed by 1 min at 600 g tightly packed the eggs. The supernatant on top of the eggs was carefully removed and the eggs were then crushed and fractionated by centrifugation at 13000 g for 10 min. The tube was carefully punctured by an 18-gauge needle and the cytoplasmic fraction in the middle was pulled out without contamination through the top layer containing huge amounts of lipids. The extract volume was estimated in the syringe before it was transferred into a precooled reaction tube and supplemented with Cytochalasin B to a final concentration of 10 μ g/ml. In order to test whether the prepared extract was still arrested in metaphase II 30 μ l of extract were supplemented with low amounts of frog sperm. 24 μ l of this mixture was transferred to a reaction containing 1 μ l of CaCl_2 (25x) to induce release into interphase. After 30 min of incubation at 30°C the condensation status of the chromatin was checked by immunofluorescence microscopy (IFM).

6.4.9 Purification of active recombinant human Separase

Five large 150 mm cell culture dishes with Hek293T cells at approximately 60% confluency were each co-transfected with 40 μ g of plasmid encoding for GFP-TEV₄-Separase and 20 μ g of plasmid encoding for Securin. After 36 h of expression, nocodazole was added for 12 h to arrest cells in mitosis. Cells were harvested and lysed in 10 ml LP2 buffer (see 6.5.9). Then, 250 μ l of preequilibrated GFP nanobodies coupled to sepharose were incubated with the lysate for 3 h at 4°C. In the meantime, a *Xenopus laevis* egg extract was prepared as described in 6.4.8 and supplemented with recombinant Δ 90-Cyclin B1 (final concentration: 57 nM) to prevent mitotic exit. The beads were washed once with LP2 buffer and once with CSF-XB buffer before they were combined with a ten-fold volume of CSF-extract. Addition of Ca^{2+} then released the extract into anaphase and started Securin degradation. After 20 min of incubation at RT the extract was diluted with CSF-XB to allow re-isolation of beads. The beads were then washed once with CSF-XB and once with TEV-cleavage buffer. Separase was eluted by adding TEV protease and incubation for 20 min at RT. The eluate was then

cleared from beads via Mobicol columns (Mobitec), aliquoted, snap-frozen in liquid nitrogen and stored at -80°C.

The described procedure was carried out with the Separase variant P1127A (Hellmuth et al., 2015) which allows purification of active enzyme, and with the Separase variant C2029S (Stemmann et al., 2001) which lacks proteolytic activity and serves as a negative control in performed cleavage assays.

6.4.10 Purification of active Plk1

Plasmids encoding for HA-tagged versions of wild type, kinase dead and constitutively active Plk1 were transfected into Hek293T cells as described in 6.5.4. Cell lysates were generated as described in 6.5.9 and incubated with HA-affinity matrix (Roche Diagnostic, Mannheim, Germany) for 3 h at 4°C and gentle shaking. The kinases were eluted with 0.1 M glycine, pH 2.8 and immediately neutralized with 1 M Tris (pH 9). Then, the eluate was dialyzed against 1x PBS at 4°C for 2 h before it was aliquoted and snap-frozen in liquid nitrogen and stored at -80°C until use.

6.5 Cell biological methods

6.5.1 Tissue culture cell lines

Hek 293T: human embryonic kidney cell line transformed with SV 40 large T antigen.

Hek 293 Flp-In: the Flp-In T-Rex 293 cell line contains a single stably integrated FRT site which allows the targeted transgene integration via Flp recombinase. Additionally, the cells constitutively express a tetracycline repressor which binds to the tetracycline operator sequence and suppresses expression in absence of tetra- or doxycycline.

HeLa K: human cervix epithelial adenocarcinoma cells, subclone K.

6.5.2 Cultivation of cell lines

Monolayer cell cultures were grown in culture dishes (Greiner Bio-One, Kremsmünster, Austria) in Dulbecco's Modified Eagle Medium (DMEM, PAA, Pasching, Austria) supplemented with 10% (v/v) heat inactivated (56°C, 30 min) fetal bovine serum (FCS, Sigma-Aldrich, Munich, Germany) at 37°C and 5% CO₂. To split the cells, medium was

removed and cells were washed with 1x PBS. Subsequently, the cells were incubated with 16 $\mu\text{l}/\text{cm}^2$ Trypsin/EDTA solution for 2-5 min to detach them from the cell culture dish. Adding fresh and prewarmed medium stopped the trypsin reaction and by pipetting up and down, the cells were further detached from the tray and from each other. The cells were then pelleted at 300 g for 3 min at RT, resuspended in prewarmed medium and distributed on new cell culture dishes. Exact numbers of cells were determined by the Vi-Cell Counter (Beckman Coulter, Krefeld, Germany) according to manufacturer's instructions.

6.5.3 Storage of mammalian cells

Cells were harvested at 60-80% confluency by trypsination, resuspended in 90% (v/v) fetal bovine serum and 10% (v/v) DMSO and aliquoted in cryo-tubes (Nalgene, Rochester, NY, USA). The cell suspension was then slowly frozen in a cardboard box or an insulated device containing isopropanol. For long time storage the tubes were transferred into a tank of liquid nitrogen. For thawing, cryo stocks were rapidly warmed in a 37°C water bath. To remove DMSO, tubes were briefly centrifuged (300 g, 1 min) and the supernatant was discarded. The cell pellet was resuspended in prewarmed DMEM and spread on cell culture dishes.

6.5.4 Transfection of Hek293 cells

Hek293T and Hek293 Flp-In cells were transfected with plasmid DNA at 50-60% confluency by the calcium phosphate method. The transfection mix was prepared as follows:

Diameter of dish	5.3 cm	10 cm	14.5 cm
Volume of medium	4 ml	10 ml	25 ml
Amount of DNA	4 μg	16 μg	30 μg
H₂O (-volume of DNA and CaCl ₂)	300 μl	800 μl	2000 μl
2 M CaCl₂	37.2 μl	99.2 μl	248 μl
2x HBS	300 μl	800 μl	2000 μl

Shortly before transfection 20 μM chloroquin was added to the cells. The plasmid DNA was first mixed with water and then with the sterile CaCl₂. The 2x HBS solution was added dropwise while gently vortexing. The transfection mix was then carefully dripped onto the surface of the medium. 8-12 h later, the medium was changed and cells continued to grow and expressed the transgene for further 24-48 h.

6.5.5 Transfection of HeLa cells

HeLa cells were transfected with the cationic polymer polyethylenimine (PEI, linear, MW 25000, Polysciences, Inc., Warrington, PA, USA). The day before transfection, cells were seeded in a density of about 2×10^5 cells per six-well. The transfection mix was prepared as follows: 300 μ l of sterile NaCl was mixed with 3 μ g of DNA and vortexed for 5 sec. 16.6 μ l of sterile 10 μ M PEI were added and again the mix was vortexed for 15 sec. After incubation at RT for 15 min, the transfection mix was added to the cells. 4 h later the medium was changed and cells were further incubated for 24-36 h.

6.5.6 Generation of stable Hek293 Flp-In cell lines

In order to generate stable cell lines, Hek293 Flp-In cells were grown at 50-60% confluency on a 14.5 cm dish. Using the calcium phosphate method, they were co-transfected with 3 μ g of a plasmid (pcDNA1-backbone) containing the gene of interest (under control of a tetracycline operator), a hygromycin resistance cassette, a FRT site (which allows the site-specific recombination and integration into the host genome) and 30 μ g of a plasmid encoding for Flp recombinase (pAG1786). 36 h after transfection, hygromycin B was added (150 μ g/ml, PAA) to put the cells under selection. For the next 7-10 days the medium was changed if necessary to remove dying cells. Surviving cells with successful integration of the plasmid then formed visible colonies which were individually isolated using small glass cylinders for trypsination and transferred into a single well of a 24-well cell culture dish. Each clone was then test-induced with doxycyclin and transgene expression was verified by Western blot analysis. The plasmid used for the integration into the FRT site also contained an additional loxP-site allowing a second round of genomic integration utilizing Cre recombinase (Buheitel & Stemmann, 2013). Hence, a single stable cell line was used for co-transfection of a plasmid carrying the second gene of interest and a plasmid expressing the Cre-recombinase. Accordingly, 27 μ g of plasmid (pcDNA5-backbone) containing the gene of interest (under control of a tetracycline operator), a G418 resistance cassette and a loxP-site were co-transfected with 3 μ g of plasmid encoding for Cre recombinase (pIC-Cre). Selection was carried out with 120 μ g/ml G418 (Gibco). Cloning and screening for double transgenic cell line clones were performed as described for single stable cell lines.

6.5.7 Synchronization of mammalian cells

For synchronization at the G1/S boundary, thymidine was added to the medium at a final concentration of 2 mM. After 16 to 20 h, cells were released from the block by washing once

with PBS and incubated in fresh medium for 2x 15 min and 1x 30 min. To synchronize the cells in metaphase of mitosis, 200 ng/ μ l nocodazole or taxol was added 3-4 h after release from thymidine block. Nocodazole/taxol treatment was carried out for 8-10 h. In case of unsynchronized cells drug treatment was prolonged to 16 h.

6.5.8 Taxol-ZM override

For the taxol-ZM experiments, HeLa cells were transfected with PEI at a confluency of 50%. The *PCNT*-encoding constructs and siRNA against endogenous *PCNT* were co-transfected. Thymidine was added with the transfection mix and after 20 h the cells were released from the G1/S-phase block. 4 h later, taxol was added for 8 h and the metaphase-to-anaphase arrest was overridden by addition of 5 μ M ZM 447439, an aurora B kinase inhibitor (Tocris Biosciences, Bristol, United Kingdom). Western blot samples were then taken at the indicated time points.

6.5.9 Generation of tissue culture cell lysates for Immunoprecipitation experiments

Cells were harvested by scraping or rinsing from a 100 mm culture dish and pelleted by centrifugation for 3 min at 300 g. Cells were washed once with 1x PBS before the pellet was resuspended in 500 μ l LP2 buffer and transferred to a dounce homogenizer (Wheaton, Millville, NJ, USA). 10 strokes with a tight pestle efficiently lysed the cells and the lysate was transferred into a reaction tube before it was further incubated for 5-10 min on ice. Centrifugation at 16000 g for 30 min at 4°C cleared the lysate from debris and the supernatant was transferred to a new reaction tube. The corresponding beads were washed with 1x PBS and LP2 buffer before they were incubated with the supernatant for 3 h or overnight at 4°C. Subsequently, the beads were gently pelleted at 300 g and washed three times with LP2 buffer. Bound protein(s) were eluted with the corresponding elution buffer. Alternatively, for the generation of Western blot samples, the beads were mixed with an adequate volume of 1x SDS sample buffer and boiled for 5 min at 95°C. The eluate was then cleared from beads by centrifugation through a Mobicol column (Mobicol, Göttingen, Germany). Then, β -mercaptoethanol was added and the sample was boiled again for 5 min at 95°C.

6.5.10 Isolation of centrosomes

In order to isolate centrosomes, mitotic arrested cells from a 10 cm dish were harvested and pelleted by centrifugation (300 g, 3 min). The pellet was washed once with 10 ml 1x PBS and then resuspended in 0.5 ml LP2 which was supplemented with 20 μ g/ml DNaseI (Roche,

Mannheim, Germany) and 0.5 $\mu\text{g}/\text{ml}$ nocodazole (Sigma-Aldrich, Germany). The cells were lysed on ice by 10 strokes in a tight glass dounce homogenizer (Wheaton, Millville, NJ, USA) and incubated for 15 min on ice. Then, the lysate was centrifuged (3800 g, 10 min, 4°C) in order to pellet and remove cell debris and chromatin. In the meantime, 15 ml COREX round bottom glass tubes were prepared. Therefore, the sterile cover slips were placed onto a glass adapter on the bottom of the glass tube and covered with 3.5 ml of the sucrose cushion. The centrosome containing supernatants were carefully transferred on top of the sucrose cushions without mixing them and the centrosomes were centrifuged onto the cover slips (13000 g, 25 min, 4°C, swing-out rotor). The cover slips were then fixed in -20° methanol overnight and further processed for IFM. For some experiments, the lysates were incubated with recombinant proteases. Therefore, the lysates cleared from debris were transferred to reaction tubes, supplemented with TEV (1 U/ μl) and/or HRV (10 ng/ μl) protease and incubated for 30 min at RT before they were transferred into the COREX round bottom glass tubes.

6.5.11 Immunofluorescence of isolated centrosomes

The cover slips that were fixed overnight in methanol at -20°C were incubated in blocking solution for 1 h at RT. Then, the cover slips were incubated with primary antibodies diluted in blocking solution for 1 h at RT, washed three times with washing solution and incubated with appropriate fluorescently labeled secondary antibodies again diluted in blocking solution for 1 h at RT. Finally, the cover slips were washed three times with washing solution and mounted with 3 μl mounting medium on a microscope slide. The cover slips were fixed and sealed with nail polish before the centrosomes were visualized by fluorescence microscopy.

7 References

- Alexandru, G., Uhlmann, F., Mechtler, K., Poupart, M.-A., & Nasmyth, K. (2001). Phosphorylation of the cohesin subunit Scc1 by Polo/Cdc5 kinase regulates sister chromatid separation in yeast. *Cell*, *105*(4), 459–472.
[https://doi.org/10.1016/s0092-8674\(01\)00362-2](https://doi.org/10.1016/s0092-8674(01)00362-2)
- Alves-Cruzeiro, J. M. da C., Nogales-Cadenas, R., & Pascual-Montano, A. D. (2014). CentrosomeDB: A new generation of the centrosomal proteins database for *Human* and *Drosophila melanogaster*. *Nucleic Acids Research*, *42*(D1), D430–D436.
<https://doi.org/10.1093/nar/gkt1126>
- Alvey, P. L. (1986). Do adult centrioles contain cartwheels and lie at right angles to each other? *Cell Biology International Reports*, *10*(8), 589–598.
[https://doi.org/10.1016/0309-1651\(86\)90136-0](https://doi.org/10.1016/0309-1651(86)90136-0)
- Amano, S. (1957). The Structure of the Centrioles and Spindle Body as Observed Under the Electron and Phase Contrast Microscope SA New Extension-fiber Theory Concerning Mitotic Mechanism in Animal Cells. *Cytologia*, *22*(2), 193–212.
- Andersen, J. S., Wilkinson, C. J., Mayor, T., Mortensen, P., Nigg, E. A., & Mann, M. (2003). Proteomic characterization of the human centrosome by protein correlation profiling. *Nature*, *426*(6966), 570–574.
<https://doi.org/10.1038/nature02166>
- Andrews, P. D., Ovechkina, Y., Morrice, N., Wagenbach, M., Duncan, K., Wordeman, L., & Swedlow, J. R. (2004). Aurora B regulates MCAK at the mitotic centromere. *Developmental Cell*, *6*(2), 253–268.
[https://doi.org/10.1016/s1534-5807\(04\)00025-5](https://doi.org/10.1016/s1534-5807(04)00025-5)
- Archambault, V., & Glover, D. M. (2009). Polo-like kinases: Conservation and divergence in their functions and regulation. *Nature Reviews Molecular Cell Biology*, *10*(4), 265–275.
<https://doi.org/10.1038/nrm2653>
- Arquint, C., Gabryjonczyk, A.-M., Imseng, S., Böhm, R., Sauer, E., Hiller, S., Nigg, E. A., & Maier, T. (2015). STIL binding to Polo-box 3 of PLK4 regulates centriole duplication. *ELife*, *4*.
<https://doi.org/10.7554/eLife.07888>
- Arquint, C., & Nigg, E. A. (2016). The PLK4–STIL–SAS-6 module at the core of centriole duplication. *Biochemical Society Transactions*, *44*(5), 1253–1263.
<https://doi.org/10.1042/BST20160116>
- Azimzadeh, J., & Marshall, W. F. (2010). Building the Centriole. *Current Biology*, *20*(18), R816–R825.
<https://doi.org/10.1016/j.cub.2010.08.010>
- Badano, J. L., Teslovich, T. M., & Katsanis, N. (2005). The centrosome in human genetic disease. *Nature Reviews Genetics*, *6*(3), 194–205.
<https://doi.org/10.1038/nrg1557>
- Bahe, S., Stierhof, Y.-D., Wilkinson, C. J., Leiss, F., & Nigg, E. A. (2005). Rootletin forms centriole-associated filaments and functions in centrosome cohesion. *The Journal of Cell Biology*, *171*(1), 27–33.
<https://doi.org/10.1083/jcb.200504107>
- Banerji, R., Skibbens, R. V., & Iovine, M. K. (2017). How many roads lead to cohesinopathies?: Mechanisms Underlying Cohesinopathies. *Developmental Dynamics*, *246*(11), 881–888.
<https://doi.org/10.1002/dvdy.24510>

- Barford, D. (2011). Structural insights into anaphase-promoting complex function and mechanism. *Philosophical Transactions of the Royal Society B: Biological Sciences*, 366(1584), 3605–3624.
<https://doi.org/10.1098/rstb.2011.0069>
- Barr, F. A., Silljé, H. H. W., & Nigg, E. A. (2004). Polo-like kinases and the orchestration of cell division. *Nature Reviews Molecular Cell Biology*, 5(6), 429–441.
<https://doi.org/10.1038/nrm1401>
- Basto, R., Lau, J., Vinogradova, T., Gardiol, A., Woods, C. G., Khodjakov, A., & Raff, J. W. (2006). Flies without Centrioles. *Cell*, 125(7), 1375–1386.
<https://doi.org/10.1016/j.cell.2006.05.025>
- Bauer, B. W., Davidson, I. F., Canena, D., Wutz, G., Tang, W., Litos, G., Horn, S., Hinterdorfer, P., & Peters, J.-M. (2021). Cohesin mediates DNA loop extrusion by a “swing and clamp” mechanism. *Cell*, 184(21), 5448–5464.e22.
<https://doi.org/10.1016/j.cell.2021.09.016>
- Baxter, J. (2015). “Breaking Up Is Hard to Do”: The Formation and Resolution of Sister Chromatid Intertwines. *Journal of Molecular Biology*, 427(3), 590–607.
<https://doi.org/10.1016/j.jmb.2014.08.022>
- Bayley, P. M., Schilstra, M. J., & Martin, S. R. (1989). A simple formulation of microtubule dynamics: Quantitative implications of the dynamic instability of microtubule populations in vivo and in vitro. *Journal of Cell Science*, 93 (Pt 2), 241–254.
<https://doi.org/10.1242/jcs.93.2.241>
- Beauchene, N. A., Díaz-Martínez, L. A., Furniss, K., Hsu, W.-S., Tsai, H.-J., Chamberlain, C., Esponda, P., Giménez-Abián, J. F., & Clarke, D. J. (2010). Rad21 is required for centrosome integrity in human cells independently of its role in chromosome cohesion. *Cell Cycle*, 9(9), 1774–1780.
<https://doi.org/10.4161/cc.9.9.11524>
- Beckouët, F., Srinivasan, M., Roig, M. B., Chan, K.-L., Scheinost, J. C., Batty, P., Hu, B., Petela, N., Gligoris, T., Smith, A. C., Strmecki, L., Rowland, B. D., & Nasmyth, K. (2016). Releasing Activity Disengages Cohesin’s Smc3/Scc1 Interface in a Process Blocked by Acetylation. *Molecular Cell*, 61(4), 563–574.
<https://doi.org/10.1016/j.molcel.2016.01.026>
- Bender, D., Da Silva, E. M. L., Chen, J., Poss, A., Gawey, L., Rulon, Z., & Rankin, S. (2020). Multivalent interaction of ESCO2 with the replication machinery is required for sister chromatid cohesion in vertebrates. *Proceedings of the National Academy of Sciences of the United States of America*, 117(2), 1081–1089.
<https://doi.org/10.1073/pnas.1911936117>
- Bennabi, I., Terret, M.-E., & Verlhac, M.-H. (2016). Meiotic spindle assembly and chromosome segregation in oocytes. *The Journal of Cell Biology*, 215(5), 611–619.
<https://doi.org/10.1083/jcb.201607062>
- Bertani G. (2004). Lysogeny at mid-twentieth century: P1, P2, and other experimental systems. *Journal of bacteriology*, 186(3), 595–600.
<https://doi.org/10.1128/JB.186.3.595-600.2004>
- Bettencourt-Dias, M., Rodrigues-Martins, A., Carpenter, L., Riparbelli, M., Lehmann, L., Gatt, M. K., Carmo, N., Balloux, F., Callaini, G., & Glover, D. M. (2005). SAK/PLK4 Is Required for Centriole Duplication and Flagella Development. *Current Biology*, 15(24), 2199–2207.
<https://doi.org/10.1016/j.cub.2005.11.042>
- Bisht, K. K., Daniloski, Z., & Smith, S. (2013). SA1 binds directly to DNA through its unique AT-hook to promote sister chromatid cohesion at telomeres. *Journal of Cell Science*, 126(Pt 15), 3493–3503.
<https://doi.org/10.1242/jcs.130872>

- Blanco-Ameijeiras, J., Lozano-Fernández, P., & Martí, E. (2022). Centrosome maturation—In tune with the cell cycle. *Journal of Cell Science*, *135*(2), jcs259395.
<https://doi.org/10.1242/jcs.259395>
- Boland, A., Martin, T. G., Zhang, Z., Yang, J., Bai, X., Chang, L., Scheres, S. H. W., & Barford, D. (2017). Cryo-EM structure of a metazoan separase–securin complex at near-atomic resolution. *Nature Structural & Molecular Biology*, *24*(4), 414–418.
<https://doi.org/10.1038/nsmb.3386>
- Brar, G. A., Kiburz, B. M., Zhang, Y., Kim, J.-E., White, F., & Amon, A. (2006). Rec8 phosphorylation and recombination promote the step-wise loss of cohesins in meiosis. *Nature*, *441*(7092), 532–536.
<https://doi.org/10.1038/nature04794>
- Brautigan, D. L. (2013). Protein Ser/ Thr phosphatases - the ugly ducklings of cell signalling: Protein Ser/Thr phosphatases. *FEBS Journal*, *280*(2), 324–325.
<https://doi.org/10.1111/j.1742-4658.2012.08609.x>
- Brouhard, G., & Sept, D. (2012). Microtubules: Sizing up the GTP cap. *Current Biology: CB*, *22*(18), R802–803.
<https://doi.org/10.1016/j.cub.2012.07.050>
- Brown, R. C., & Lemmon, B. E. (2011). Dividing without centrioles: Innovative plant microtubule organizing centres organize mitotic spindles in bryophytes, the earliest extant lineages of land plants. *AoB Plants*, *2011*(0), plr028–plr028.
<https://doi.org/10.1093/aobpla/plr028>
- Brun, L., Rupp, B., Ward, J. J., & Nédélec, F. (2009). A theory of microtubule catastrophes and their regulation. *Proceedings of the National Academy of Sciences*, *106*(50), 21173–21178.
<https://doi.org/10.1073/pnas.0910774106>
- Buchman, J. J., Tseng, H.-C., Zhou, Y., Frank, C. L., Xie, Z., & Tsai, L.-H. (2010). Cdk5rap2 Interacts with Pericentrin to Maintain the Neural Progenitor Pool in the Developing Neocortex. *Neuron*, *66*(3), 386–402.
<https://doi.org/10.1016/j.neuron.2010.03.036>
- Bugnard, E., Zaal, K. J. M., & Ralston, E. (2005). Reorganization of microtubule nucleation during muscle differentiation. *Cell Motility and the Cytoskeleton*, *60*(1), 1–13.
<https://doi.org/10.1002/cm.20042>
- Buheitel, J., & Stemmann, O. (2013). Prophase pathway-dependent removal of cohesin from human chromosomes requires opening of the Smc3–Scc1 gate. *The EMBO Journal*, *32*(5), 666–676.
<https://doi.org/10.1038/emboj.2013.7>
- Bürmann, F., Lee, B.-G., Than, T., Sinn, L., O'Reilly, F. J., Yatskevich, S., Rappsilber, J., Hu, B., Nasmyth, K., & Löwe, J. (2019). A folded conformation of MukBEF and cohesin. *Nature Structural & Molecular Biology*, *26*(3), 227–236.
<https://doi.org/10.1038/s41594-019-0196-z>
- Cabral, G., Sanegre Sans, S., Cowan, C. R., & Dammermann, A. (2013). Multiple Mechanisms Contribute to Centriole Separation in *C. elegans*. *Current Biology*, *23*(14), 1380–1387.
<https://doi.org/10.1016/j.cub.2013.06.043>
- Çamdere, G., Guacci, V., Stricklin, J., & Koshland, D. (2015). The ATPases of cohesin interface with regulators to modulate cohesin-mediated DNA tethering. *Elife*, *4*, e11315.
<https://doi.org/10.7554/eLife.11315>
- Canudas, S., & Smith, S. (2009). Differential regulation of telomere and centromere cohesion by the Scc3 homologues SA1 and SA2, respectively, in human cells. *The Journal of Cell Biology*, *187*(2), 165–173.

- <https://doi.org/10.1083/jcb.200903096>
- Carazo-Salas, R. E., Guarguaglini, G., Gruss, O. J., Segref, A., Karsenti, E., & Mattaj, I. W. (1999). Generation of GTP-bound Ran by RCC1 is required for chromatin-induced mitotic spindle formation. *Nature*, *400*(6740), 178–181.
<https://doi.org/10.1038/22133>
- Cardozo, T., & Pagano, M. (2004). The SCF ubiquitin ligase: Insights into a molecular machine. *Nature Reviews Molecular Cell Biology*, *5*(9), 739–751.
<https://doi.org/10.1038/nrm1471>
- Carmena, M., Wheelock, M., Funabiki, H., & Earnshaw, W. C. (2012). The chromosomal passenger complex (CPC): From easy rider to the godfather of mitosis. *Nature Reviews Molecular Cell Biology*, *13*(12), 789–803.
<https://doi.org/10.1038/nrm3474>
- Carramolino, L., Lee, B. C., Zaballos, A., Peled, A., Barthelemy, I., Shav-Tal, Y., Prieto, I., Carmi, P., Gothelf, Y., González de Buitrago, G., Aracil, M., Márquez, G., Barbero, J. L., & Zipori, D. (1997). SA-1, a nuclear protein encoded by one member of a novel gene family: Molecular cloning and detection in hemopoietic organs. *Gene*, *195*(2), 151–159.
[https://doi.org/10.1016/s0378-1119\(97\)00121-2](https://doi.org/10.1016/s0378-1119(97)00121-2)
- Carvalho-Santos, Z., Machado, P., Alvarez-Martins, I., Gouveia, S. M., Jana, S. C., Duarte, P., Amado, T., Branco, P., Freitas, M. C., Silva, S. T. N., Antony, C., Bandejas, T. M., & Bettencourt-Dias, M. (2012). BLD10/CEP135 Is a Microtubule-Associated Protein that Controls the Formation of the Flagellum Central Microtubule Pair. *Developmental Cell*, *23*(2), 412–424.
<https://doi.org/10.1016/j.devcel.2012.06.001>
- Cassimeris, L. (2002). The oncoprotein 18/stathmin family of microtubule destabilizers. *Current Opinion in Cell Biology*, *14*(1), 18–24.
[https://doi.org/10.1016/s0955-0674\(01\)00289-7](https://doi.org/10.1016/s0955-0674(01)00289-7)
- Cavanaugh, A. M., & Jaspersen, S. L. (2017). Big Lessons from Little Yeast: Budding and Fission Yeast Centrosome Structure, Duplication, and Function. *Annual Review of Genetics*, *51*, 361–383.
<https://doi.org/10.1146/annurev-genet-120116-024733>
- Chan, J., Sambade, A., Calder, G., & Lloyd, C. (2009). Arabidopsis Cortical Microtubules Are Initiated along, as Well as Branching from, Existing Microtubules. *THE PLANT CELL ONLINE*, *21*(8), 2298–2306.
<https://doi.org/10.1105/tpc.109.069716>
- Chan, K.-L., Gligoris, T., Upcher, W., Kato, Y., Shirahige, K., Nasmyth, K., & Beckouët, F. (2013). Pds5 promotes and protects cohesin acetylation. *Proceedings of the National Academy of Sciences*, *110*(32), 13020–13025.
<https://doi.org/10.1073/pnas.1306900110>
- Chang, L., Zhang, Z., Yang, J., McLaughlin, S. H., & Barford, D. (2014). Molecular architecture and mechanism of the anaphase-promoting complex. *Nature*, *513*(7518), 388–393.
<https://doi.org/10.1038/nature13543>
- Chen, H., Gos, A., Morris, M. A., & Antonarakis, S. E. (1996). Localization of a human homolog of the mouse pericentrin gene (PCNT) to chromosome 21qter. *Genomics*, *35*(3), 620–624.
<https://doi.org/10.1006/geno.1996.0411>
- Choi, Y.-K., Liu, P., Sze, S. K., Dai, C., & Qi, R. Z. (2010). CDK5RAP2 stimulates microtubule nucleation by the γ -tubulin ring complex. *The Journal of Cell Biology*, *191*(6), 1089–1095.
<https://doi.org/10.1083/jcb.201007030>

- Choksi, S. P., Lauter, G., Swoboda, P., & Roy, S. (2014). Switching on cilia: Transcriptional networks regulating ciliogenesis. *Development*, *141*(7), 1427–1441.
<https://doi.org/10.1242/dev.074666>
- Ciosk, R., Shirayama, M., Shevchenko, A., Tanaka, T., Toth, A., Shevchenko, A., & Nasmyth, K. (2000). Cohesin's binding to chromosomes depends on a separate complex consisting of Scc2 and Scc4 proteins. *Molecular Cell*, *5*(2), 243–254.
[https://doi.org/10.1016/s1097-2765\(00\)80420-7](https://doi.org/10.1016/s1097-2765(00)80420-7)
- Ciosk, R., Zachariae, W., Michaelis, C., Shevchenko, A., Mann, M., & Nasmyth, K. (1998). An ESP1/PDS1 complex regulates loss of sister chromatid cohesion at the metaphase to anaphase transition in yeast. *Cell*, *93*(6), 1067–1076.
[https://doi.org/10.1016/s0092-8674\(00\)81211-8](https://doi.org/10.1016/s0092-8674(00)81211-8)
- Coelho, P. A., Bury, L., Shahbazi, M. N., Liakath-Ali, K., Tate, P. H., Wormald, S., Hindley, C. J., Huch, M., Archer, J., Skarnes, W. C., Zernicka-Goetz, M., & Glover, D. M. (2015). Over-expression of Plk4 induces centrosome amplification, loss of primary cilia and associated tissue hyperplasia in the mouse. *Open Biology*, *5*(12), 150209.
<https://doi.org/10.1098/rsob.150209>
- Collier, J. E., Lee, B.-G., Roig, M. B., Yatskevich, S., Petela, N. J., Metson, J., Voulgaris, M., Gonzalez Llamazares, A., Löwe, J., & Nasmyth, K. A. (2020). Transport of DNA within cohesin involves clamping on top of engaged heads by Scc2 and entrapment within the ring by Scc3. *ELife*, *9*, e59560.
<https://doi.org/10.7554/eLife.59560>
- Collier, J. E., & Nasmyth, K. A. (2022). DNA passes through cohesin's hinge as well as its Smc3-kleisin interface. *ELife*, *11*, e80310.
<https://doi.org/10.7554/eLife.80310>
- Collins, G. A., & Goldberg, A. L. (2017). The Logic of the 26S Proteasome. *Cell*, *169*(5), 792–806.
<https://doi.org/10.1016/j.cell.2017.04.023>
- Cordingley, M. G., Callahan, P. L., Sardana, V. V., Garsky, V. M., & Colonno, R. J. (1990). Substrate requirements of human rhinovirus 3C protease for peptide cleavage in vitro. *Journal of Biological Chemistry*, *265*(16), 9062–9065.
- Cosenza, M. R., & Krämer, A. (2016). Centrosome amplification, chromosomal instability and cancer: Mechanistic, clinical and therapeutic issues. *Chromosome Research*, *24*(1), 105–126.
<https://doi.org/10.1007/s10577-015-9505-5>
- Countryman, P., Fan, Y., Gorthi, A., Pan, H., Strickland, J., Kaur, P., Wang, X., Lin, J., Lei, X., White, C., You, C., Wirth, N., Tessmer, I., Piehler, J., Riehn, R., Bishop, A. J. R., Tao, Y. J., & Wang, H. (2018). Cohesin SA2 is a sequence-independent DNA-binding protein that recognizes DNA replication and repair intermediates. *The Journal of Biological Chemistry*, *293*(3), 1054–1069.
<https://doi.org/10.1074/jbc.M117.806406>
- Culver, B. P., Meehl, J. B., Giddings, T. H., & Winey, M. (2009). The two SAS-6 homologs in *Tetrahymena thermophila* have distinct functions in basal body assembly. *Molecular Biology of the Cell*, *20*(6), 1865–1877.
<https://doi.org/10.1091/mbc.e08-08-0838>
- Cunha-Ferreira, I., Bento, I., & Bettencourt-Dias, M. (2009). From Zero to Many: Control of Centriole Number in Development and Disease. *Traffic*, *10*(5), 482–498.
<https://doi.org/10.1111/j.1600-0854.2009.00905.x>
- Cuschieri, L., Nguyen, T., & Vogel, J. (2007). Control At The Cell Center: The Role Of Spindle Poles In Cytoskeletal Organization And Cell Cycle Regulation. *Cell Cycle*, *6*(22), 2788–2794.
<https://doi.org/10.4161/cc.6.22.4941>

- da Silva, E. S., & Naghavi, M. H. (2023). Microtubules and viral infection. *Advances in Virus Research*, *115*, 87–134.
<https://doi.org/10.1016/bs.aivir.2023.02.003>
- Davidson, I. F., Barth, R., Zaczek, M., van der Torre, J., Tang, W., Nagasaka, K., Janissen, R., Kerssemakers, J., Wutz, G., Dekker, C., & Peters, J.-M. (2023). CTCF is a DNA-tension-dependent barrier to cohesin-mediated loop extrusion. *Nature*, *616*(7958), 822–827.
<https://doi.org/10.1038/s41586-023-05961-5>
- Davidson, I. F., Bauer, B., Goetz, D., Tang, W., Wutz, G., & Peters, J.-M. (2019). DNA loop extrusion by human cohesin. *Science*, *366*(6471), 1338–1345.
<https://doi.org/10.1126/science.aaz3418>
- Dawe, H. R., Farr, H., & Gull, K. (2006). Centriole/basal body morphogenesis and migration during ciliogenesis in animal cells. *Journal of Cell Science*, *120*(1), 7–15.
<https://doi.org/10.1242/jcs.03305>
- Deardorff, M. A., Bando, M., Nakato, R., Watrin, E., Itoh, T., Minamino, M., Saitoh, K., Komata, M., Katou, Y., Clark, D., Cole, K. E., De Baere, E., Decroos, C., Di Donato, N., Ernst, S., Francey, L. J., Gyftodimou, Y., Hirashima, K., Hullings, M., ... Shirahige, K. (2012). HDAC8 mutations in Cornelia de Lange syndrome affect the cohesin acetylation cycle. *Nature*, *489*(7415), 313–317.
<https://doi.org/10.1038/nature11316>
- Deardorff, M. A., Kaur, M., Yaeger, D., Rampuria, A., Korolev, S., Pie, J., Gil-Rodríguez, C., Arnedo, M., Loeys, B., Kline, A. D., Wilson, M., Lillquist, K., Siu, V., Ramos, F. J., Musio, A., Jackson, L. S., Dorsett, D., & Krantz, I. D. (2007). Mutations in Cohesin Complex Members SMC3 and SMC1A Cause a Mild Variant of Cornelia de Lange Syndrome with Predominant Mental Retardation. *The American Journal of Human Genetics*, *80*(3), 485–494.
<https://doi.org/10.1086/511888>
- Delattre, M., & Gönczy, P. (2004). The arithmetic of centrosome biogenesis. *Journal of Cell Science*, *117*(9), 1619–1630.
<https://doi.org/10.1242/jcs.01128>
- Delaval, B., & Doxsey, S. J. (2010). Pericentrin in cellular function and disease. *The Journal of Cell Biology*, *188*(2), 181–190.
<https://doi.org/10.1083/jcb.200908114>
- Delgehyr, N., Sillibourne, J., & Bornens, M. (2005). Microtubule nucleation and anchoring at the centrosome are independent processes linked by ninein function. *Journal of Cell Science*, *118*(8), 1565–1575.
<https://doi.org/10.1242/jcs.02302>
- Dephoure, N., Zhou, C., Villén, J., Beausoleil, S. A., Bakalarski, C. E., Elledge, S. J., & Gygi, S. P. (2008). A quantitative atlas of mitotic phosphorylation. *Proceedings of the National Academy of Sciences*, *105*(31), 10762–10767.
<https://doi.org/10.1073/pnas.0805139105>
- Díaz-Martínez, L. A., Beauchene, N. A., Furniss, K., Esponda, P., Giménez-Abián, J. F., & Clarke, D. J. (2010). Cohesin is needed for bipolar mitosis in human cells. *Cell Cycle*, *9*(9), 1764–1773.
<https://doi.org/10.4161/cc.9.9.11525>
- Ding, R., West, R. R., Morphew, D. M., Oakley, B. R., & McIntosh, J. R. (1997). The spindle pole body of *Schizosaccharomyces pombe* enters and leaves the nuclear envelope as the cell cycle proceeds. *Molecular Biology of the Cell*, *8*(8), 1461–1479.
<https://doi.org/10.1091/mbc.8.8.1461>

- Dippell, R. V. (1968). The development of basal bodies in paramecium. *Proceedings of the National Academy of Sciences of the United States of America*, 61(2), 461–468.
<https://doi.org/10.1073/pnas.61.2.461>
- Doxsey, S. J., Stein, P., Evans, L., Calarco, P. D., & Kirschner, M. (1994). Pericentrin, a highly conserved centrosome protein involved in microtubule organization. *Cell*, 76(4), 639–650.
[https://doi.org/10.1016/0092-8674\(94\)90504-5](https://doi.org/10.1016/0092-8674(94)90504-5)
- Elia, A. E., Rellos, P., Haire, L. F., Chao, J. W., Ivins, F. J., Hoepker, K., Mohammad, D., Cantley, L. C., Smerdon, S. J., & Yaffe, M. B. (2003). The molecular basis for phosphodependent substrate targeting and regulation of Plks by the Polo-box domain. *Cell*, 115(1), 83–95.
[https://doi.org/10.1016/s0092-8674\(03\)00725-6](https://doi.org/10.1016/s0092-8674(03)00725-6)
- Enserink, J. M., & Kolodner, R. D. (2010). An overview of Cdk1-controlled targets and processes. *Cell Division*, 5(1), 11.
<https://doi.org/10.1186/1747-1028-5-11>
- Eytan, E., Wang, K., Miniowitz-Shemtov, S., Sitry-Shevah, D., Kaisari, S., Yen, T. J., Liu, S.-T., & Hershko, A. (2014). Disassembly of mitotic checkpoint complexes by the joint action of the AAA-ATPase TRIP13 and p31(comet). *Proceedings of the National Academy of Sciences of the United States of America*, 111(33), 12019–12024.
<https://doi.org/10.1073/pnas.1412901111>
- Fang, G., Zhang, D., Yin, H., Zheng, L., Bi, X., & Yuan, L. (2014). Centlein mediates an interaction between C-Nap1 and Cep68 to maintain centrosome cohesion. *Journal of Cell Science*, 127(8), 1631–1639.
<https://doi.org/10.1242/jcs.139451>
- Faragher, A. J., & Fry, A. M. (2003). Nek2A kinase stimulates centrosome disjunction and is required for formation of bipolar mitotic spindles. *Molecular Biology of the Cell*, 14(7), 2876–2889.
<https://doi.org/10.1091/mbc.e03-02-0108>
- Farcas, A.-M., Uluocak, P., Helmhart, W., & Nasmyth, K. (2011). Cohesin's Concatenation of Sister DNAs Maintains Their Intertwining. *Molecular Cell*, 44(1), 97–107.
<https://doi.org/10.1016/j.molcel.2011.07.034>
- Firat-Karalar, E. N., & Stearns, T. (2014). The centriole duplication cycle. *Philosophical Transactions of the Royal Society B: Biological Sciences*, 369(1650), 20130460–20130460.
<https://doi.org/10.1098/rstb.2013.0460>
- Flory, M. R., & Davis, T. N. (2003). The centrosomal proteins pericentrin and kendrin are encoded by alternatively spliced products of one gene. *Genomics*, 82(3), 401–405.
[https://doi.org/10.1016/S0888-7543\(03\)00119-8](https://doi.org/10.1016/S0888-7543(03)00119-8)
- Fu, J., & Glover, D. (2016). How the newborn centriole becomes a mother. *Cell Cycle*, 15(12), 1521–1522.
<https://doi.org/10.1080/15384101.2016.1164566>
- Fu, J., & Glover, D. M. (2012). Structured illumination of the interface between centriole and peri-centriolar material. *Open Biology*, 2(8), 120104–120104.
<https://doi.org/10.1098/rsob.120104>
- Fujita, H., Yoshino, Y., & Chiba, N. (2016). Regulation of the centrosome cycle. *Molecular & Cellular Oncology*, 3(2), e1075643.
<https://doi.org/10.1080/23723556.2015.1075643>
- Galaktionov, K., & Beach, D. (1991). Specific activation of cdc25 tyrosine phosphatases by B-type cyclins: Evidence for multiple roles of mitotic cyclins. *Cell*, 67(6), 1181–1194.
[https://doi.org/10.1016/0092-8674\(91\)90294-9](https://doi.org/10.1016/0092-8674(91)90294-9)

- Gandhi, R., Gillespie, P. J., & Hirano, T. (2006). Human Wapl Is a Cohesin-Binding Protein that Promotes Sister-Chromatid Resolution in Mitotic Prophase. *Current Biology*, *16*(24), 2406–2417.
<https://doi.org/10.1016/j.cub.2006.10.061>
- Geimer, S., & Melkonian, M. (2004). The ultrastructure of the *Chlamydomonas reinhardtii* basal apparatus: Identification of an early marker of radial asymmetry inherent in the basal body. *Journal of Cell Science*, *117*(13), 2663–2674.
<https://doi.org/10.1242/jcs.01120>
- Gerlich, D., Koch, B., Dupeux, F., Peters, J.-M., & Ellenberg, J. (2006). Live-cell imaging reveals a stable cohesin-chromatin interaction after but not before DNA replication. *Current Biology: CB*, *16*(15), 1571–1578.
<https://doi.org/10.1016/j.cub.2006.06.068>
- Gibbons, I. R., & Grimstone, A. V. (1960). On flagellar structure in certain flagellates. *The Journal of Cell Biology*, *7*(4), 697–716.
- Gillingham, A. K., & Munro, S. (2000). The PACT domain, a conserved centrosomal targeting motif in the coiled-coil proteins AKAP450 and pericentrin. *EMBO Reports*, *1*(6), 524–529.
<https://doi.org/10.1093/embo-reports/kvd105>
- Giménez-Abián, J. F., Díaz-Martínez, L. A., Beauchene, N. A., Hsu, W.-S., Tsai, H.-J., & Clarke, D. J. (2010). Determinants of Rad21 localization at the centrosome in human cells. *Cell Cycle*, *9*(9), 1759–1763.
<https://doi.org/10.4161/cc.9.9.11523>
- Gligoris, T. G., Scheinost, J. C., Bürmann, F., Petela, N., Chan, K.-L., Uluocak, P., Beckouët, F., Gruber, S., Nasmyth, K., & Löwe, J. (2014). Closing the cohesin ring: structure and function of its Smc3-kleisin interface. *Science*, *346*(6212), 963–967.
<https://doi.org/10.1126/science.1256917>
- Golsteyn, R. M., Mundt, K. E., Fry, A. M., & Nigg, E. A. (1995). Cell cycle regulation of the activity and subcellular localization of Plk1, a human protein kinase implicated in mitotic spindle function. *The Journal of Cell Biology*, *129*(6), 1617–1628.
<https://doi.org/10.1083/jcb.129.6.1617>
- Graser, S., Stierhof, Y.-D., & Nigg, E. A. (2007). Cep68 and Cep215 (Cdk5rap2) are required for centrosome cohesion. *Journal of Cell Science*, *120*(24), 4321–4331.
<https://doi.org/10.1242/jcs.020248>
- Gregson, H. C., Schmiesing, J. A., Kim, J.-S., Kobayashi, T., Zhou, S., & Yokomori, K. (2001). A Potential Role for Human Cohesin in Mitotic Spindle Aster Assembly. *Journal of Biological Chemistry*, *276*(50), 47575–47582.
<https://doi.org/10.1074/jbc.M103364200>
- Gruber, S., Arumugam, P., Katou, Y., Kuglitsch, D., Helmhart, W., Shirahige, K., & Nasmyth, K. (2006). Evidence that Loading of Cohesin Onto Chromosomes Involves Opening of Its SMC Hinge. *Cell*, *127*(3), 523–537.
<https://doi.org/10.1016/j.cell.2006.08.048>
- Gruber, S., Haering, C. H., & Nasmyth, K. (2003). Chromosomal cohesin forms a ring. *Cell*, *112*(6), 765–777.
[https://doi.org/10.1016/s0092-8674\(03\)00162-4](https://doi.org/10.1016/s0092-8674(03)00162-4)
- Guichard, P., Chrétien, D., Marco, S., & Tassin, A.-M. (2010). Procentriole assembly revealed by cryo-electron tomography. *The EMBO Journal*, *29*(9), 1565–1572.
<https://doi.org/10.1038/emboj.2010.45>

- Gundersen, G. G., Khawaja, S., & Bulinski, J. C. (1987). Postpolymerization detyrosination of α -tubulin: A mechanism for subcellular differentiation of microtubules. *J. Cell Biol.*, *105*(25), 1–264.
<https://doi.org/10.1083/jcb.105.1.251>
- Gupta, G. D., Coyaud, É., Gonçalves, J., Mojarad, B. A., Liu, Y., Wu, Q., Gheiratmand, L., Comartin, D., Tkach, J. M., Cheung, S. W. T., Bashkurov, M., Hasegan, M., Knight, J. D., Lin, Z.-Y., Schueler, M., Hildebrandt, F., Moffat, J., Gingras, A.-C., Raught, B., & Pelletier, L. (2015). A Dynamic Protein Interaction Landscape of the Human Centrosome-Cilium Interface. *Cell*, *163*(6), 1484–1499.
<https://doi.org/10.1016/j.cell.2015.10.065>
- Haarhuis, J. H. I., Elbatsh, A. M. O., & Rowland, B. D. (2014). Cohesin and Its Regulation: On the Logic of X-Shaped Chromosomes. *Developmental Cell*, *31*(1), 7–18.
<https://doi.org/10.1016/j.devcel.2014.09.010>
- Habedanck, R., Stierhof, Y.-D., Wilkinson, C. J., & Nigg, E. A. (2005). The Polo kinase Plk4 functions in centriole duplication. *Nature Cell Biology*, *7*(11), 1140–1146.
<https://doi.org/10.1038/ncb1320>
- Haering, C. H., Farcas, A.-M., Arumugam, P., Metson, J., & Nasmyth, K. (2008). The cohesin ring concatenates sister DNA molecules. *Nature*, *454*(7202), 297–301.
<https://doi.org/10.1038/nature07098>
- Haering, C. H., Löwe, J., Hochwagen, A., & Nasmyth, K. (2002). Molecular architecture of SMC proteins and the yeast cohesin complex. *Molecular Cell*, *9*(4), 773–788.
[https://doi.org/10.1016/s1097-2765\(02\)00515-4](https://doi.org/10.1016/s1097-2765(02)00515-4)
- Hall, N. A., & Hehnlly, H. (2021). A centriole's subdistal appendages: Contributions to cell division, ciliogenesis and differentiation. *Open Biology*, *11*(2), 200399.
<https://doi.org/10.1098/rsob.200399>
- Haren, L., Stearns, T., & Lüders, J. (2009). Plk1-dependent recruitment of gamma-tubulin complexes to mitotic centrosomes involves multiple PCM components. *PLoS One*, *4*(6), e5976.
<https://doi.org/10.1371/journal.pone.0005976>
- Hauf, S., Roitinger, E., Koch, B., Dittrich, C. M., Mechtler, K., & Peters, J.-M. (2005). Dissociation of Cohesin from Chromosome Arms and Loss of Arm Cohesion during Early Mitosis Depends on Phosphorylation of SA2. *PLoS Biology*, *3*(3), e69.
<https://doi.org/10.1371/journal.pbio.0030069>
- Hauf, S., Waizenegger, I. C., & Peters, J.-M. (2001). Cohesin cleavage by separase required for anaphase and cytokinesis in human cells. *Science*, *293*(5533), 1320–1323.
<https://doi.org/10.1126/science.1061376>
- Heald, R., Tournebize, R., Blank, T., Sandaltzopoulos, R., Becker, P., Hyman, A., & Karsenti, E. (1996). Self-organization of microtubules into bipolar spindles around artificial chromosomes in *Xenopus* egg extracts. *Nature*, *382*(6590), 420–425.
<https://doi.org/10.1038/382420a0>
- Heald, R., Tournebize, R., Habermann, A., Karsenti, E., & Hyman, A. (1997). Spindle assembly in *Xenopus* egg extracts: Respective roles of centrosomes and microtubule self-organization. *The Journal of Cell Biology*, *138*(3), 615–628.
<https://doi.org/10.1083/jcb.138.3.615>
- Hellmuth, S., Gómez-H, L., Pendás, A. M., & Stemmann, O. (2020). Securin-independent regulation of separase by checkpoint-induced shugoshin-MAD2. *Nature*, *580*(7804), 536–541.
<https://doi.org/10.1038/s41586-020-2182-3>

- Hellmuth, S., Rata, S., Brown, A., Heidmann, S., Novak, B., & Stemmann, O. (2015). Human Chromosome Segregation Involves Multi-Layered Regulation of Separase by the Peptidyl-Prolyl-Isomerase Pin1. *Molecular Cell*, *58*(3), 495–506.
<https://doi.org/10.1016/j.molcel.2015.03.025>
- Hellmuth, S., & Stemmann, O. (2020). Separase-triggered apoptosis enforces minimal length of mitosis. *Nature*, *580*(7804), 542–547.
<https://doi.org/10.1038/s41586-020-2187-y>
- Heroes, E., Lesage, B., Görnemann, J., Beullens, M., Van Meervelt, L., & Bollen, M. (2013). The PP1 binding code: A molecular-lego strategy that governs specificity: The PP1 binding code. *FEBS Journal*, *280*(2), 584–595.
<https://doi.org/10.1111/j.1742-4658.2012.08547.x>
- Higashi, T. L., Eickhoff, P., Sousa, J. S., Locke, J., Nans, A., Flynn, H. R., Snijders, A. P., Papageorgiou, G., O'Reilly, N., Chen, Z. A., O'Reilly, F. J., Rappsilber, J., Costa, A., & Uhlmann, F. (2020). A Structure-Based Mechanism for DNA Entry into the Cohesin Ring. *Molecular Cell*, *79*(6), 917–933.e9.
<https://doi.org/10.1016/j.molcel.2020.07.013>
- Hiraki, M., Nakazawa, Y., Kamiya, R., & Hirono, M. (2007). Bld10p Constitutes the Cartwheel-Spoke Tip and Stabilizes the 9-Fold Symmetry of the Centriole. *Current Biology*, *17*(20), 1778–1783.
<https://doi.org/10.1016/j.cub.2007.09.021>
- Hirano, T. (2006). At the heart of the chromosome: SMC proteins in action. *Nature Reviews Molecular Cell Biology*, *7*(5), 311–322.
<https://doi.org/10.1038/nrm1909>
- Hirono, M. (2014). Cartwheel assembly. *Philosophical Transactions of the Royal Society B: Biological Sciences*, *369*(1650), 20130458–20130458.
<https://doi.org/10.1098/rstb.2013.0458>
- Hornig, N. C., & Uhlmann, F. (2004). Preferential cleavage of chromatin-bound cohesin after targeted phosphorylation by Polo-like kinase. *The EMBO Journal*, *23*(15), 3144–3153.
<https://doi.org/10.1038/sj.emboj.7600303>
- Hou, F., & Zou, H. (2005). Two human orthologues of Eco1/Ctf7 acetyltransferases are both required for proper sister-chromatid cohesion. *Molecular Biology of the Cell*, *16*(8), 3908–3918.
<https://doi.org/10.1091/mbc.e04-12-1063>
- Huis in 't Veld, P. J., Herzog, F., Ladurner, R., Davidson, I. F., Piric, S., Kreidl, E., Bhaskara, V., Aebersold, R., & Peters, J.-M. (2014). Characterization of a DNA exit gate in the human cohesin ring. *Science*, *346*(6212), 968–972.
<https://doi.org/10.1126/science.1256904>
- Hunter, T., & Sefton, B. M. (1980). Transforming gene product of Rous sarcoma virus phosphorylates tyrosine. *Proceedings of the National Academy of Sciences*, *77*(3), 1311–1315.
- Ivanov, D., & Nasmyth, K. (2005). A Topological Interaction between Cohesin Rings and a Circular Minichromosome. *Cell*, *122*(6), 849–860.
<https://doi.org/10.1016/j.cell.2005.07.018>
- Ivanov, D., Schleiffer, A., Eisenhaber, F., Mechtler, K., Haering, C. H., & Nasmyth, K. (2002). Eco1 is a novel acetyltransferase that can acetylate proteins involved in cohesion. *Current Biology*, *12*(4), 323–328.
[https://doi.org/10.1016/s0960-9822\(02\)00681-4](https://doi.org/10.1016/s0960-9822(02)00681-4)
- Iyer, D. R., & Rhind, N. (2017). The Intra-S Checkpoint Responses to DNA Damage. *Genes*, *8*(2), 74.
<https://doi.org/10.3390/genes8020074>

- Jakobsen, L., Vanselow, K., Skogs, M., Toyoda, Y., Lundberg, E., Poser, I., Falkenby, L. G., Bennetzen, M., Westendorf, J., Nigg, E. A., & others. (2011). Novel asymmetrically localizing components of human centrosomes identified by complementary proteomics methods. *The EMBO Journal*, *30*(8), 1520–1535.
<https://doi.org/10.1038/emboj.2011.63>
- Janson, M. E., Setty, T. G., Paoletti, A., & Tran, P. T. (2005). Efficient formation of bipolar microtubule bundles requires microtubule-bound γ -tubulin complexes. *The Journal of Cell Biology*, *169*(2), 297–308.
<https://doi.org/10.1083/jcb.200410119>
- Janssens, V., Longin, S., & Goris, J. (2008). PP2A holoenzyme assembly: In cauda venenum (the sting is in the tail). *Trends in Biochemical Sciences*, *33*(3), 113–121.
<https://doi.org/10.1016/j.tibs.2007.12.004>
- Jaspersen, S. L., Charles, J. F., & Morgan, D. O. (1999). Inhibitory phosphorylation of the APC regulator Hct1 is controlled by the kinase Cdc28 and the phosphatase Cdc14. *Current Biology*, *9*(5), 227–236.
[https://doi.org/10.1016/s0960-9822\(99\)80111-0](https://doi.org/10.1016/s0960-9822(99)80111-0)
- Joglekar, A. (2016). A Cell Biological Perspective on Past, Present and Future Investigations of the Spindle Assembly Checkpoint. *Biology*, *5*(4), 44.
<https://doi.org/10.3390/biology5040044>
- Joukov, V., Walter, J. C., & De Nicolo, A. (2014). The Cep192-Organized Aurora A-Plk1 Cascade Is Essential for Centrosome Cycle and Bipolar Spindle Assembly. *Molecular Cell*, *55*(4), 578–591.
<https://doi.org/10.1016/j.molcel.2014.06.016>
- Kaldis, P. (1999). The cdk-activating kinase (CAK): From yeast to mammals. *Cellular and Molecular Life Sciences*, *55*(2), 284–296.
<https://doi.org/10.1007/s000180050290>
- Kalous, J., & Aleshkina, D. (2023). Multiple Roles of PLK1 in Mitosis and Meiosis. *Cells*, *12*(1), 187. <https://doi.org/10.3390/cells12010187>
- Kapust, R. B., Tözser, J., Copeland, T. D., & Waugh, D. S. (2002). The P1' specificity of tobacco etch virus protease. *Biochemical and Biophysical Research Communications*, *294*(5), 949–955.
[https://doi.org/10.1016/S0006-291X\(02\)00574-0](https://doi.org/10.1016/S0006-291X(02)00574-0)
- Katis, V. L., Lipp, J. J., Imre, R., Bogdanova, A., Okaz, E., Habermann, B., Mechtler, K., Nasmyth, K., & Zachariae, W. (2010). Rec8 Phosphorylation by Casein Kinase 1 and Cdc7-Dbf4 Kinase Regulates Cohesin Cleavage by Separase during Meiosis. *Developmental Cell*, *18*(3), 397–409.
<https://doi.org/10.1016/j.devcel.2010.01.014>
- Keck, J. M., Jones, M. H., Wong, C. C. L., Binkley, J., Chen, D., Jaspersen, S. L., Holinger, E. P., Xu, T., Niepel, M., Rout, M. P., Vogel, J., Sidow, A., Yates, J. R., & Winey, M. (2011). A cell cycle phosphoproteome of the yeast centrosome. *Science*, *332*(6037), 1557–1561.
<https://doi.org/10.1126/science.1205193>
- Kim, J., Lee, K., & Rhee, K. (2015). PLK1 regulation of PCNT cleavage ensures fidelity of centriole separation during mitotic exit. *Nature Communications*, *6*, 10076.
<https://doi.org/10.1038/ncomms10076>
- Kim, S., & Rhee, K. (2014). Importance of the CEP215-pericentrin interaction for centrosome maturation during mitosis. *PLoS One*, *9*(1), e87016.
<https://doi.org/10.1371/journal.pone.0087016>
- Kim, T.-S., Park, J.-E., Shukla, A., Choi, S., Murugan, R. N., Lee, J. H., Ahn, M., Rhee, K., Bang, J. K., Kim, B. Y., Loncarek, J., Erikson, R. L., & Lee, K. S. (2013). Hierarchical recruitment of Plk4 and regulation of centriole biogenesis by two

- centrosomal scaffolds, Cep192 and Cep152. *Proceedings of the National Academy of Sciences*, *110*(50), E4849–E4857.
<https://doi.org/10.1073/pnas.1319656110>
- Kim, Y., Shi, Z., Zhang, H., Finkelstein, I. J., & Yu, H. (2019). Human cohesin compacts DNA by loop extrusion. *Science*, *366*(6471), 1345–1349.
<https://doi.org/10.1126/science.aaz4475>
- Kitagawa, D., Vakonakis, I., Olieric, N., Hilbert, M., Keller, D., Olieric, V., Bortfeld, M., Erat, M. C., Flückiger, I., Gönczy, P., & Steinmetz, M. O. (2011). Structural Basis of the 9-Fold Symmetry of Centrioles. *Cell*, *144*(3), 364–375.
<https://doi.org/10.1016/j.cell.2011.01.008>
- Kitajima, T. S., Sakuno, T., Ishiguro, K., Iemura, S., Natsume, T., Kawashima, S. A., & Watanabe, Y. (2006). Shugoshin collaborates with protein phosphatase 2A to protect cohesin. *Nature*, *441*(7089), 46–52.
<https://doi.org/10.1038/nature04663>
- Klebba, J. E., Buster, D. W., McLamarrah, T. A., Rusan, N. M., & Rogers, G. C. (2015). Autoinhibition and relief mechanism for Polo-like kinase 4. *Proceedings of the National Academy of Sciences*, *112*(7), E657–E666.
<https://doi.org/10.1073/pnas.1417967112>
- Kleiger, G., & Mayor, T. (2014). Perilous journey: A tour of the ubiquitin-proteasome system. *Trends in Cell Biology*, *24*(6), 352–359.
<https://doi.org/10.1016/j.tcb.2013.12.003>
- Klingseisen, A., & Jackson, A. P. (2011). Mechanisms and pathways of growth failure in primordial dwarfism. *Genes & Development*, *25*(19), 2011–2024.
<https://doi.org/10.1101/gad.169037>
- Kobayashi, T., Tsang, W. Y., Li, J., Lane, W., & Dynlacht, B. D. (2011). Centriolar Kinesin Kif24 Interacts with CP110 to Remodel Microtubules and Regulate Ciliogenesis. *Cell*, *145*(6), 914–925.
<https://doi.org/10.1016/j.cell.2011.04.028>
- Kobe, B., & Kajava, A. V. (2001). The leucine-rich repeat as a protein recognition motif. *Current Opinion in Structural Biology*, *11*(6), 725–732.
[https://doi.org/10.1016/s0959-440x\(01\)00266-4](https://doi.org/10.1016/s0959-440x(01)00266-4)
- Kollman, J. M., Merdes, A., Mourey, L., & Agard, D. A. (2011). Microtubule nucleation by γ -tubulin complexes. *Nature Reviews Molecular Cell Biology*, *12*(11), 709–721.
<https://doi.org/10.1038/nrm3209>
- Kollman, J. M., Polka, J. K., Zelter, A., Davis, T. N., & Agard, D. A. (2010). Microtubule nucleating γ -TuSC assembles structures with 13-fold microtubule-like symmetry. *Nature*, *466*(7308), 879–882.
<https://doi.org/10.1038/nature09207>
- Kollman, J. M., Zelter, A., Muller, E. G. D., Fox, B., Rice, L. M., Davis, T. N., & Agard, D. A. (2008). The structure of the gamma-tubulin small complex: Implications of its architecture and flexibility for microtubule nucleation. *Molecular Biology of the Cell*, *19*(1), 207–215.
<https://doi.org/10.1091/mbc.e07-09-0879>
- Kong, D., Farmer, V., Shukla, A., James, J., Gruskin, R., Kiriya, S., & Loncarek, J. (2014). Centriole maturation requires regulated Plk1 activity during two consecutive cell cycles. *The Journal of Cell Biology*, *206*(7), 855–865.
<https://doi.org/10.1083/jcb.201407087>

- Kong, X., Ball, A. R., Sonoda, E., Feng, J., Takeda, S., Fukagawa, T., Yen, T. J., & Yokomori, K. (2009). Cohesin associates with spindle poles in a mitosis-specific manner and functions in spindle assembly in vertebrate cells. *Molecular Biology of the Cell*, *20*(5), 1289–1301.
<https://doi.org/10.1091/mbc.e08-04-0419>
- Kraft, C., Herzog, F., Gieffers, C., Mechtler, K., Hagting, A., Pines, J., & Peters, J.-M. (2003). Mitotic regulation of the human anaphase-promoting complex by phosphorylation. *The EMBO Journal*, *22*(24), 6598–6609.
<https://doi.org/10.1093/emboj/cdg627>
- Krämer, A., Mailand, N., Lukas, C., Syljuåsen, R. G., Wilkinson, C. J., Nigg, E. A., Bartek, J., & Lukas, J. (2004). Centrosome-associated Chk1 prevents premature activation of cyclin-B-Cdk1 kinase. *Nature Cell Biology*, *6*(9), 884–891.
<https://doi.org/10.1038/ncb1165>
- Kramer, E. R., Scheuringer, N., Podtelejnikov, A. V., Mann, M., & Peters, J.-M. (2000). Mitotic regulation of the APC activator proteins CDC20 and CDH1. *Molecular Biology of the Cell*, *11*(5), 1555–1569.
<https://doi.org/10.1091/mbc.11.5.1555>
- Krantz, I. D., McCallum, J., DeScipio, C., Kaur, M., Gillis, L. A., Yaeger, D., Jukofsky, L., Wasserman, N., Bottani, A., Morris, C. A., Nowaczyk, M. J. M., Toriello, H., Bamshad, M. J., Carey, J. C., Rappaport, E., Kawauchi, S., Lander, A. D., Calof, A. L., Li, H., ... Jackson, L. G. (2004). Cornelia de Lange syndrome is caused by mutations in NIPBL, the human homolog of *Drosophila melanogaster* Nipped-B. *Nature Genetics*, *36*(6), 631–635.
<https://doi.org/10.1038/ng1364>
- Kratz, A.-S., Barenz, F., Richter, K. T., & Hoffmann, I. (2015). Plk4-dependent phosphorylation of STIL is required for centriole duplication. *Biology Open*, *4*(3), 370–377.
<https://doi.org/10.1242/bio.201411023>
- Kueng, S., Hegemann, B., Peters, B. H., Lipp, J. J., Schleiffer, A., Mechtler, K., & Peters, J.-M. (2006). Wapl Controls the Dynamic Association of Cohesin with Chromatin. *Cell*, *127*(5), 955–967.
<https://doi.org/10.1016/j.cell.2006.09.040>
- Ladurner, R., Kreidl, E., Ivanov, M. P., Ekker, H., Idarraga-Amado, M. H., Busslinger, G. A., Wutz, G., Cisneros, D. A., & Peters, J. (2016). Sororin actively maintains sister chromatid cohesion. *The EMBO Journal*, *35*(6), 635–653.
<https://doi.org/10.15252/emboj.201592532>
- Laloraya, S., Guacci, V., & Koshland, D. (2000). Chromosomal addresses of the cohesin component Mcd1p. *J Cell Biol*, *151*(5), 1047–1056.
<https://doi.org/10.1083/jcb.151.5.1047>
- Lammens, A., Schele, A., & Hopfner, K.-P. (2004). Structural biochemistry of ATP-driven dimerization and DNA-stimulated activation of SMC ATPases. *Current Biology*, *14*(19), 1778–1782.
<https://doi.org/10.1016/j.cub.2004.09.044>
- Lara-Gonzalez, P., Westhorpe, F. G., & Taylor, S. S. (2012). The Spindle Assembly Checkpoint. *Current Biology*, *22*(22), R966–R980.
<https://doi.org/10.1016/j.cub.2012.10.006>
- Lawo, S., Hasegan, M., Gupta, G. D., & Pelletier, L. (2012). Subdiffraction imaging of centrosomes reveals higher-order organizational features of pericentriolar material. *Nature Cell Biology*, *14*(11), 1148–1158.
<https://doi.org/10.1038/ncb2591>

- Lee, K., & Rhee, K. (2011). PLK1 phosphorylation of pericentrin initiates centrosome maturation at the onset of mitosis. *The Journal of Cell Biology*, *195*(7), 1093–1101. <https://doi.org/10.1083/jcb.201106093>
- Lee, K., & Rhee, K. (2012). Separase-dependent cleavage of pericentrin B is necessary and sufficient for centriole disengagement during mitosis. *Cell Cycle*, *11*(13), 2476–2485. <https://doi.org/10.4161/cc.20878>
- Li, Q., Hansen, D., Killilea, A., Joshi, H. C., Palazzo, R. E., & Balczon, R. (2001). Kendrin/pericentrin-B, a centrosome protein with homology to pericentrin that complexes with PCM-1. *Journal of Cell Science*, *114*(4), 797–809. <https://doi.org/10.1242/jcs.114.4.797>
- Li, S., Fernandez, J.-J., Marshall, W. F., & Agard, D. A. (2019). Electron cryo-tomography provides insight into procentriole architecture and assembly mechanism. *ELife*, *8*, e43434. <https://doi.org/10.7554/eLife.43434>
- Li, Y., Haarhuis, J. H. I., Sedeño Cacciatore, Á., Oldenkamp, R., van Ruiten, M. S., Willems, L., Teunissen, H., Muir, K. W., de Wit, E., Rowland, B. D., & Panne, D. (2020). The structural basis for cohesin-CTCF-anchored loops. *Nature*, *578*(7795), 472–476. <https://doi.org/10.1038/s41586-019-1910-z>
- Lin, Z., Luo, X., & Yu, H. (2016). Structural basis of cohesin cleavage by separase. *Nature*, *532*(7597), 131–134. <https://doi.org/10.1038/nature17402>
- Liu, B., & Lee, Y.-R. J. (2022). Spindle Assembly and Mitosis in Plants. *Annual Review of Plant Biology*, *73*, 227–254. <https://doi.org/10.1146/annurev-arplant-070721-084258>
- Liu, H., Rankin, S., & Yu, H. (2013). Phosphorylation-enabled binding of SGO1-PP2A to cohesin protects sororin and centromeric cohesion during mitosis. *Nature Cell Biology*, *15*(1), 40–49. <https://doi.org/10.1038/ncb2637>
- Liu, J., & Krantz, I. D. (2008). Cohesin and Human Disease. *Annual Review of Genomics and Human Genetics*, *9*(1), 303–320. <https://doi.org/10.1146/annurev.genom.9.081307.164211>
- Lobjois, V., Jullien, D., Bouché, J.-P., & Ducommun, B. (2009). The polo-like kinase 1 regulates CDC25B-dependent mitosis entry. *Biochimica et Biophysica Acta (BBA) - Molecular Cell Research*, *1793*(3), 462–468. <https://doi.org/10.1016/j.bbamcr.2008.12.015>
- Lončarek, J., Hergert, P., & Khodjakov, A. (2010). Centriole Reduplication during Prolonged Interphase Requires Procentriole Maturation Governed by Plk1. *Current Biology*, *20*(14), 1277–1282. <https://doi.org/10.1016/j.cub.2010.05.050>
- Loncarek, J., Hergert, P., Magidson, V., & Khodjakov, A. (2008). Control of daughter centriole formation by the pericentriolar material. *Nature Cell Biology*, *10*(3), 322–328. <https://doi.org/10.1038/ncb1694>
- Losada, A., Yokochi, T., Kobayashi, R., & Hirano, T. (2000). Identification and characterization of SA/Scc3p subunits in the Xenopus and human cohesin complexes. *The Journal of Cell Biology*, *150*(3), 405–416. <https://doi.org/10.1083/jcb.150.3.405>
- Luo, S., & Tong, L. (2017). Molecular mechanism for the regulation of yeast separase by securin. *Nature*, *542*(7640), 255–259. <https://doi.org/10.1038/nature21061>

- Ma, D., Wang, F., Teng, J., Huang, N., & Chen, J. (2023). Structure and function of distal and subdistal appendages of the mother centriole. *Journal of Cell Science*, *136*(3), jcs260560.
<https://doi.org/10.1242/jcs.260560>
- Ma, S., Liu, M.-A., Yuan, Y.-L. O., & Erikson, R. L. (2003). The serum-inducible protein kinase Snk is a G 1 phase polo-like kinase that is inhibited by the calcium-and integrin-binding protein CIB. *Molecular Cancer Research*, *1*(5), 376–384.
- Maier, N. K., Ma, J., Lampson, M. A., & Cheeseman, I. M. (2021). Separase cleaves the kinetochore protein Meikin at the meiosis I/II transition. *Developmental Cell*, *56*(15), 2192-2206.e8.
<https://doi.org/10.1016/j.devcel.2021.06.019>
- Marcos-Alcalde, Í., Mendieta-Moreno, J. I., Puisac, B., Gil-Rodríguez, M. C., Hernández-Marcos, M., Soler-Polo, D., Ramos, F. J., Ortega, J., Pié, J., Mendieta, J., & Gómez-Puertas, P. (2017). Two-step ATP-driven opening of cohesin head. *Scientific Reports*, *7*(1).
<https://doi.org/10.1038/s41598-017-03118-9>
- Mardin, B. R., & Schiebel, E. (2012). Breaking the ties that bind: New advances in centrosome biology. *The Journal of Cell Biology*, *197*(1), 11–18.
<https://doi.org/10.1083/jcb.201108006>
- Margolin, G., Gregoret, I. V., Cickovski, T. M., Li, C., Shi, W., Alber, M. S., & Goodson, H. V. (2012). The mechanisms of microtubule catastrophe and rescue: Implications from analysis of a dimer-scale computational model. *Molecular Biology of the Cell*, *23*(4), 642–656.
<https://doi.org/10.1091/mbc.E11-08-0688>
- Martinez-Campos, M., Basto, R., Baker, J., Kernan, M., & Raff, J. W. (2004). The Drosophila pericentrin-like protein is essential for cilia/flagella function, but appears to be dispensable for mitosis. *The Journal of Cell Biology*, *165*(5), 673–683.
<https://doi.org/10.1083/jcb.200402130>
- Matsuo, K., Ohsumi, K., Iwabuchi, M., Kawamata, T., Ono, Y., & Takahashi, M. (2012). Kendrin Is a Novel Substrate for Separase Involved in the Licensing of Centriole Duplication. *Current Biology*, *22*(10), 915–921.
<https://doi.org/10.1016/j.cub.2012.03.048>
- Mayor, T., Stierhof, Y.-D., Tanaka, K., Fry, A. M., & Nigg, E. A. (2000). The centrosomal protein C-Nap1 is required for cell cycle-regulated centrosome cohesion. *The Journal of Cell Biology*, *151*(4), 837–846.
<https://doi.org/10.1083/jcb.151.4.837>
- McGowan, C. H., & Russell, P. (1993). Human Wee1 kinase inhibits cell division by phosphorylating p34cdc2 exclusively on Tyr15. *The EMBO Journal*, *12*(1), 75.
<https://doi.org/10.1002/j.1460-2075.1993.tb05633.x>
- McGuinness, B. E., Hirota, T., Kudo, N. R., Peters, J.-M., & Nasmyth, K. (2005). Shugoshin Prevents Dissociation of Cohesin from Centromeres During Mitosis in Vertebrate Cells. *PLoS Biology*, *3*(3), e86.
<https://doi.org/10.1371/journal.pbio.0030086>
- Mennella, V., Agard, D. A., Huang, B., & Pelletier, L. (2014). Amorphous no more: Subdiffraction view of the pericentriolar material architecture. *Trends in Cell Biology*, *24*(3), 188–197.
<https://doi.org/10.1016/j.tcb.2013.10.001>

- Mennella, V., Keszthelyi, B., McDonald, K. L., Chhun, B., Kan, F., Rogers, G. C., Huang, B., & Agard, D. A. (2012). Subdiffraction-resolution fluorescence microscopy reveals a domain of the centrosome critical for pericentriolar material organization. *Nature Cell Biology*, *14*(11), 1159–1168.
<https://doi.org/10.1038/ncb2597>
- Metzger, M. B., Hristova, V. A., & Weissman, A. M. (2012). HECT and RING finger families of E3 ubiquitin ligases at a glance. *Journal of Cell Science*, *125*(3), 531–537.
<https://doi.org/10.1242/jcs.091777>
- Michaelis, C., Ciosk, R., & Nasmyth, K. (1997). Cohesins: Chromosomal proteins that prevent premature separation of sister chromatids. *Cell*, *91*(1), 35–45.
[https://doi.org/10.1016/s0092-8674\(01\)80007-6](https://doi.org/10.1016/s0092-8674(01)80007-6)
- Misulovin, Z., Schwartz, Y. B., Li, X.-Y., Kahn, T. G., Gause, M., MacArthur, S., Fay, J. C., Eisen, M. B., Pirrotta, V., Biggin, M. D., & Dorsett, D. (2008). Association of cohesin and Nipped-B with transcriptionally active regions of the *Drosophila melanogaster* genome. *Chromosoma*, *117*(1), 89–102.
<https://doi.org/10.1007/s00412-007-0129-1>
- Mitchison, T. J., & Salmon, E. D. (2001). Mitosis: A history of division. *Nature Cell Biology*, *3*(1), E17.
<https://doi.org/10.1038/35050656>
- Mitchison, T., & Kirschner, M. (1984). Dynamic instability of microtubule growth. *Nature*, *312*(5991), 237–242.
<https://doi.org/10.1038/312237a0>
- Miyoshi, K., Asanuma, M., Miyazaki, I., Matsuzaki, S., Tohyama, M., & Ogawa, N. (2006). Characterization of pericentrin isoforms in vivo. *Biochemical and Biophysical Research Communications*, *351*(3), 745–749.
<https://doi.org/10.1016/j.bbrc.2006.10.101>
- Moens, P. B., & Rapport, E. (1971). Spindles, spindle plaques, and meiosis in the yeast *Saccharomyces cerevisiae* (Hansen). *The Journal of Cell Biology*, *50*(2), 344–361.
<https://doi.org/10.1083/jcb.50.2.344>
- Mohr, L., Buheitel, J., Schöckel, L., Karalus, D., Mayer, B., & Stemmann, O. (2015). An Alternatively Spliced Bifunctional Localization Signal Reprograms Human Shugoshin 1 to Protect Centrosomal Instead of Centromeric Cohesin. *Cell Reports*, *12*(12), 2156–2168.
<https://doi.org/10.1016/j.celrep.2015.08.045>
- Moldovan, G.-L., Pfander, B., & Jentsch, S. (2006). PCNA Controls Establishment of Sister Chromatid Cohesion during S Phase. *Molecular Cell*, *23*(5), 723–732.
<https://doi.org/10.1016/j.molcel.2006.07.007>
- Moyer, T. C., Clutario, K. M., Lambrus, B. G., Daggubati, V., & Holland, A. J. (2015). Binding of STIL to Plk4 activates kinase activity to promote centriole assembly. *The Journal of Cell Biology*, *209*(6), 863–878.
<https://doi.org/10.1083/jcb.201502088>
- Mullee, L. I., & Morrison, C. G. (2016). Centrosomes in the DNA damage response—The hub outside the centre. *Chromosome Research*, *24*(1), 35–51.
<https://doi.org/10.1007/s10577-015-9503-7>
- Müller, H., Schmidt, D., Steinbrink, S., Mirgorodskaya, E., Lehmann, V., Habermann, K., Dreher, F., Gustavsson, N., Kessler, T., & Lehrach, H. (2010). Proteomic and functional analysis of the mitotic *Drosophila* centrosome. *The EMBO Journal*, *29*(19), 3344–3357.
<https://doi.org/10.1038/emboj.2010.210>

- Murata, T., Sonobe, S., Baskin, T. I., Hyodo, S., Hasezawa, S., Nagata, T., Horio, T., & Hasebe, M. (2005). Microtubule-dependent microtubule nucleation based on recruitment of γ -tubulin in higher plants. *Nature Cell Biology*, 7(10), 961–968.
<https://doi.org/10.1038/ncb1306>
- Murayama, Y., Samora, C. P., Kurokawa, Y., Iwasaki, H., & Uhlmann, F. (2018). Establishment of DNA-DNA Interactions by the Cohesin Ring. *Cell*, 172(3), 465–477.e15.
<https://doi.org/10.1016/j.cell.2017.12.021>
- Murayama, Y., & Uhlmann, F. (2013). Biochemical reconstitution of topological DNA binding by the cohesin ring. *Nature*, 505(7483), 367–371.
<https://doi.org/10.1038/nature12867>
- Murayama, Y., & Uhlmann, F. (2015). DNA Entry into and Exit out of the Cohesin Ring by an Interlocking Gate Mechanism. *Cell*, 163(7), 1628–1640.
<https://doi.org/10.1016/j.cell.2015.11.030>
- Murray, A. W. (2004). Recycling the cell cycle: Cyclins revisited. *Cell*, 116(2), 221–234.
[https://doi.org/10.1016/s0092-8674\(03\)01080-8](https://doi.org/10.1016/s0092-8674(03)01080-8)
- Musacchio, A. (2015). The Molecular Biology of Spindle Assembly Checkpoint Signaling Dynamics. *Current Biology*, 25(20), R1002–R1018.
<https://doi.org/10.1016/j.cub.2015.08.051>
- Naghavi, M. H., & Walsh, D. (2017). Microtubule Regulation and Function during Virus Infection. *Journal of Virology*, 91(16), e00538-17.
<https://doi.org/10.1128/JVI.0053817>
- Nasa, I., & Kettenbach, A. N. (2018). Coordination of Protein Kinase and Phosphoprotein Phosphatase Activities in Mitosis. *Frontiers in Cell and Developmental Biology*, 6.
<https://doi.org/10.3389/fcell.2018.00030>
- Nishiyama, T., Ladurner, R., Schmitz, J., Kreidl, E., Schleiffer, A., Bhaskara, V., Bando, M., Shirahige, K., Hyman, A. A., Mechtler, K., & Peters, J.-M. (2010). Sororin Mediates Sister Chromatid Cohesion by Antagonizing Wapl. *Cell*, 143(5), 737–749.
<https://doi.org/10.1016/j.cell.2010.10.031>
- Nishiyama, T., Sykora, M. M., Huis in 't Veld, P. J., Mechtler, K., & Peters, J.-M. (2013). Aurora B and Cdk1 mediate Wapl activation and release of acetylated cohesin from chromosomes by phosphorylating Sororin. *Proceedings of the National Academy of Sciences*, 110(33), 13404–13409.
<https://doi.org/10.1073/pnas.1305020110>
- Norbury, C., Blow, J., & Nurse, P. (1991). Regulatory phosphorylation of the p34cdc2 protein kinase in vertebrates. *The EMBO Journal*, 10(11), 3321.
<https://doi.org/10.1002/j.1460-2075.1991.tb04896.x>
- Nurse, P. (1997). Regulation of the eukaryotic cell cycle. *European Journal of Cancer*, 33(7), 1002–1004.
[https://doi.org/10.1016/s0959-8049\(97\)00091-9](https://doi.org/10.1016/s0959-8049(97)00091-9)
- Oegema, K., Wiese, C., Martin, O. C., Milligan, R. A., Iwamatsu, A., Mitchison, T. J., & Zheng, Y. (1999). Characterization of two related Drosophila gamma-tubulin complexes that differ in their ability to nucleate microtubules. *The Journal of Cell Biology*, 144(4), 721–733.
<https://doi.org/10.1083/jcb.144.4.721>
- Ohta, M., Ashikawa, T., Nozaki, Y., Kozuka-Hata, H., Goto, H., Inagaki, M., Oyama, M., & Kitagawa, D. (2014). Direct interaction of Plk4 with STIL ensures formation of a single procentriole per parental centriole. *Nature Communications*, 5, 5267.
<https://doi.org/10.1038/ncomms6267>

- Oliveira, R. A., & Nasmyth, K. (2013). Cohesin cleavage is insufficient for centriole disengagement in *Drosophila*. *Current Biology: CB*, *23*(14), R601–603.
<https://doi.org/10.1016/j.cub.2013.04.003>
- Ouyang, Z., Zheng, G., Tomchick, D. R., Luo, X., & Yu, H. (2016). Structural Basis and IP 6 Requirement for Pds5-Dependent Cohesin Dynamics. *Molecular Cell*, *62*(2), 248–259.
<https://doi.org/10.1016/j.molcel.2016.02.033>
- Paintrand, M., Moudjou, M., Delacroix, H., & Bornens, M. (1992). Centrosome organization and centriole architecture: Their sensitivity to divalent cations. *Journal of Structural Biology*, *108*(2), 107–128.
[https://doi.org/10.1016/1047-8477\(92\)90011-x](https://doi.org/10.1016/1047-8477(92)90011-x)
- Panic, M., Hata, S., Neuner, A., & Schiebel, E. (2015). The Centrosomal Linker and Microtubules Provide Dual Levels of Spatial Coordination of Centrosomes. *PLOS Genetics*, *11*(5), e1005243.
<https://doi.org/10.1371/journal.pgen.1005243>
- Parelho, V., Hadjur, S., Spivakov, M., Leleu, M., Sauer, S., Gregson, H. C., Jarmuz, A., Canzonetta, C., Webster, Z., Nesterova, T., Cobb, B. S., Yokomori, K., Dillon, N., Aragon, L., Fisher, A. G., & Merckenschlager, M. (2008). Cohesins functionally associate with CTCF on mammalian chromosome arms. *Cell*, *132*(3), 422–433.
<https://doi.org/10.1016/j.cell.2008.01.011>
- Park, S.-Y., Park, J.-E., Kim, T.-S., Kim, J. H., Kwak, M.-J., Ku, B., Tian, L., Murugan, R. N., Ahn, M., Komiya, S., Hojo, H., Kim, N.-H., Kim, B. Y., Bang, J. K., Erikson, R. L., Lee, K. W., Kim, S. J., Oh, B.-H., Yang, W., & Lee, K. S. (2014). Molecular basis for unidirectional scaffold switching of human Plk4 in centriole biogenesis. *Nature Structural & Molecular Biology*, *21*(8), 696–703.
<https://doi.org/10.1038/nsmb.2846>
- Pashkova, N., Gakhar, L., Winistorfer, S. C., Yu, L., Ramaswamy, S., & Piper, R. C. (2010). WD40 Repeat Propellers Define a Ubiquitin-Binding Domain that Regulates Turnover of F Box Proteins. *Molecular Cell*, *40*(3), 433–443.
<https://doi.org/10.1016/j.molcel.2010.10.018>
- Paturle-Lafanechère, L., Manier, M., Trigault, N., Pirollet, F., Mazarguil, H., & Job, D. (1994). Accumulation of delta 2-tubulin, a major tubulin variant that cannot be tyrosinated, in neuronal tissues and in stable microtubule assemblies. *Journal of Cell Science*, *107*(6), 1529–1543.
<https://doi.org/10.1242/jcs.107.6.1529>
- Peel, N., Stevens, N. R., Basto, R., & Raff, J. W. (2007). Overexpressing Centriole-Replication Proteins In Vivo Induces Centriole Overduplication and De Novo Formation. *Current Biology*, *17*(10), 834–843.
<https://doi.org/10.1016/j.cub.2007.04.036>
- Pehlivan, D., Hullings, M., Carvalho, C. M. B., Gonzaga-Jauregui, C. G., Loy, E., Jackson, L. G., Krantz, I. D., Deardorff, M. A., & Lupski, J. R. (2012). NIPBL rearrangements in Cornelia de Lange syndrome: Evidence for replicative mechanism and genotype–phenotype correlation. *Genetics in Medicine*, *14*(3), 313–322.
<https://doi.org/10.1038/gim.2011.13>
- Pereira, G., & Schiebel, E. (2016). Mitotic exit: Determining the PP2A dephosphorylation program. *J Cell Biol*, jcb–201608019.
<https://doi.org/10.1083/jcb.201608019>
- Petela, N. J., Gligoris, T. G., Metson, J., Lee, B.-G., Voulgaris, M., Hu, B., Kikuchi, S., Chapard, C., Chen, W., Rajendra, E., Srinivisan, M., Yu, H., Löwe, J., & Nasmyth, K. A. (2018). Scc2 Is a Potent Activator of Cohesin’s ATPase that Promotes Loading by Binding Scc1 without Pds5. *Molecular Cell*, *70*(6), 1134–1148.e7.
<https://doi.org/10.1016/j.molcel.2018.05.022>

- Peter, M., Le Peuch, C., Labbé, J.-C., Meyer, A. N., Donoghue, D. J., & Dorée, M. (2002). Initial activation of cyclin-B1–cdc2 kinase requires phosphorylation of cyclin B1. *EMBO Reports*, 3(6), 551–556.
<https://doi.org/10.1093/embo-reports/kvfl11>
- Peters, J.-M. (2006). The anaphase promoting complex/cyclosome: A machine designed to destroy. *Nature Reviews Molecular Cell Biology*, 7(9), 644–656.
<https://doi.org/10.1038/nrm1988>
- Petronczki, M., Lénárt, P., & Peters, J.-M. (2008). Polo on the Rise—From Mitotic Entry to Cytokinesis with Plk1. *Developmental Cell*, 14(5), 646–659.
<https://doi.org/10.1016/j.devcel.2008.04.014>
- Pines, J. (1991). Cyclins: Wheels within wheels. *Cell Growth & Differentiation: The Molecular Biology Journal of the American Association for Cancer Research*, 2(6), 305–310.
- Qian, Y. W., Erikson, E., & Maller, J. L. (1999). Mitotic effects of a constitutively active mutant of the *Xenopus* polo-like kinase Plx1. *Molecular and Cellular Biology*, 19(12), 8625–8632.
<https://doi.org/10.1128/MCB.19.12.8625>
- Rankin, S., Ayad, N. G., & Kirschner, M. W. (2005). Sororin, a substrate of the anaphase-promoting complex, is required for sister chromatid cohesion in vertebrates. *Molecular Cell*, 18(2), 185–200.
<https://doi.org/10.1016/j.molcel.2005.03.017>
- Rauch, A., Thiel, C. T., Schindler, D., Wick, U., Crow, Y. J., Ekici, A. B., van Essen, A. J., Goecke, T. O., Al-Gazali, L., Chrzanowska, K. H., Zweier, C., Brunner, H. G., Becker, K., Curry, C. J., Dallapiccola, B., Devriendt, K., Dörfler, A., Kinning, E., Megarbane, A., ... Reis, A. (2008). Mutations in the pericentrin (PCNT) gene cause primordial dwarfism. *Science*, 319(5864), 816–819.
<https://doi.org/10.1126/science.1151174>
- Remsburg, C. M., Konrad, K. D., & Song, J. L. (2023). RNA localization to the mitotic spindle is essential for early development and is regulated by kinesin-1 and dynein. *Journal of Cell Science*, 136(5), jcs260528.
<https://doi.org/10.1242/jcs.260528>
- Rodrigues-Martins, A., Bettencourt-Dias, M., Riparbelli, M., Ferreira, C., Ferreira, I., Callaini, G., & Glover, D. M. (2007). DSAS-6 organizes a tube-like centriole precursor, and its absence suggests modularity in centriole assembly. *Current Biology*, 17(17), 1465–1472.
<https://doi.org/10.1016/j.cub.2007.07.034>
- Rolet Ben-Shahar, T., Heeger, S., Lehane, C., East, P., Flynn, H., Skehel, M., & Uhlmann, F. (2008). Eco1-dependent cohesin acetylation during establishment of sister chromatid cohesion. *Science*, 321(5888), 563–566. <https://doi.org/10.1126/science.1157774>
- Roostalu, J., & Surrey, T. (2017). Microtubule nucleation: Beyond the template. *Nature Reviews Molecular Cell Biology*, 18(11), 702–710.
<https://doi.org/10.1038/nrm.2017.75>
- Rudra, S., & Skibbens, R. V. (2012). Sister chromatid cohesion establishment occurs in concert with lagging strand synthesis. *Cell Cycle (Georgetown, Tex.)*, 11(11), 2114–2121.
<https://doi.org/10.4161/cc.20547>
- Rudra, S., & Skibbens, R. V. (2013). Chl1 DNA Helicase Regulates Scc2 Deposition Specifically during DNA-Replication in *Saccharomyces cerevisiae*. *PLoS ONE*, 8(9), e75435.
<https://doi.org/10.1371/journal.pone.0075435>

- Ruthmann, A. (1959). The fine structure of the meiotic spindle of the crayfish. *The Journal of Biophysical and Biochemical Cytology*, 5(1), 177.
- Salisbury, J. L. (2003). Centrosomes: Coiled-coils organize the cell center. *Current Biology*, 13(3), R88–R90.
[https://doi.org/10.1016/s0960-9822\(03\)00033-2](https://doi.org/10.1016/s0960-9822(03)00033-2)
- Sampath, S. C., Ohi, R., Leismann, O., Salic, A., Pozniakovski, A., & Funabiki, H. (2004). The chromosomal passenger complex is required for chromatin-induced microtubule stabilization and spindle assembly. *Cell*, 118(2), 187–202.
<https://doi.org/10.1016/j.cell.2004.06.026>
- Scheer, U. (2014). Historical roots of centrosome research: Discovery of Boveri's microscope slides in Wurzburg. *Philosophical Transactions of the Royal Society B: Biological Sciences*, 369(1650), 20130469–20130469.
<https://doi.org/10.1098/rstb.2013.0469>
- Schmidt, T. I., Kleylein-Sohn, J., Westendorf, J., Le Clech, M., Lavoie, S. B., Stierhof, Y.-D., & Nigg, E. A. (2009). Control of Centriole Length by CPAP and CP110. *Current Biology*, 19(12), 1005–1011.
<https://doi.org/10.1016/j.cub.2009.05.016>
- Schöckel, L., Möckel, M., Mayer, B., Boos, D., & Stemmann, O. (2011). Cleavage of cohesin rings coordinates the separation of centrioles and chromatids. *Nature Cell Biology*, 13(8), 966–972.
<https://doi.org/10.1038/ncb2280>
- Sepulveda, G., Antkowiak, M., Brust-Mascher, I., Mahe, K., Ou, T., Castro, N. M., Christensen, L. N., Cheung, L., Jiang, X., Yoon, D., Huang, B., & Jao, L.-E. (2018). Co-translational protein targeting facilitates centrosomal recruitment of PCNT during centrosome maturation in vertebrates. *ELife*, 7, e34959.
<https://doi.org/10.7554/eLife.34959>
- Shi, Y. (2009). Serine/Threonine Phosphatases: Mechanism through Structure. *Cell*, 139(3), 468–484.
<https://doi.org/10.1016/j.cell.2009.10.006>
- Shukla, A., Kong, D., Sharma, M., Magidson, V., & Loncarek, J. (2015). Plk1 relieves centriole block to reduplication by promoting daughter centriole maturation. *Nature Communications*, 6, 8077.
<https://doi.org/10.1038/ncomms9077>
- Sir, J.-H., Pütz, M., Daly, O., Morrison, C. G., Dunning, M., Kilmartin, J. V., & Gergely, F. (2013). Loss of centrioles causes chromosomal instability in vertebrate somatic cells. *The Journal of Cell Biology*, 203(5), 747–756.
<https://doi.org/10.1083/jcb.201309038>
- Skowyra, D., Craig, K. L., Tyers, M., Elledge, S. J., & Harper, J. W. (1997). F-box proteins are receptors that recruit phosphorylated substrates to the SCF ubiquitin-ligase complex. *Cell*, 91(2), 209–219.
[https://doi.org/10.1016/s0092-8674\(00\)80403-1](https://doi.org/10.1016/s0092-8674(00)80403-1)
- Sluder, G. (2013). Centriole engagement: It's not just cohesin any more. *Current Biology: CB*, 23(15), R659–660.
<https://doi.org/10.1016/j.cub.2013.06.064>
- Smith, E., Hégarat, N., Vesely, C., Roseboom, I., Larch, C., Streicher, H., Straatman, K., Flynn, H., Skehel, M., Hirota, T., & others. (2011). Differential control of Eg5-dependent centrosome separation by Plk1 and Cdk1. *The EMBO Journal*, 30(11), 2233–2245.
<https://doi.org/10.1038/emboj.2011.120>

- Sonnen, K. F., Gabryjonczyk, A.-M., Anselm, E., Stierhof, Y.-D., & Nigg, E. A. (2013). Human Cep192 and Cep152 cooperate in Plk4 recruitment and centriole duplication. *Journal of Cell Science*, *126*(14), 3223–3233.
<https://doi.org/10.1242/jcs.129502>
- Sonnen, K. F., Schermelleh, L., Leonhardt, H., & Nigg, E. A. (2012). 3D-structured illumination microscopy provides novel insight into architecture of human centrosomes. *Biology Open*, *1*(10), 965–976.
<https://doi.org/10.1242/bio.20122337>
- Srinivasan, M., Fumasoni, M., Petela, N. J., Murray, A., & Nasmyth, K. A. (2020). Cohesion is established during DNA replication utilising chromosome associated cohesin rings as well as those loaded de novo onto nascent DNAs. *ELife*, *9*, e56611.
<https://doi.org/10.7554/eLife.56611>
- Stemmann, O., Zou, H., Gerber, S. A., Gygi, S. P., & Kirschner, M. W. (2001). Dual inhibition of sister chromatid separation at metaphase. *Cell*, *107*(6), 715–726.
[https://doi.org/10.1016/s0092-8674\(01\)00603-1](https://doi.org/10.1016/s0092-8674(01)00603-1)
- Strnad, P., & Gönczy, P. (2008). Mechanisms of procentriole formation. *Trends in Cell Biology*, *18*(8), 389–396.
<https://doi.org/10.1016/j.tcb.2008.06.004>
- Strnad, P., Leidel, S., Vinogradova, T., Euteneuer, U., Khodjakov, A., & Gönczy, P. (2007). Regulated HsSAS-6 levels ensure formation of a single procentriole per centriole during the centrosome duplication cycle. *Developmental Cell*, *13*(2), 203–213.
<https://doi.org/10.1016/j.devcel.2007.07.004>
- Sulimenko, V., Hájková, Z., Klebanovych, A., & Dráber, P. (2017). Regulation of microtubule nucleation mediated by γ -tubulin complexes. *Protoplasma*, *254*(3), 1187–1199.
<https://doi.org/10.1007/s00709-016-1070-z>
- Sun, Y., Kucej, M., Fan, H.-Y., Yu, H., Sun, Q.-Y., & Zou, H. (2009). Separase Is Recruited to Mitotic Chromosomes to Dissolve Sister Chromatid Cohesion in a DNA-Dependent Manner. *Cell*, *137*(1), 123–132.
<https://doi.org/10.1016/j.cell.2009.01.040>
- Sunkel, C. E., & Glover, D. M. (1988). Polo, a mitotic mutant of *Drosophila* displaying abnormal spindle poles. *Journal of Cell Science*, *89*(1), 25–38.
<https://doi.org/10.1242/jcs.89.1.25>
- Takahashi, M., Yamagiwa, A., Nishimura, T., Mukai, H., & Ono, Y. (2002). Centrosomal proteins CG-NAP and kendrin provide microtubule nucleation sites by anchoring γ -tubulin ring complex. *Molecular Biology of the Cell*, *13*(9), 3235–3245.
<https://doi.org/10.1091/mbc.e02-02-0112>
- Tang, C.-J. C., Fu, R.-H., Wu, K.-S., Hsu, W.-B., & Tang, T. K. (2009). CPAP is a cell-cycle regulated protein that controls centriole length. *Nature Cell Biology*, *11*(7), 825–831.
<https://doi.org/10.1038/ncb1889>
- Tang, N., & Marshall, W. F. (2012). Centrosome positioning in vertebrate development. *Journal of Cell Science*, *125*(21), 4951–4961.
<https://doi.org/10.1242/jcs.038083>
- Tang, Z., Shu, H., Qi, W., Mahmood, N. A., Mumby, M. C., & Yu, H. (2006). PP2A is required for centromeric localization of Sgo1 and proper chromosome segregation. *Developmental Cell*, *10*(5), 575–585.
<https://doi.org/10.1016/j.devcel.2006.03.010>
- Tanos, B. E., Yang, H.-J., Soni, R., Wang, W.-J., Macaluso, F. P., Asara, J. M., & Tsou, M.-F. B. (2013). Centriole distal appendages promote membrane docking, leading to cilia initiation. *Genes & Development*, *27*(2), 163–168.
<https://doi.org/10.1101/gad.207043.112>

- Tavernier, N., Panbianco, C., Gotta, M., & Pintard, L. (2015). Cdk1 plays matchmaker for the Polo-like kinase and its activator SPAT-1/Bora. *Cell Cycle*, *14*(15), 2394–2398.
<https://doi.org/10.1080/15384101.2015.1053673>
- Thomas, X., Afonso, C., Destoumieux-Garzón, D., Peduzzi, J., Rebuffat, S., & Tabet, J.-C. (2004). Characterization of a posttranslational modification of Microcin E492 by ESI-ITMS. *52nd Conference of the American Society for Mass Spectrometry (ASMS)*.
<https://hal.archives-ouvertes.fr/hal-00013612/>
- Tibelius, A., Marhold, J., Zentgraf, H., Heilig, C. E., Neitzel, H., Ducommun, B., Rauch, A., Ho, A. D., Bartek, J., & Krämer, A. (2009). Microcephalin and pericentrin regulate mitotic entry via centrosome-associated Chk1. *The Journal of Cell Biology*, *185*(7), 1149–1157.
<https://doi.org/10.1083/jcb.200810159>
- Tilney, L. G., Bryan, J., Bush, D. J., Fujiwara, K., Mooseker, M. S., Murphy, D. B., & Snyder, D. H. (1973). Microtubules: Evidence for 13 protofilaments. *The Journal of Cell Biology*, *59*(2 Pt 1), 267–275.
<https://doi.org/10.1083/jcb.59.2.267>
- Tonkin, E. T., Wang, T.-J., Lisgo, S., Bamshad, M. J., & Strachan, T. (2004). NIPBL, encoding a homolog of fungal Scc2-type sister chromatid cohesion proteins and fly Nipped-B, is mutated in Cornelia de Lange syndrome. *Nature Genetics*, *36*(6), 636–641.
<https://doi.org/10.1038/ng1363>
- Tonks, N. K. (2006). Protein tyrosine phosphatases: From genes, to function, to disease. *Nature Reviews Molecular Cell Biology*, *7*(11), 833–846.
<https://doi.org/10.1038/nrm2039>
- Tóth, A., Ciosk, R., Uhlmann, F., Galova, M., Schleiffer, A., & Nasmyth, K. (1999). Yeast cohesin complex requires a conserved protein, Eco1p(Ctf7), to establish cohesion between sister chromatids during DNA replication. *Genes & Development*, *13*(3), 320–333.
<https://doi.org/10.1101/gad.13.3.320>
- Tsou, M.-F. B., & Stearns, T. (2006). Mechanism limiting centrosome duplication to once per cell cycle. *Nature*, *442*(7105), 947–951.
<https://doi.org/10.1038/nature04985>
- Tsou, M.-F. B., Wang, W.-J., George, K. A., Uryu, K., Stearns, T., & Jallepalli, P. V. (2009). Polo Kinase and Separase Regulate the Mitotic Licensing of Centriole Duplication in Human Cells. *Developmental Cell*, *17*(3), 344–354.
<https://doi.org/10.1016/j.devcel.2009.07.015>
- Uhlmann, F. (2016). SMC complexes: From DNA to chromosomes. *Nature Reviews Molecular Cell Biology*, *17*(7), 399–412.
<https://doi.org/10.1038/nrm.2016.30>
- Uhlmann, F., Lottspeich, F., & Nasmyth, K. (1999). Sister-chromatid separation at anaphase onset is promoted by cleavage of the cohesin subunit Scc1. *Nature*, *400*(6739), 37.
<https://doi.org/10.1038/21831>
- Uhlmann, F., & Nasmyth, K. (1998). Cohesion between sister chromatids must be established during DNA replication. *Current Biology: CB*, *8*(20), 1095–1101.
[https://doi.org/10.1016/s0960-9822\(98\)70463-4](https://doi.org/10.1016/s0960-9822(98)70463-4)
- Uhlmann, F., Wernic, D., Poupard, M. A., Koonin, E. V., & Nasmyth, K. (2000). Cleavage of cohesin by the CD clan protease separin triggers anaphase in yeast. *Cell*, *103*(3), 375–386.
[https://doi.org/10.1016/s0092-8674\(00\)00130-6](https://doi.org/10.1016/s0092-8674(00)00130-6)

- Uzbekov, R., & Alieva, I. (2018). Who are you, subdistal appendages of centriole? *Open Biology*, 8(7), 180062.
<https://doi.org/10.1098/rsob.180062>
- van Breugel, M., Hirono, M., Andreeva, A., Yanagisawa, H., Yamaguchi, S., Nakazawa, Y., Morgner, N., Petrovich, M., Ebong, I.-O., Robinson, C. V., & others. (2011). Structures of SAS-6 suggest its organization in centrioles. *Science*, 331(6021), 1196–1199.
<https://doi.org/10.1126/science.1199325>
- van der Lelij, P., Chrzanowska, K. H., Godthelp, B. C., Rooimans, M. A., Oostra, A. B., Stumm, M., Zdzienicka, M. Z., Joenje, H., & de Winter, J. P. (2010). Warsaw Breakage Syndrome, a Cohesinopathy Associated with Mutations in the XPD Helicase Family Member DDX11/ChlR1. *The American Journal of Human Genetics*, 86(2), 262–266.
<https://doi.org/10.1016/j.ajhg.2010.01.008>
- Vega, H., Waisfisz, Q., Gordillo, M., Sakai, N., Yanagihara, I., Yamada, M., van Gosliga, D., Kayserili, H., Xu, C., Ozono, K., Wang Jabs, E., Inui, K., & Joenje, H. (2005). Roberts syndrome is caused by mutations in ESCO2, a human homolog of yeast ECO1 that is essential for the establishment of sister chromatid cohesion. *Nature Genetics*, 37(5), 468–470.
<https://doi.org/10.1038/ng1548>
- Vermeulen, K., Van Bockstaele, D. R., & Berneman, Z. N. (2003). The cell cycle: A review of regulation, deregulation and therapeutic targets in cancer. *Cell Proliferation*, 36(3), 131–149.
- Vertii, A., Hung, H.-F., Hehnly, H., & Doxsey, S. (2016). Human basal body basics. *Cilia*, 5(1).
<https://doi.org/10.1186/s13630-016-0030-8>
- Vodermaier, H. C. (2004). APC/C and SCF: Controlling Each Other and the Cell Cycle. *Current Biology*, 14(18), R787–R796.
<https://doi.org/10.1016/j.cub.2004.09.020>
- Voter, W. A., & Erickson, H. P. (1984). The kinetics of microtubule assembly. Evidence for a two-stage nucleation mechanism. *Journal of Biological Chemistry*, 259(16), 10430–10438.
- Waizenegger, I. C., Hauf, S., Meinke, A., & Peters, J.-M. (2000). Two distinct pathways remove mammalian cohesin from chromosome arms in prophase and from centromeres in anaphase. *Cell*, 103(3), 399–410.
[https://doi.org/10.1016/s0092-8674\(00\)00132-x](https://doi.org/10.1016/s0092-8674(00)00132-x)
- Wang, W.-J., Soni, R. K., Uryu, K., & Bryan Tsou, M.-F. (2011). The conversion of centrioles to centrosomes: Essential coupling of duplication with segregation. *The Journal of Cell Biology*, 193(4), 727–739.
<https://doi.org/10.1083/jcb.201101109>
- Wang, X., Yang, Y., & Dai, W. (2006). Differential subcellular localizations of two human Sgo1 isoforms: Implications in regulation of sister chromatid cohesion and microtubule dynamics. *Cell Cycle*, 5(6), 636–641.
- Wang, X., Yang, Y., Duan, Q., Jiang, N., Huang, Y., Darzynkiewicz, Z., & Dai, W. (2008). SSgo1, a Major Splice Variant of Sgo1, Functions in Centriole Cohesion Where It Is Regulated by Plk1. *Developmental Cell*, 14(3), 331–341.
<https://doi.org/10.1016/j.devcel.2007.12.007>
- Wang, Y., Dantas, T. J., Lator, P., Dockery, P., & Morrison, C. G. (2013). Promoter hijack reveals pericentrin functions in mitosis and the DNA damage response. *Cell Cycle*, 12(4), 635–646.
<https://doi.org/10.4161/cc.23516>

- Watanabe, N., Arai, H., Iwasaki, J., Shiina, M., Ogata, K., Hunter, T., & Osada, H. (2005). Cyclin-dependent kinase (CDK) phosphorylation destabilizes somatic Wee1 via multiple pathways. *Proceedings of the National Academy of Sciences of the United States of America*, *102*(33), 11663–11668.
<https://doi.org/10.1073/pnas.0500410102>
- Watanabe, N., Arai, H., Nishihara, Y., Taniguchi, M., Watanabe, N., Hunter, T., & Osada, H. (2004). M-phase kinases induce phospho-dependent ubiquitination of somatic Wee1 by SCF β -TrCP. *Proceedings of the National Academy of Sciences of the United States of America*, *101*(13), 4419–4424.
<https://doi.org/10.1073/pnas.0307700101>
- Wells, J. N., Gligoris, T. G., Nasmyth, K. A., & Marsh, J. A. (2017). Evolution of condensin and cohesin complexes driven by replacement of Kite by Hawk proteins. *Current Biology*, *27*(1), R17–R18.
<https://doi.org/10.1016/j.cub.2016.11.050>
- Wendt, K. S., Yoshida, K., Itoh, T., Bando, M., Koch, B., Schirghuber, E., Tsutsumi, S., Nagae, G., Ishihara, K., Mishiro, T., Yahata, K., Imamoto, F., Aburatani, H., Nakao, M., Imamoto, N., Maeshima, K., Shirahige, K., & Peters, J.-M. (2008). Cohesin mediates transcriptional insulation by CCCTC-binding factor. *Nature*, *451*(7180), 796–801.
<https://doi.org/10.1038/nature06634>
- Wheatley, D. N. (1982). The centriole: a central enigma of cell biology. Elsevier Biomedical Press, S. 21.
- Wittmann, T., Hyman, A., & Desai, A. (2001). The spindle: a dynamic assembly of microtubules and motors. *Nature cell biology*, *3*(1), E28–E34.
<https://doi.org/10.1038/35050669>
- Wollman, R., Cytrynbaum, E. N., Jones, J. T., Meyer, T., Scholey, J. M., & Mogilner, A. (2005). Efficient Chromosome Capture Requires a Bias in the ‘Search-and-Capture’ Process during Mitotic-Spindle Assembly. *Current Biology*, *15*(9), 828–832.
<https://doi.org/10.1016/j.cub.2005.03.019>
- Wong, C., & Stearns, T. (2003). Centrosome number is controlled by a centrosome-intrinsic block to reduplication. *Nature Cell Biology*, *5*(6), 539.
<https://doi.org/10.1038/ncb993>
- Wong, R. W. (2010). An update on cohesin function as a ‘molecular glue’ on chromosomes and spindles. *Cell Cycle*, *9*(9), 1754–1758.
<https://doi.org/10.4161/cc.9.9.11806>
- Wong, R. W., & Blobel, G. (2008). Cohesin subunit SMC1 associates with mitotic microtubules at the spindle pole. *Proceedings of the National Academy of Sciences*, *105*(40), 15441–15445.
<https://doi.org/10.1073/pnas.0807660105>
- Woodruff, J. B., Wueseke, O., & Hyman, A. A. (2014). Pericentriolar material structure and dynamics. *Philosophical Transactions of the Royal Society of London. Series B, Biological Sciences*, *369*(1650), 20130459.
<https://doi.org/10.1098/rstb.2013.0459>
- Wu, F. M., Nguyen, J. V., & Rankin, S. (2011). A Conserved Motif at the C Terminus of Sororin Is Required for Sister Chromatid Cohesion. *Journal of Biological Chemistry*, *286*(5), 3579–3586.
<https://doi.org/10.1074/jbc.M110.196758>
- Wu, J., & Akhmanova, A. (2017). Microtubule-organizing centers. *Annual Review of Cell and Developmental Biology*, *33*, 51–75.
<https://doi.org/10.1146/annurev-cellbio-100616-060615>

- Wutz, G., Várnai, C., Nagasaka, K., Cisneros, D. A., Stocsits, R. R., Tang, W., Schoenfelder, S., Jessberger, G., Muhar, M., Hossain, M. J., Walther, N., Koch, B., Kueblbeck, M., Ellenberg, J., Zuber, J., Fraser, P., & Peters, J.-M. (2017). Topologically associating domains and chromatin loops depend on cohesin and are regulated by CTCF, WAPL, and PDS5 proteins. *The EMBO Journal*, *36*(24), 3573–3599.
<https://doi.org/10.15252/embj.201798004>
- Xie, S., Wu, H., Wang, Q., Cogswell, J. P., Husain, I., Conn, C., Stambrook, P., Jhanwar-Uniyal, M., & Dai, W. (2001). Plk3 Functionally Links DNA Damage to Cell Cycle Arrest and Apoptosis at Least in Part via the p53 Pathway. *Journal of Biological Chemistry*, *276*(46), 43305–43312.
<https://doi.org/10.1074/jbc.M106050200>
- Yang, M., Li, B., Tomchick, D. R., Machius, M., Rizo, J., Yu, H., & Luo, X. (2007). P31comet blocks Mad2 activation through structural mimicry. *Cell*, *131*(4), 744–755.
<https://doi.org/10.1016/j.cell.2007.08.048>
- Yoshida, Y., Chiba, T., Tokunaga, F., Kawasaki, H., Iwai, K., Suzuki, T., Ito, Y., Matsuoka, K., Yoshida, M., Tanaka, K., & Tai, T. (2002). E3 ubiquitin ligase that recognizes sugar chains. *Nature*, *418*(6896), 438–442.
<https://doi.org/10.1038/nature00890>
- Young, A., Dichtenberg, J. B., Purohit, A., Tuft, R., & Doxsey, S. J. (2000). Cytoplasmic dynein-mediated assembly of pericentrin and γ tubulin onto centrosomes. *Molecular Biology of the Cell*, *11*(6), 2047–2056.
<https://doi.org/10.1091/mbc.11.6.2047>
- Yu, H. (2016). Magic Acts with the Cohesin Ring. *Molecular Cell*, *61*(4), 489–491.
<https://doi.org/10.1016/j.molcel.2016.02.003>
- Yu, J., Raia, P., Ghent, C. M., Raisch, T., Sadian, Y., Cavadini, S., Sabale, P. M., Barford, D., Raunser, S., Morgan, D. O., & Boland, A. (2021). Structural basis of human separase regulation by securin and CDK1-cyclin B1. *Nature*, *596*(7870), 138–142.
<https://doi.org/10.1038/s41586-021-03764-0>
- Zhang, J., Shi, X., Li, Y., Kim, B.-J., Jia, J., Huang, Z., Yang, T., Fu, X., Jung, S. Y., Wang, Y., Zhang, P., Kim, S.-T., Pan, X., & Qin, J. (2008). Acetylation of Smc3 by Eco1 is required for S phase sister chromatid cohesion in both human and yeast. *Molecular Cell*, *31*(1), 143–151.
<https://doi.org/10.1016/j.molcel.2008.06.006>
- Zhang, N., Kuznetsov, S. G., Sharan, S. K., Li, K., Rao, P. H., & Pati, D. (2008). A handcuff model for the cohesin complex. *The Journal of Cell Biology*, *183*(6), 1019–1031.
<https://doi.org/10.1083/jcb.200801157>
- Zhang, N., Panigrahi, A. K., Mao, Q., & Pati, D. (2011). Interaction of Sororin Protein with Polo-like Kinase 1 Mediates Resolution of Chromosomal Arm Cohesion. *Journal of Biological Chemistry*, *286*(48), 41826–41837.
<https://doi.org/10.1074/jbc.M111.305888>
- Zhang, N., & Pati, D. (2009). Handcuff for sisters: A new model for sister chromatid cohesion. *Cell Cycle*, *8*(3), 399–402.
<https://doi.org/10.4161/cc.8.3.7586>
- Zhang, N., & Pati, D. (2015). C-terminus of Sororin interacts with SA2 and regulates sister chromatid cohesion. *Cell Cycle*, *14*(6), 820–826.
<https://doi.org/10.1080/15384101.2014.1000206>
- Zhang, X., Chen, Q., Feng, J., Hou, J., Yang, F., Liu, J., Jiang, Q., & Zhang, C. (2009). Sequential phosphorylation of Nedd1 by Cdk1 and Plk1 is required for targeting of the TuRC to the centrosome. *Journal of Cell Science*, *122*(13), 2240–2251.
<https://doi.org/10.1242/jcs.042747>

- Zhang, X., Lan, W., Ems-McClung, S. C., Stukenberg, P. T., & Walczak, C. E. (2007). Aurora B phosphorylates multiple sites on mitotic centromere-associated kinesin to spatially and temporally regulate its function. *Molecular Biology of the Cell*, *18*(9), 3264–3276.
<https://doi.org/10.1091/mbc.e07-01-0086>
- Zheng, Y., Wong, M. L., Alberts, B., & Mitchison, T. (1995). Nucleation of microtubule assembly by a gamma-tubulin-containing ring complex. *Nature*, *378*(6557), 578–583.
<https://doi.org/10.1038/378578a0>
- Zhu, X., & Kaverina, I. (2013). Golgi as an MTOC: Making microtubules for its own good. *Histochemistry and Cell Biology*, *140*(3), 361–367.
<https://doi.org/10.1007/s00418-013-1119-4>
- Zimmerman, W. C., Sillibourne, J., Rosa, J., & Doxsey, S. J. (2004). Mitosis-specific anchoring of γ tubulin complexes by pericentrin controls spindle organization and mitotic entry. *Molecular Biology of the Cell*, *15*(8), 3642–3657.
<https://doi.org/10.1091/mbc.e03-11-0796>
- Zitouni, S., Nabais, C., Jana, S. C., Guerrero, A., & Bettencourt-Dias, M. (2014). Polo-like kinases: Structural variations lead to multiple functions. *Nature Reviews Molecular Cell Biology*, *15*(7), 433–452.
<https://doi.org/10.1038/nrm3819>

8 Abbreviations

3D-SIM	3-dimensional structured illumination microscopy
A	alanine
aa	amino acids
ABC	ATP binding cassette
Ala	alanine
APC/C	anaphase promoting complex or cyclosome
ATP	adenosine triphosphate
BCL-XL	B-cell lymphoma- extra large
BCR-ABL	breakpoint cluster region-abelson murine leukemia viral oncogene homolog 1
bp	base pair
BSA	bovine serum albumin
Bub	budding uninhibited by benzimidazoles
<i>C. elegans</i>	<i>Caenorhabditis elegans</i>
C-Nap1	centrosomal Nek2-associated protein 1
ca	circa or constitutively active
CAK	Cdk-activating kinase
CAR	Cohesin associated region
Cep	centrosomal protein
Cdc	cell division cycle
Cdh1	cdc20 homolog 1
Cdk	cyclin-dependent kinase
CdLS	Cornelia de Lange syndrome
CG-Nap	centrosome and Golgi localized PKN-associated protein
CHD	chromodomain helicase DNA-binding protein
Chk1	checkpoint kinase 1
Chl1	close homolog of L1
CHO	Chinese hamster ovary
CIN	chromosomal instability
Cnn	Centrosomin
CPAP	centrosomal P4.1-associated protein
CPC	chromosomal passenger complex
Cre	Cyclization recombinase
CTCF	CCCTC-binding factor

Abbreviations

C-terminus	carboxy terminus (C-terminal carboxyterminal)
D	aspartate
<i>D. melanogaster</i>	<i>Drosophila melanogaster</i>
Da	Dalton
DAP	distal appendages
DAPI	4',6'-diamino-2-phenylindol
DNA	deoxyribonucleic acid
dNTP	deoxyribonucleotide triphosphate
dox	doxycycline
D-PLP	Drosophila Pericentrin-like protein
D-Box	destruction box
<i>E. coli</i>	<i>Escherichia coli</i>
Eco	establishment of cohesion protein
EDTA	ethylenediamine tetraacetic acid
EGTA	ethylene glycol tetraacetic acid
EM	electron microscopy
Fig.	figure
Flag	epitope tag (aa sequence DYKDDDDK)
Flp	flippase
FRT	flippase recombination target
g	gram or gravitational constant (9.81 m/sec ²)
GCP	γ -tubulin complex protein
GFP	green fluorescence protein
h	hour or human
HAWK	HEAT proteins associated with Kleisins
HEAT	Huntingtin, elongation factor 3, PP2A subunit A, TOR1
HECT	homologous to the E6-AP carboxyl terminus
Hek	human embryonic kidney
HeLa	Henrietta Lacks (patient from whom cell line is derived)
HEPES	4-(2-hydroxyethyl)-1-piperazineethanesulfonic acid
HBS	HEPES buffered saline
HRP	horse radish peroxidase
HRV	human rhinovirus 3C
IFM	immunofluorescence microscopy
INCENP	inner centromere protein
IP	Immunoprecipitation
IVT/T	<i>in vitro</i> transcription/translation

Abbreviations

kb	kilo base pairs
LB	lysogeny broth
loxP	locus of X-over P1
Mad	mitotic arrest deficient
MBP	myelin basic protein
MCAK	mitotic centromere associated kinesin
MCC	mitotic checkpoint complex
Mcl	myeloid cell leukemia
min	minute
mRNA	messenger RNA
MT	microtubule
MTOC	microtubule organizing center
NBD	nucleotide binding domain
NC	non-cleavable
NHS	N-Hydroxysuccinimide
N-terminus	amino terminus (N-terminal aminoterminal)
OD	optical density
ORF	open reading frame
PAGE	polyacrylamide gel electrophoresis
PB	polo box
PBD	polo box domain
PBS	phosphate buffered saline
PCM	pericentriolar matrix
PCNT	Pericentrin
PCR	polymerase chain reaction
PD	protease dead
PDS	precocious dissociation of sisters
PKA	proteinkinase A
Plk	polo-like kinase
PLP	proteolipid protein
PP	protein phosphatase
PVDF	polyvinylidene fluoride
PTM	posttranslational modification
pHH3	phosphohistone H3
RBS	Roberts syndrome
RING	really interesting new gene
RNA	ribonucleic acid

Abbreviations

RNAi	RNA interference
rpm	revolutions per minute
RT	room temperature
SA	stromal antigen
SAP	subdistal appendages
Scc	sister chromatid cohesion
SCF	Skp-cullin-F-Box class ubiquitin ligase
SCI	sister chromatid intertwining
SCS	sister chromatid separation
SDS	sodium dodecylsulfate
siRNA	small interfering RNA
Sgo	shugoshin
Smc	structural maintenance of chromosomes
Ser/Thr	serine and threonine residues
TEV	tobacco etch virus
Tet	tetracycline
U	unit
UTR	untranslated region
v/v	volume per volume
W/v	weight per volume
Wapl	wings apart-like
WB	Western blot
WBS	Warsaw breakage syndrome
WT	wild type
<i>X. laevis</i>	<i>Xenopus laevis</i>
ZM	ZM447439
γ -TuRC	γ -tubulin ring complex
γ -TuSC	γ -tubulin small complex

(Eidestattliche) Versicherungen und Erklärungen

(§ 8 Satz 2 Nr. 3 PromO Fakultät)

Hiermit versichere ich eidesstattlich, dass ich die Arbeit selbstständig verfasst und keine anderen als die von mir angegebenen Quellen und Hilfsmittel benutzt habe (vgl. Art. 97 Abs. 1 Satz 8 BayHIG).

(§ 8 Satz 2 Nr. 3 PromO Fakultät)

Hiermit erkläre ich, dass ich die Dissertation nicht bereits zur Erlangung eines akademischen Grades eingereicht habe und dass ich nicht bereits diese oder eine gleichartige Doktorprüfung endgültig nicht bestanden habe.

(§ 8 Satz 2 Nr. 4 PromO Fakultät)

Hiermit erkläre ich, dass ich Hilfe von gewerblichen Promotionsberatern bzw. -vermittlern oder ähnlichen Dienstleistern weder bisher in Anspruch genommen habe noch künftig in Anspruch nehmen werde.

(§ 8 Satz 2 Nr. 7 PromO Fakultät)

Hiermit erkläre ich mein Einverständnis, dass die elektrische Fassung der Dissertation unter Wahrung meiner Urheberrechte und des Datenschutzes einer gesonderten Überprüfung unterzogen werden kann.

(§ 8 Satz 2 Nr. 8 PromO Fakultät)

Hiermit erkläre ich mein Einverständnis, dass bei Verdacht wissenschaftlichen Fehlverhaltens Ermittlungen durch universitätsinterne Organe der wissenschaftlichen Selbstkontrolle stattfinden können.

.....

Ort, Datum, Unterschrift